uOttawa

L'Université canadienne
Canada's university

FACULTÉ DES ÉTUDES SUPÉRIEURES ET POSTOCTORALES

uOttawa

L'Université canadienne
Canada's university

FACULTY OF GRADUATE AND POSDOCTORAL STUDIES

Adrienne Gowing
AUTEUR DE LA THÈSE / AUTHOR OF THESIS

Ph.D. (Biochemistry)
GRADE / DEGREE

Department of Biochemistry, Microbiology and Immunology
FACULTÉ, ÉCOLE, DÉPARTEMENT / FACULTY, SCHOOL, DEPARTMENT

Metabolic Characterization of Human FOXC2 in Adipose Tissue

TITRE DE LA THÈSE / TITLE OF THESIS

Mary-Ellen Harper
DIRECTEUR (DIRECTRICE) DE LA THÈSE / THESIS SUPERVISOR

CO-DIRECTEUR (CO-DIRECTRICE) DE LA THÈSE / THESIS CO-SUPERVISOR

Rosalind Labow

Alexander Sorisky

Gary W. Slater
Le Doyen de la Faculté des études supérieures et postdoctorales / Dean of the Faculty of Graduate and Postdoctoral Studies

Metabolic Characterization of Human FOXC2 in Adipose Tissue

By: Adrienne Gowing

Supervisor: Dr. Mary-Ellen Harper

Department of Biochemistry, Microbiology and Immunology
Faculty of Medicine
University of Ottawa

Thesis submitted to the Faculty of Graduate and Postdoctoral Studies
In partial fulfillment of the requirements for the M.Sc. degree in Biochemistry

Your file Votre référence
ISBN: 978-0-494-66264-9
Our file Notre référence
ISBN: 978-0-494-66264-9

TABLE OF CONTENTS

Title **Page**

Acknowledgments

I would like to thank my brilliant and compassionate supervisor Dr. Mary-Ellen Harper. I could not have done any of this without her guidance. I would also like to thank the entire Harper lab for all of their technical support and guidance. I would like to thank Jian Xuan for her unbelievable concern and help with the isolated fat cells, Linda Jui for all of her histology work, and Mahmoud Salkhordeh for his incredible technical support. Furthermore, I would like to thank Peter Ripstein of the Ottawa Heart Institute for embedding, sectioning, and staining tissues for electron microscopy and Mitra Abaeian for her help in the optimization of the protocol for the isolation of primary adipocytes. Finally, I would like to thank my family for always being there for me through thick and thin and for always believing in me.

List of Figures

Title **Page**

List of Acronyms

4-HNE: 4-hydroxynonenal
aP2: adipocyte protein 2
ATP: adenosine-triphosphate
βAR: beta-adrenergic receptor
BAT: brown adipose tissue
BMI: body mass index
cAMP: cyclic adenosine monophosphate
C/EBP: CCAAT-enhancer-binding proteins
CRE: cAMP response element
CREB: cAMP response element binding
CVD: cardiovascular disease
ddH2O: double distilled water
DMEM: Dulbecco's Modified Eagle Medium
DNA: deoxyribonucleic acid
DR: dynamic range
E: energy
ECAR: extracellular acidification rate
FCCP: carbonyl cyanide-p-trifluoromethoxyphenylhydrazone (mitochondrial uncoupler)
FFA: free fatty acids
FOX: forkhead box
FOXC2 tg: FOXC2 transgenic
GDP: guanosine diphosphate
GLUT4: insulin-responsive glucose transporter-4
H&E: Haematoxylin & Eosin
HCl: hydrochloric acid
HNF: hepatic nuclear factor
HSL: hormone sensitive lipase
IBAT: interscapular brown adipose tissue
IBMX: isobutylmethylxanthine (PDE inhibitor)
IHC: immunohistochemistry
IRS1: insulin-receptor substrate-1
MEF: mouse embryonic fibroblasts
Mfn: mitofusin
mRNA: messenger ribonucleic acid
mtDNA: mitochondrial DNA
NRF: normalized relative fluorescence
O_2: molecular oxygen
OCR: oxygen consumption rate
PBS: phosphate buffer saline
PDE: phosphodiesterase
PRCF: percent relative cumulative frequency
PGC1α: peroxisome proliferator-activated (PPAR)-γ coactivator-1-alpha
PPARγ: peroxisome proliferator-activated receptor-gamma
PKA: protein kinase A

RER: respiratory exchange ratio
ROS: reactive oxygen species
SAT: subcutaneous adipose tissue
SEM: standard error of the mean
SNS: sympathetic nervous system
SREBP: Sterol Regulatory Element Binding Protein
T2DM: Type 2 Diabetes Mellitus
TEM: transmission electron microscopy
Tfam: mitochondrial transcription factor A
TZD: thiazolidinedione
UCP1: uncoupling protein-1
VAT: visceral adipose tissue
WAT: white adipose tissue
wt: wild type

Abstract

In mice, the overexpression of the nuclear transcription factor FOXC2 in adipose tissue counteracts obesity and diet-induced insulin resistance. Transgenic mice that overexpress FOXC2 in adipose tissue (FOXC2 tg mice) have the key feature of an apparent "conversion" of their intra-abdominal white adipose tissue (WAT) depot into brown adipose tissue (BAT). BAT is very different structurally and metabolically from WAT as it effectively "wastes" energy in the form of heat because of the expression of uncoupling protein-1 (UCP1). In brown adipocytes, thermogenesis is activated through sympathetic stimulation of β_3 adrenergic receptors (β_3ARs) and it is believed that FOXC2 increases the sensitivity of this pathway in adipocytes. FOXC2 tg mice show an increased energy expenditure at 24°C, and 30°C (thermoneutrality) when compared with wild type (wt) mice. However, the FOXC2 tg mice have a blunted response to the β_3AR agonist, CL-316,243 while wt mice show a normal increase in whole body O_2 consumption. O_2 consumption of isolated BAT and WAT from FOXC2 tg and wt mice was assessed and it was observed that "converted" FOXC2 tg WAT had a similar O_2 consumption profile to that of wt BAT. Furthermore, transmission electron microscopy (TEM) of tissues demonstrated an increased multilocularity of cellular lipid droplets and increased mitochondrial content in FOXC2 tg WAT similar to that of FOXC2 tg and wt BAT. Moreover, the oxidative capacity of differentiated mouse embryonic fibroblasts (MEFs) from FOXC2 tg mice was increased compared with wt differentiated MEFs. Taken together, these findings clearly indicate important roles of FOXC2 in adipocyte energy metabolism, affecting mitochondrial energetics, in particular.

1. Introduction

Obesity, a condition characterized by the excessive accumulation of adipose tissue, is reaching epidemic proportions in societies worldwide. In adult humans the main type of adipose tissue is white adipose tissue. While it has its limitations, the body mass index (BMI), is the most commonly used method of identifying overweight and underweight conditions. It is a measure of a person's weight in relation to their height, and is calculated as follows:

$$\text{BMI} = \text{body weight (kg)}/\text{height (metres)}^2$$

A BMI between 18.4 and 24.9 is considered healthy. A BMI between 25 and 30 is considered overweight and a BMI over 30 is considered obese. Using these criteria, in 2004, 23.1% of Canadian adults were obese and 36.1% were overweight (Statistics Canada). In fact, Canadian population studies show that there has been a sharp increase in obesity prevalence since the 1970's (Statistics Canada).

Obesity usually develops gradually due to a prolonged state of positive energy balance, a state in which energy intake exceeds energy expenditure. In contrast, during energy (E) balance, energy intake is equal overall to energy expenditure and this is maintained through complex control networks involving sensors and feedback control structures in the periphery and in the central nervous system. There are both genetic and environmental factors involved in overeating and the development of obesity. For example, the hormone leptin, secreted by adipocytes, acts on the hypothalamus to signal satiety and also stimulates energy expenditure in the periphery (Farooqi and O'Rahilly, 2009). Thus, humans with an extremely rare mutation in the leptin gene (Rau *et al*,

1999), and *ob/ob* mice, which have a mutant form of leptin, (Zhang *et al*, 1994, Pelleymounter *et al*, 1995) become morbidly obese.

A fact not widely known amongst the general population is that there are two types of adipose tissue, white adipose tissue (WAT) and brown adipose tissue (BAT). In obesity there is a large accumulation of WAT. The main function of WAT is energy storage and the release of certain hormones and other factors (Frühbeck, 2008; Wozniak *et al*, 2008). In contrast the main function of BAT is energy expenditure for the purpose of thermogenesis (heat production). Brown adipocytes have abundant mitochondria, and are unique in that they express the mitochondrial inner membrane protein, uncoupling protein-1 (UCP1). UCP1 uncouples mitochondrial respiration from ATP synthesis and the energy is dissipated as heat (Nedergaard *et al*, 2001; Porter, 2008). As the energy expenditure of BAT is high, much research has focused on the idea that increased amounts of BAT may protect against obesity development. However, the molecular mechanisms underlying the development of BAT are poorly understood. The focus of the research reported herein is on a specific nuclear transcription factor, called FOXC2, which apparently 'converts' thermogenically inactive WAT to highly metabolic BAT. In fact, the overexpression of FOXC2 protein in adipocytes of mice results in an apparent conversion of WAT into BAT (Cederberg *et al*, 2001).

The overall goal of the research reported in this thesis was to determine the *in vivo* and *in vitro* metabolic implications of FOXC2 expression in adipose tissues. The overall hypothesis was that the increased expression of FOXC2 increases adipocyte energy metabolism due to the conversion of metabolically quiescent WAT to metabolically active BAT. Thus, FOXC2 is hypothesized to play an important

metaboregulatory role in adipocytes, favouring increased energy expenditure and leanness. To test this hypothesis a number of experimental systems were employed. These included transgenic mice that overexpress human FOXC2 protein specifically in adipose tissues (FOXC2 tg mice), and differentiated mouse embryonic fibroblasts (MEFs) that overexpress human FOXC2 protein (FOXC2 tg MEFs). An integrative approach was used and involved studies at the whole animal level, the tissue level and at the level of isolated adipocytes. In the following introductory sections, the major concepts and literature relevant to this research will be examined. It is hoped that these studies and others of molecular control 'switches' in adipose tissue will shed light on the mechanisms of brown adipocyte development and function. In the long term, such research may yield new anti-obesity strategies.

1.1. *Obesity and Insulin Resistance*

Obesity is an independent risk factor for a number of diseases such as Type 2 Diabetes Mellitus (T2DM), cardiovascular disease (CVD), gallbladder disease, high blood pressure, and various cancers (Must *et al,* 1999; Kahn and Flier, 2000). Like obesity, T2DM is reaching epidemic proportions worldwide and itself is a risk factor for CVD, blindness, renal failure, strokes and neuropathy (O'Rahilly, 1997). Two of the main pathophysiological signs of T2DM are insulin resistance and hyperinsulinemia. Insulin is critical in adipocyte metabolism and adipocytes are one of the most insulin-sensitive types of cells in the body. Insulin is also important for most aspects of adipocyte metabolism, including adipocyte differentiation, and the inhibition of lipolysis (Kahn and Flier, 2000; Abdul-Ghani and DeFronzo, 2009).

T2DM develops gradually and generally begins with a state of insulin resistance in which cells do not respond normally to insulin (*i.e.,* impaired insulin-stimulated glucose uptake). The pancreas must then secrete more insulin for a given response; thus there are higher than normal levels of insulin in the circulation (*i.e.,* hyperinsulinemia). Eventually, the pancreatic β cells become damaged and lose the ability to compensate for the reduced sensitivity of peripheral tissues, and this leads to hypoinsulinemia and a hyperglycemic state (Muoio and Newgard, 2008). The major risk factor for insulin resistance is obesity. The regulation of a wide variety of cytokines released by adipocytes is altered in obesity leading to insulin resistance and cardiovascular problems (Sorisky, 2002). Along with insulin resistance, obesity is also a risk factor for hypertension, hyperlipidemia and atherosclerosis. Taken together these are symptoms of the metabolic syndrome or 'syndrome X' (Kahn and Flier, 2000; Hajer *et al*, 2008). The metabolic syndrome is important in that it identifies patients at risk for developing T2DM and CVD. Weight loss in patients with T2DM and the metabolic syndrome can lead to improvements in insulin resistance and other metabolic dysfunctions (Huang, 2009). Therefore it is important to better understand obesity and how it affects the ability of cells to respond to insulin.

1.2. *Two Types of Adipose Tissue: White and Brown Adipose Tissues*

As mentioned, there are two types of adipose tissue in mammals, WAT and BAT. When energy is abundant WAT synthesizes and takes up non-esterified fatty acids and converts them into triacylglycerols which are stored inside a large lipid droplet inside the adipocytes. This lipid droplet takes up the majority of the cell volume. WAT functions

mainly as a lipid storage site but it also functions as a dynamic endocrine tissue which secretes various paracrine and endocrine factors (Hauner, 2005). White adipocytes secrete factors called adipokines that are central to many processes in the body such as energy balance, insulin sensitivity and immune system responses (Wang *et al*, 2008; Hauner, 2005; Gregoire, 2001). Leptin and adiponectin are adipokine hormones synthesized and secreted by adipocytes (Fain *et al*, 2004).

BAT, on the other hand, evolved as a key thermogenic tissue in mammals. Conrad Gessner discovered BAT in 1551 in the interscapular region of the marmot (Smith and Horwitz, 1969). Robert Smith in 1961 subsequently discovered that BAT produces heat in response to cold (Smith, 1961). In 1962 Smith then showed that this heat is released into the vascular system (BAT is highly vascularized) in areas near the spine, heart and other thoracic structures (Smith, 1962). Thus a thermoregulatory role for BAT was identified.

Although many subsequent studies revealed a great deal about the thermoregulatory properties of brown adipose tissue, it was not until 1978 that the UCP1 protein was discovered as a 32-kDa protein (Heaton *et al*, 1978). It was originally referred to as 'thermogenin' and was later called uncoupling protein, and then, following the discovery of other uncoupling proteins, was specifically referred to as UCP1. cDNA cloning of the rat mitochondrial uncoupling protein was first published in 1985 (Bouillaud *et al*, 1985) while the actual gene sequence of rat UCP1 was first published in 1988 (Bouillaud *et al*, 1988). Results indicated that UCP1 has 306 residues. In 1990, the human UCP1 gene was isolated and sequenced having 305 amino acids and 79% homology to the rat homologue (Casard *et al*, 1990).

BAT dissipates energy in the form of heat through a process called adaptive thermogenesis. This occurs primarily in response to cold due to the unique presence of UCP1 in the mitochondrial inner membrane of this tissue. UCP1 is a member of the mitochondrial transporter family and is therefore a tripartite structure, meaning it consists of 3 semi-conserved repeats of approximately 100-amino acids (Nedergaard *et al*, 2001). UCP1, an integral membrane protein, functions as a homodimer and each subunit has 6 transmembrane domains with a guanosine-diphosphate (GDP)-binding domain (GDP-binding is known to inhibit UCP1) on the cytosolic side (Kozak and Harper, 2000; Nedergaard *et al*, 2001). UCP1 uncouples energy expenditure from ATP synthesis by causing a leak of protons across the mitochondrial inner membrane resulting in dissipation of the proton electrochemical gradient. This proton leak increases the flux through fatty acid oxidation and therefore the activity of the electron transport chain (Kozak and Harper, 2000; Nedergaard *et al*, 2001; Porter, 2008). BAT has a great deal of mitochondria in order to support thermogenesis. A schematic of oxidative phosphorylation including the electron transport chain and UCP1-mediated proton leak pathways can be seen in Figure 1.

BAT responds to environmental stimuli through the sympathetic nervous system (SNS), by norepinephrine acting through the β-adrenergic receptors (βARs) (Himms-Hagen, 2001, Sell *et al*, 2004, Wijers *et al*, 2009). The acute activation through adrenergic mechanisms in BAT results in thermogenesis through fatty acid activation of UCP1. Chronic β-adrenergic stimulation results in increased UCP1 content and activation (Himms-Hagen, 2001; Porter, 2008). Chronic cold exposure of rodents and

Figure 1. Mitochondrial oxidative phosphorylation and UCP1 thermogenesis. Fuel oxidation from metabolic pathways such as glycolysis, the Krebs cycle, fatty acid oxidation, and amino acid metabolism ultimately lead to two high-energy electron donors, NADH and $FADH_2$. Electrons (red arrows) from these donors are passed through the electron transport chain along the mitochondrial inner membrane to oxygen which is reduced to water. Electrons are passed from NADH and $FADH_2$ to Complex I and Complex II, respectively. Ubiquinone (UQ) receives electrons from Complex I and II. UQ passes electrons to Complex III, which passes them to cytochrome c (cyt c). Cyt c then passes electrons to Complex IV which uses the electrons and hydrogen ions to ultimately reduce oxygen to water. During electron transport, Complex I, Complex III, and Complex IV create a proton gradient across the mitochondrial inner membrane by pumping protons from the matrix into the inter-membrane space. This proton gradient is then used by ATP synthase to generate ATP. The mitochondrial inner membrane of brown adipose tissue contains a large amount of uncoupling protein-1 (UCP1) which acts as an uncoupler by forming an alternative pathway for the flow of protons back into the matrix. This essentially uncouples electron transport activity from ATP production by ATP synthase and releases energy in the form of heat due to an increase in the preceding oxidative reactions in response to the uncoupling (increase in respiration=increase in heat production).

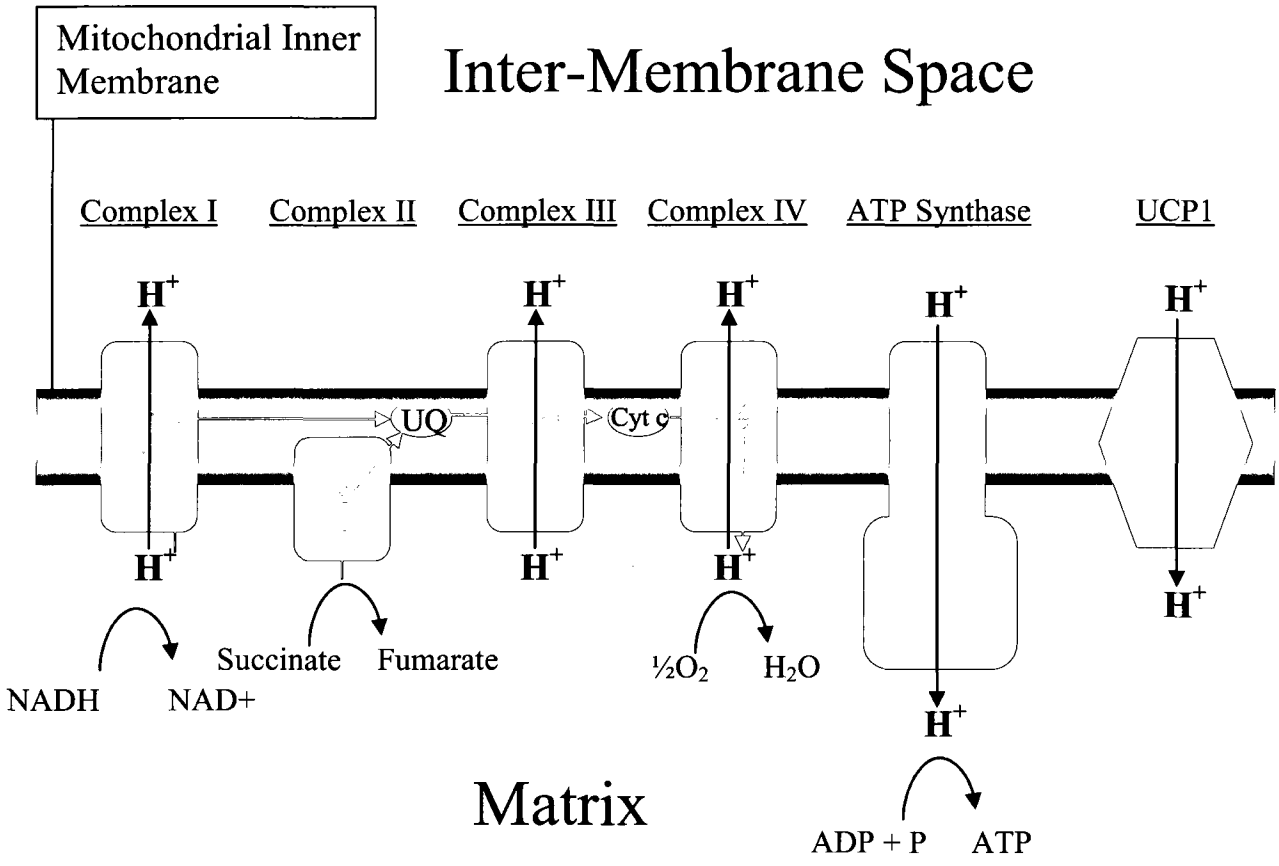
Mitochondrial Inner Membrane
Inter-Membrane Space
Complex I
Complex II
Complex III
Complex IV
ATP Synthase
UCP1
H+
UQ
Cyt c
NADH
NAD+
Succinate
Fumarate
½O2
H2O
ADP + P
ATP
Matrix

humans is sensed by the central nervous system; the subsequent increases in norepinephrine and epinephrine in BAT leads to its activation, differentiation, and hypertrophy (Klingenspor, 2003). There is also a great increase in blood flow and metabolic fuel supply to BAT at this time (Ma and Foster, 1989; Bukowiecki *et al*, 1982). Sympathetic stimulation of brown adipocytes also activates the α-adrenergic receptors (αARs). Stimulation of the α_2ARs leads to the inhibition of thermogenesis through the inactivation of adenylyl cyclase (Cannon and Nedergaard, 2004). In obesity there is evidence for increases in the ratio of α_2ARs/βARs (Lafontan *et al*, 2000). The stimulation of the α_1ARs by the SNS is believed to activate thermogenesis, although its contribution is less than that of the βARs and is less well understood (Cannon and Nedergaard, 2004).

Active BAT is present in small mammals such as rodents, hibernating mammals, and also in newborn humans; in all of these species it functions to maintain body temperature. The amount of active BAT in adult humans is much less than it is in infants (Tiraby and Langin, 2003). However, very recently positron emission topography combined with computerized tomography (PET-CT) and actual tissue biopsies have definitively demonstrated the presence of active brown adipose tissue in adults (Cinti, 2006; Nedergaard *et al*, 2007; Celi, 2009). The presence of cold activated brown adipose tissue in humans was discovered by morphological analysis of biopsies from patients following positron emission topography (Virtanen *et al*, 2009). Furthermore, after analyzing a large amount of test subjects who had undergone PET-CT it was determined that the probability of detection of BAT (UCP1-immunopositive) was inversely correlated with age, BMI and fasting plasma glucose (Cypess *et al*, 2009). van Marken

Lichtenbelt *et al*, (2009) examined the presence, distribution, and activity of BAT in lean *vs.* obese men. Using PET-CT, BAT activity was observed after cold exposure in 23 of 24 subjects and was inversely correlated with BMI and body fat percentage while BAT activity was positively correlated with resting energy expenditure (van Marken Lichtenbelt *et al*, 2009). These data indicate that BAT does in fact exist in adult humans and that it may represent a natural way to increase energy expenditure in humans.

1.3. *The β_3 Adrenergic Pathway in Adipocytes*

There are three types of βARs (1, 2, and 3), all of which are G-protein coupled receptors and are expressed in rodent WAT and BAT. Only one, the β_3AR, is expressed primarily and most abundantly in adipose tissue and is known to activate thermogenesis and lipolysis in adipocytes in rodents (Emorine *et al*, 1992; Collins *et al*, 2001; Skeberdis, 2004). In rodents, the β_3AR is the most highly expressed βAR in the mature brown adipocyte and most significant in terms of thermogenesis, while the β_1AR is active in the brown preadipocyte but not coupled to any signalling processes in mature adipocytes (Cannon and Nedergaard, 2004). WAT is also sympathetically innervated although to a lesser degree than BAT. At times of caloric deprivation the SNS mediates lipolysis through β-adrenergic pathways in WAT (Collins *et al*, 2004). While β_3ARs are expressed in both WAT and BAT in rodents, they are expressed primarily in BAT and not WAT in humans (Ito *et al*, 1998). Therefore, specifically increasing the amount of BAT in humans has been an important line of research into potential thermogenic anti-obesity strategies.

The βARs consist of seven transmembrane domains with three intracellular and three extracellular loops (Skeberdis, 2004). β_3AR stimulation results in the activation of the heterotrimeric G protein, G_s, which, in turn, activates adenylyl cyclase. Adenylyl cyclase then produces cAMP which binds to the regulatory subunit of PKA, releasing the catalytic subunit. The catalytic subunit then participates in cAMP dependent phosphorylation and stimulates lipolysis and uncoupled thermogenesis (Cannon and Nedergaard, 2004).

PKA is composed of both regulatory and catalytic subunits in its inactive state. The subunits form a tetramer composed of two catalytic and two regulatory subunits. There are several forms of the regulatory subunits, which have their own unique tissue distribution. They are called RIα, RIβ, RIIα, and RIIβ (Imaizumi-Scherrer *et al*, 1996). PKA phosphorylates nuclear related proteins such as CREB, which are then believed to activate the expression of genes involved in thermogenesis such as UCP1, as well as cytosolic proteins such as those that mediate lipolysis. The PKA dependent lipolytic activation is believed to occur via the activation of hormone sensitive lipase (HSL) and deactivation of perilipin, both by phosphorylation (Cannon and Nedergaard, 2004). Perilipin covers lipid droplets and protects them from lipolysis by HSL. When perilipin is deactivated, the lipid droplets are exposed for attack by lipases. While HSL was once the only enzyme known to hydrolyze lipids in adipose tissue, another enzyme called adipose triglyceride lipase (ATGL) has recently been shown to be important in fatty acid mobilization in adipose tissue (Zimmermann *et al*, 2004). ATGL (*aka* desnutrin, Ca-independent phospholipase A2ς) catalyzes the first step in triglyceride hydrolysis and is highly expressed in mouse and human adipose tissue. However, while it is regulated by

nutritional status, it is not phosphorylated by PKA and its molecular regulation has yet to be deciphered (Zimmermann *et al*, 2004; Zechner *et al*, 2005). The fatty acids released through lipolysis by lipases can then act as thermogenic substrates. As well as being substrates, the fatty acids are believed to activate UCP1 allosterically, as coactivators, or as proton shuttles in association with UCP1 (Cannon and Nedergaard, 2004). Figure 2 depicts the acute activation of the β_3AR.

Norepinephrine also induces brown adipocyte proliferation via β_1/cAMP mediated processes (Bronnikov *et al.,* 1992), though the processes are as yet poorly understood. Furthermore, it is believed that norepinephrine induces differentiation of brown adipocytes through a cAMP/PKA/CREB phosphorylation pathway (Cannon and Nedergaard, 1996). This leads to an increase in transcription factors that promote BAT differentiation such as peroxisome proliferator-activated (PPAR)-γ coactivator-1-alpha (PGC1α) (Gomez-Ambrosi *et al*, 2001).

1.4. *Brown Adipose Tissue and Protection from Obesity and Insulin Resistance*

There is a great deal of evidence from animal studies that increased BAT activity protects against obesity and insulin resistance. Hamman *et al* (1996) used a UCP1-DTA transgenic mouse model with toxigene mediated ablation of BAT. It was shown that these mice became obese and were more susceptible to diet-induced insulin resistance and hyperlipidemia than control mice. Furthermore, ectopic expression of BAT in muscle has been shown to mitigate obesity. Almind *et al* (2007) compared 129S6/SvEvTac mice to C57BL/6 control mice and found that the former mice have a

Figure 2. Norepinephrine induced β_3AR/cAMP/PKA activation of acute thermogenesis and UCP1 transcription in brown adipocytes. Norepinephrine, released by the sympathetic nervous system (SNS), interacts with the β_3-adrenergic receptor (β_3AR) on the surface of the brown adipocyte. The β_3AR is a G protein coupled receptor protein coupled to Gs. Stimulation causes activation of Gs by exchange of GDP for GTP. The activated Gs subunit in turn activates adenylyl cyclase which begins producing cAMP. cAMP then binds to the regulatory subunit of PKA (R) releasing the catalytic subunit (c). The catalytic subunit then phosphorylates and activates hormone sensitive lipase (HSL) to cleave and release free fatty acids (FFA) from triglyceride droplets (TG). Phosphorylation and deactivation of perilipin exposes the TGs to HSL as well as adipocyte triaglyceride lipase (ATGL) Monoacylglyceride lipase (MGL). The FFAs then act as an energy substrate for thermogenesis and an allosteric activator of uncoupling protein-1 (UCP1). Furthermore, the catalytic subunit of PKA phosphorylates and activates CREB which induces the transcription of UCP1 by binding to a cAMP-response element (CRE) on the promotor of the UCP1 gene.

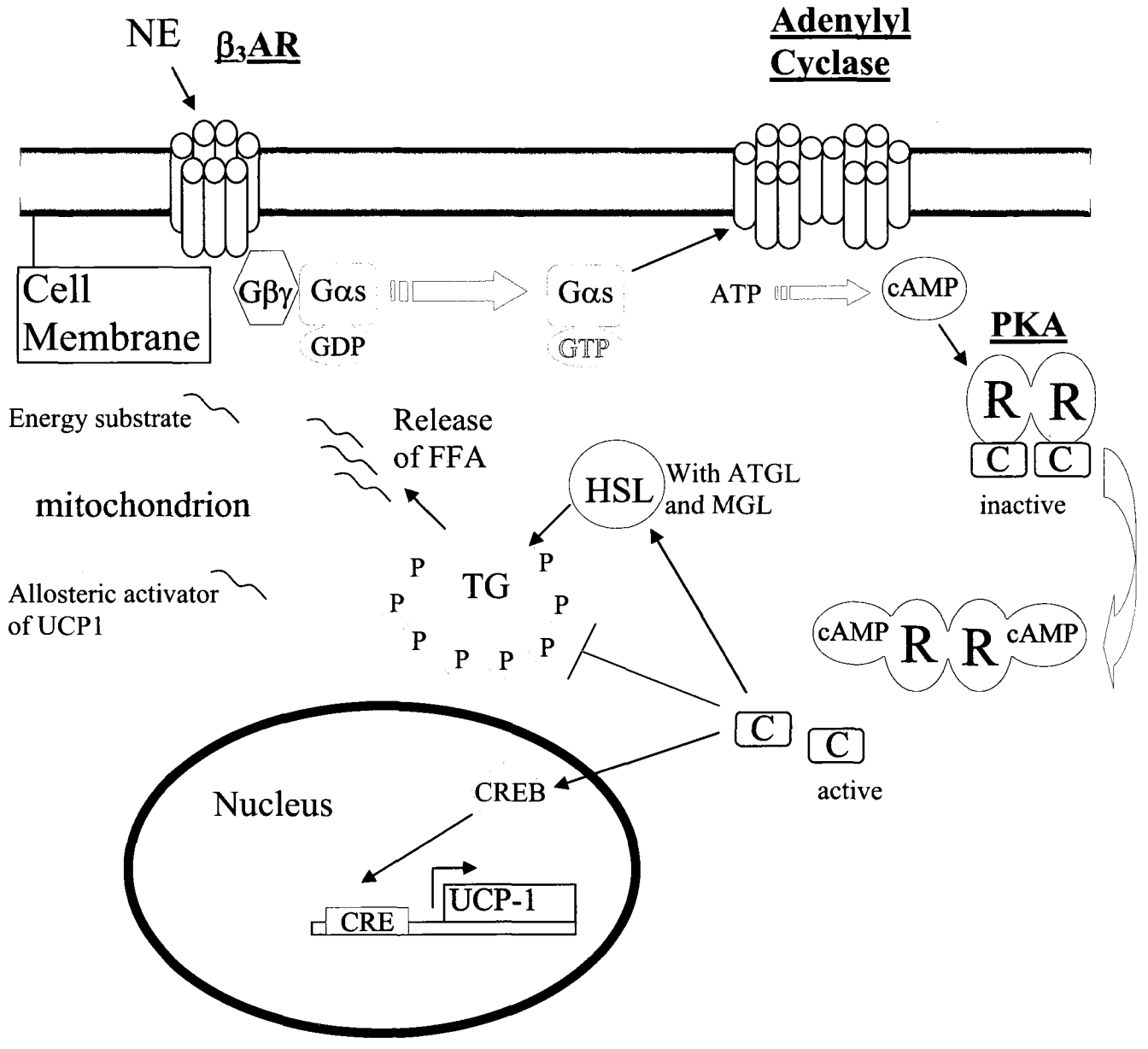
NE
β3AR
Adenylyl Cyclase
Cell Membrane
Gβγ
Gαs
GDP
Gαs
GTP
ATP
cAMP
PKA
R R
C C
inactive
Energy substrate
Release of FFA
mitochondrion
HSL
With ATGL and MGL
Allosteric activator of UCP1
P
TG
cAMP R R cAMP
C C
active
Nucleus
CREB
CRE
UCP-1

700-fold higher intramuscular BAT content (between muscle bundles) than the C57BL/6 controls. This increase was further amplified by β_3 adrenergic stimulation. Unlike C57BL/6 mice, 129 mice are somewhat resistant to diet-induced obesity, hyperinsulimemia and insulin resistance.

There is also evidence that overeating induces BAT thermogenesis, a process referred to as diet-induced thermogenesis (Rothwell and Stock, 1979). This is accomplished through activation of the SNS. It was shown by Rothwell and Stock (1979) that over-eating induced thermogenesis in the BAT of rats, suggesting that it may protect not only against cold but also against obesity. Furthermore, Lupien *et al* (1985) found that in rats, the binding of radiolabeled GDP to isolated BAT mitochondria was increased after a single meal, indicating that UCP1 was activated.

1.5. *The Origins of Brown Adipocytes*

It is generally thought that BAT originated as an internal 'heating system' through evolution; however, it is also thought to have become less important as human behaviour and technologies have developed (*i.e.,* wearing warm clothes, and heating our environments as needed). Nonetheless, researchers have explored the question of the 'reawakening' of BAT thermogenesis in adulthood, and there is an intriguing literature on this subject. Indeed this is the basis of my research.

Cold acclimation causes hypertrophy in BAT (Dicker *et al*, 1995) and importantly, UCP1 expressing multilocular BAT depots in WAT depots (Young *et al*, 1984; Cousin *et al*, 1996). There is also plenty of evidence that increases in UCP1 in mouse WAT increase energy expenditure, and reduce insulin resistance, obesity, and

dislipidemia. CL-316,243 is a highly selective β_3AR agonist and has been used as a tool to achieve this end. For example, it was shown by Himms-Hagen *et al* (1994) that chronic stimulation of rats with CL-316,243 had profound effects on their metabolism. These rats had an increased resting metabolic rate, hypertrophied interscapular BAT (IBAT), and decreased weight of WAT depots, as well as the appearance of multilocular adipocytes in WAT. Furthermore, it was seen by Ghorbani and Himms-Hagen (1997) that CL-316,243 stimulation of WAT in fa/fa Zucker rats caused formation of UCP1 expressing BAT clusters, reduced abdominal fat, and increased resting metabolic rate. These results indicate that β_3AR stimulation can help reverse obesity. It was subsequently determined by Himms-Hagen *et al* (2000) that CL-316,243 stimulated the formation of multilocular, mitochondria-rich adipocytes in WAT of rats and that these adipocytes were derived from mature white adipocytes. These studies demonstrate the importance of the β_3 adrenergic pathway in the conversion of WAT to BAT and the profound metabolic impact that this conversion can have. Therefore, the conversion of mature white adipocytes or white preadipocytes could be important in increased energy metabolism.

There are two important lines of research that focus on the acquisition or re-awakening of BAT in adult humans. These are the development of BAT from preadipocytes and the conversion of mature WAT to BAT. The differentiation of WAT is known to involve PPARγ, which activates white adipocyte differentiation in conjunction with other factors such as C/EBPs and SREBPs, and is an important regulator of adipocyte differentiation (Tontonoz and Spiegelman, 2008). PPARγ binds to promoter sequences as a heterodimer with retinoid X receptor in response to ligands

(Kliewer *et al*, 1992). The antidiabetic drugs, the thiazolidinediones (TZDs), are synthetic PPARγ ligands. While they are able to treat T2DM, they are known to cause increased adiposity and overall weight gain (Lehmann *et al*, 1995). PPARγ is induced in the differentiation of both brown and white adipocytes (Nedergaard *et al*, 2005). The differentiation of BAT is fundamentally different than that of WAT in that it involves induction of the UCP1 gene and mitochondrial biogenesis. The differentiation of BAT is less well understood however, like WAT differentiation, it is known to involve PPARγ. It is also known that the expression of PPARγ coactivator-1α (PGC1α) is important for BAT differentiation (Puigserver *et al*, 1998; Seale *et al*, 2009). PGC1α expression is mediated by cAMP and is induced in BAT but not WAT upon cold exposure and β_3 adrenergic stimulation in mice (Puigserver *et al*, 1998). Furthermore ectopic expression of PGC1α induces expression of mitochondrial genes such as UCP1 in WAT cells (Puigserver *et al*, 1998). It has been shown by Karamanlidis *et al* (2007), that a BAT gene expression pattern could be induced in the mouse white preadipocyte cell line 3T3-L1; this included the expression of PGC1α and UCP1. These data demonstrated that differentiation of preadipocytes towards the BAT rather than the WAT phenotype is controlled in part by the action of C/EBPß on the CRE of the PGC-1α proximal promoter (Karamanlidis *et al*, 2007). This indicates that preadipocytes may have the capability of becoming brown or white adipocyte cells and that the differentiation processes depend on environmental stimuli to some extent.

It is important to note that the transcription factor PRDM16 has been shown to be important in BAT differentiation (Seale *et al*, 2009). When ectopically expressed in cultured white preadipocytes PRDM16 induces brown adipocyte differentiation including

the activation of UCP1, PPARγ, and PGC1α and depletion of PRDM16 from cultured brown fat cells leads to a loss in BAT characteristics (Seale *et al*, 2007). This indicates that PRDM16 is necessary and critical in events leading to BAT differentiation. Furthermore, while it has been generally believed that WAT and BAT cells arise from the same precursor cells, recent evidence suggests that this may not be the case. It was shown by Seale *et al*, 2009 that knockdown of PRDM16 in brown fat cell precursor induces skeletal myogenesis and that PRDN16 induces induces adipogenesis in primary myogenic cells. Morover, it was revealed through in vivo lineage studies that brown adipocytes and skeletal muscle cells arise from the same *Myf5*-expresing precursor cells. However, brown adipocytes induced by chronic β_3 adrenergic stimulation were shown to have a different origin than the BAT depots that develop before birth.

1.6. *The Winged Helix/Fork Head Transcription Factors*

Since the discovery of the of the *Drosophila* transcription factor, fork head, the understanding of the winged helix/fork head class of transcription factors has greatly increased (Weigel *et al*, 1989). This transcription factor was labelled fork head because murine embryos with mutant forms of the transcription factor did not properly form the anterior and posterior gut; instead mutations resulted in two spiked head structures (Weigel *et al*, 1989). Shortly after this, hepatic nuclear factors (HNFs) were described by Lai *et al* (1990, 1991). HNFs share homology with the *Drosophila* fork head transcription factor in the DNA binding region (Weigel and Jackel, 1990). Over 100 members of the fork head family have now been identified in species ranging from yeast to humans. All contain a 100 amino acid monomeric DNA binding domain. Insights into the three-dimensional structure of the DNA binding domain have been derived from the

co-crystal structure of the HNF-3/fork head DNA recognition motif with a target DNA sequence (Clark *et al*, 1993). The core of α-helices and β-strands gives the domain the name "winged helix" (Clark *et al*, 1993). A schematic of this structure is shown in Figure 3. The overall structure of this domain resembles that of a butterfly. While all members of the winged helix/fork head family contain homologous DNA binding domains, other domains of the transcription factor proteins are quite divergent (Kaestner *et al*, 2000). Because many different laboratories discovered the forkhead family members almost simultaneously, various names and classification systems arose for these proteins. Subsequently a unified classification system was developed in 2000 (Kaestner *et al*, 2000).

In this thesis, the symbol Fox (for Fork head box) has been adopted as the abbreviation for the winged helix/fork head transcription factor gene. Moreover, it is important to note that the Fox proteins are divided into subclasses based on phylogenetic analysis, and these are designated by letters (A to Q). Within the subclasses, proteins are given an Arabic numeral. Uppercase letters are used for human (FOXC2), and only the first letter is capitalized for mice (Foxc2); in all other chordates the first and subclass letters capitalized (FoxC2).

Fox proteins display a wide variety of functions in many different tissues. In rodents, FoxA proteins are involved in hepatic and pancreatic metabolism, as well as axial mesodermic development (Lehmann *et al*, 2003). FOXP2 has been shown to play a role in speech and language development in humans (Lai *et al*, 2001). Mutations in FOXC1, one of the first human fork head genes to be studied, cause a range of glaucoma-associated ocular developmental anomalies (Lehmann *et al*, 2003). The function of

Figure 3. The conserved DNA binding domain of winged-helix/fork head proteins. This DNA binding domain is conserved and exists in over 100 members of the fork head family. The N-terminus of the winged-helix/fork head DNA binding domain contains three α-helices (H1, H2, H3). There is a loop region between H2 and H3. Three β-strands form an anti-parallel β-sheet towards the C-terminus. One β-strand (S1) is situated between H1 and H2, while S2 and S3 are located after H3 and are separated by a winged-like region called W1. Another winged-like region is found towards the C-terminus of S3. The overall three-dimensional structure resembles that of a butterfly.

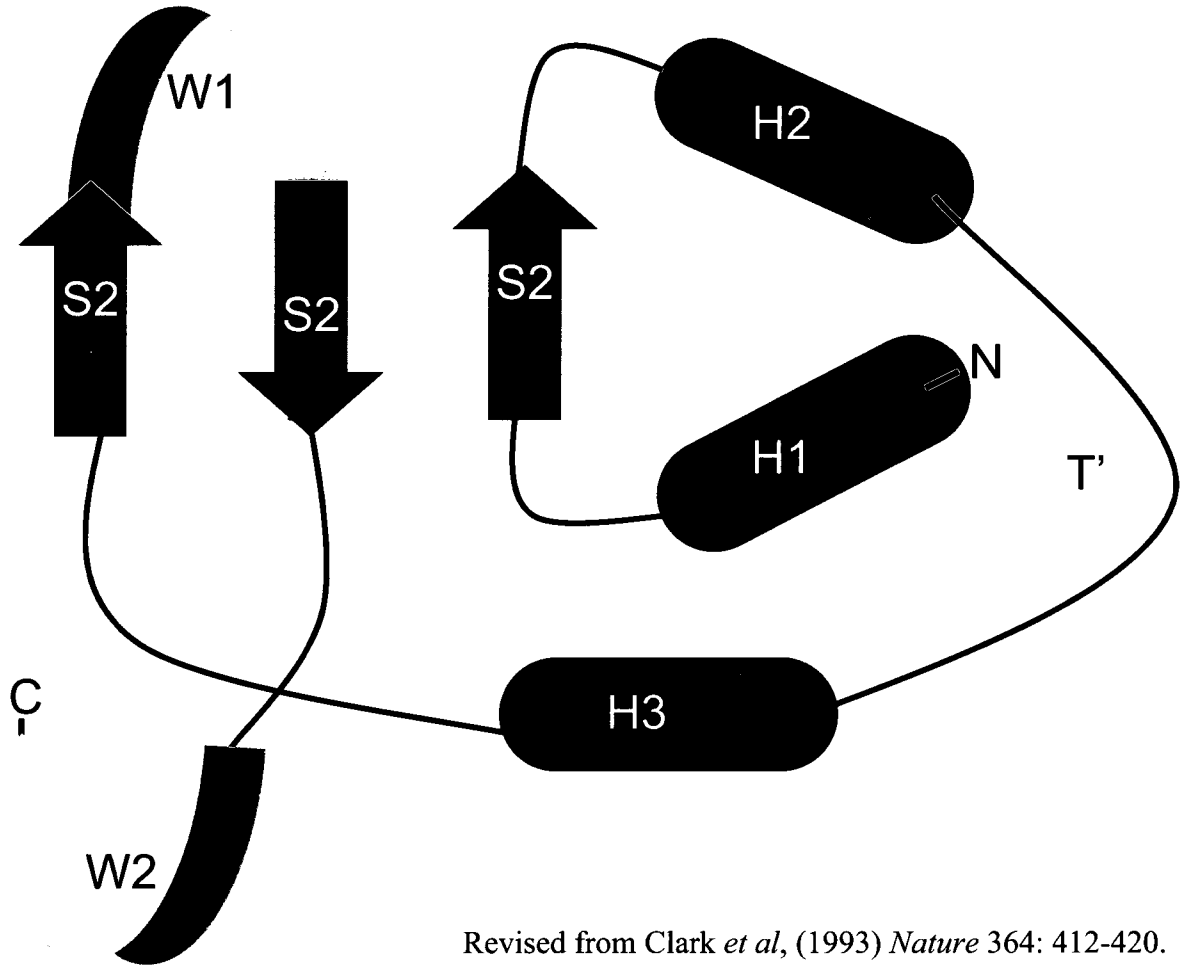

Revised from Clark *et al*, (1993) *Nature* 364: 412-420.

FOXC2 appears to be different in embryonic and adult tissues. The homozygous knockout of Foxc2 is lethal with skeletal, genitourinary, and cardiovascular defects and therefore is involved in mesodermic patterning (Kume *et al*, 2001). It has been shown in adult humans that FOXC2 may play a role in energy expenditure and glucose metabolism; FOXC2 expression is decreased with obesity and insulin resistance (Yang *et al*, 2003). Furthermore, a FOXC2 512C>T polymorphism has been identified and the T allele associated with enhanced insulin sensitivity in humans (Ridderstrale *et al*, 2002). The C-allele has been shown to be associated with obesity and metabolic dysregulation (Carlsson *et al*, 2004; Carlsson *et al*, 2005). Moreover, a frameshift mutation in the human FOXC2 was shown to be associated with T2DM (Yildirim-Toruner *et al*, 2004). Therefore, the role of FOXC2 in human energy expenditure needs to be investigated further.

1.7. *FOXC2 tg Mice and Energy Metabolism*

Mice overexpressing human FOXC2 specifically in adipose tissue with the use of an aP2 promoter (FOXC2 tg mice) are lean and resist diet-induced obesity and insulin resistance (Cederberg *et al*, 2001). Importantly, the intra-abdominal WAT depot of these mice acquires a BAT-like appearance. The previous work of Cederberg *et al* (2001) shows the induction of UCP1 in WAT and the upregulation of genes associated with mitochondrial function, such as coxII, pgc1, as well as mRNAs for the β_3AR and an increase in the sensitivity of the β_3-adrenergic pathway. Serum levels of free fatty acids (FFAs) and glucose are also decreased compared to wt mice. This indicates that the overexpression of FOXC2 has had a profound impact on the metabolism of these mice.

The underlying cause of these changes appears to be a shift in the differentiation of preadipocytes into brown adipocytes instead of white adipocytes, or possibly that the overexpression has caused a "conversion" of mature white adipocytes to BAT or brown-like adipose tissue. Prior to the work described herein there have been no reports characterizing the metabolic activity of this "converted" WAT.

FOXC2 accomplishes this "conversion" through amplification of the β_3AR/cAMP/PKA pathway. As mentioned above, there is more than one kind of PKA regulatory subunit in mice. It was shown by Dostmann *et al* (1990) that the $RI\alpha_2C_2$ PKA subtype binds cAMP with more affinity than the $RII\beta_2C_2$ subunit, both of which are expressed in adipose tissue. Mice with a mutant form of RIIβ have a lean phenotype and resist diet-induced obesity. PKA in BAT of these mice is more sensitive to cAMP signaling and the mice have an increased basal metabolic rate and body temperature, further implicating BAT thermogenesis in their phenotype (Cummings *et al*, 1996). It was shown that FOXC2 increased reporter activity of a construct driven by the promoter of the RIα gene; increased levels of RIα are thought to confer greater sensitivity in this pathway (Cederberg *et al*, 2001).

1.8. *FOXC2 Induction of Brown Adipogenesis and Apparent Decrease in White Adipogenesis: Potential Mechanisms*

It was observed by Davis *et al* (2004) that the expression of Foxc2 in 3T3-L1 preadipocytes inhibited the differentiation of these cells into mature white adipocytes. FOXC2 also inhibits the ability of PPARγ to induce adipogenic gene expression in response to differentiation compounds, such as IBMX and dexamethasone (Davis *et al*,

2004). Furthermore, the expression of FOXC2 did not induce brown adipocyte differentiation in these cells (Davis *et al*, 2004). These results support the idea that FOXC2 represses WAT differentiation; however, whether it is necessary or important in BAT differentiation has yet to be shown. While insulin sensitizing therapy using TZDs, which are synthetic PPARγ ligands, is thought to increase insulin sensitivity by decreasing lipotoxicity and increasing storage and therefore fat mass (Medina-Gomez *et al*, 2007), the role of FOXC2 in increasing insulin sensitivity appears to be through decreasing WAT and increasing BAT (Cederberg *et al*, 2001). FOXC2 overexpression in mice increased the expression of PGC1α in both WAT and BAT of the FOXC2 tg mice (Cederberg *et al*, 2001). Furthermore, it has been communicated to us by our collaborator, Dr. Sven Enerback (personal communication) that PGC1α and PPARγ do not induce transcription of FOXC2 *in vivo* but that with enhanced levels of FOXC2, PGC1α is upregulated. However, wt levels of PGC1α are not affected by FOXC2 expression since MEFs lacking FOXC2 (-/-) had no difference in PGC1 mRNA levels when compared with wt levels (Westergren *et al*, 2009; submitted). Therefore, while PGC1α levels are enhanced by overexpression of FOXC2, the expression of PGC1α is not dependant on FOXC2. Because PGC1α expression is induced by the PKA-CREB pathway, it is possible that FOXC2 helps to amplify its expression through sensitization of the β_3AR/cAMP/PKA pathway (Seale *et al*, 2009). Furthermore, FOXC2 has been shown to control the promoter activity of angiotensin-2, an important transcription factor in vascular remodeling (Xue *et al*, 2008). Increased vascularity is needed in BAT because of enhanced metabolic activity.

Furthermore, it has been communicated to us by our collaborator (Dr. Sven Enerback; personal communication) that through a promoter construct, FOXC2 activates the expression of insulin-receptor substrate-1 (IRS1), UCP1, insulin-responsive glucose transporter-4 (GLUT4), HSL, and of FOXC2 itself (Westergren *et al*, 2009; submitted). This shows that FOXC2 has diverse functions in adipocyte metabolism functioning in pathways involved in insulin signaling, glucose uptake, mitochondrial uncoupling, and lipolysis. However, the findings show that other adipocyte proteins such as adiponectin, adipsin and LPL are not activated directly by FOXC2. However, these are also known to be important in the endocrine function of WAT (Frühbeck, 2008).

Moreover, FOXC2 was shown to up-regulate nuclear encoded mitochondrial transcription factor A (Tfam) expression, and in FOXC2 tg mice Tfam expression is upregulated in WAT (Westergren *et al*, 2009; submitted). It is well known that Tfam is involved in mtDNA transcription and replication. Mice deficient in Tfam have an extreme decrease in mtDNA and oxidative phosphorylation (Larsson *et al*, 1998) and mice lacking Tfam in pancreatic β-cells develop Type 1 diabetes (Silva *et al*, 2000). These results indicate a role for FOXC2 in mitochondrial biogenesis and further shed light on the importance of FOXC2 in the BAT phenotype.

Phosphodiesterases (PDEs) cleave cAMP and therefore decrease the activity of PKA. Thus, the expression of the different phosphodiesterases in FOXC2 tg *vs.* wt mouse adipose tissue was investigated by Gronning *et al* (2006). It was found that PDE4 and PDE4A5 levels were decreased in FOXC2 tg WAT compared with wt WAT (Gronning *et al*, 2006). The decreased expression of these PDEs most likely contributes to the metabolic phenotype of the FOXC2 tg mice.

1.9. *Summary*

In summary, Fox transcription factors are found in a wide range of organisms and display a wide variety of functions. Importantly, in adult humans, FOXC2 is believed to be important in energy expenditure and glucose metabolism. Indeed, FOXC2 expression is decreased in human subjects with insulin resistance (Yang *et al*, 2003). Obesity is a major risk factor for many disorders including T2DM, and obesity-related disorders are on the rise worldwide. It is well recognized that there are many genetic and environmental components underlying obesity. Therefore, an improved understanding of the genetic risks behind obesity and T2DM is very important. The research described in this thesis focuses to a large extent on adaptive thermogenesis and the role of BAT in reducing obesity. BAT mitochondria exclusively express UCP1 for the purpose of uncoupled oxidative phosphorylation and the resulting thermogenesis. BAT thermogenesis is activated by the SNS, which responds to environmental stimuli such as a caloric overload or the cold. The original report of the overexpression of FOXC2 in adipocytes of mice (Cederberg *et al*, 2001) demonstrated an apparent conversion of WAT to BAT. It was hypothesized that this is accomplished through sensitization of the β_3AR/cAMP/PKA pathway. Because the amount of active BAT in adult humans is thought to be limited, the conversion of WAT to functional BAT may be an important future means to combat obesity and obesity-related disorders. An improved understanding of the genetic risk factors underlying obesity is greatly needed, and it is hoped that the research described herein contributes to some extent in this regard.

2. Hypothesis and Research Objectives

2.1. *Overall Goal:*

The overall goal of this study was to characterize, using a variety of *in vivo* and *in vitro* approaches, the metabolic impact of the overexpression of FOXC2 in adipose tissue.

2.2. *Hypotheses*

Since the overexpression of FOXC2 in adipocytes of mice has such a powerful effect on the metabolic phenotype of the mice, the overall hypothesis was that FOXC2 has thermogenic effects in adipocytes, favouring BAT thermogenesis, and leanness. It was specifically hypothesized that energy expenditure in the FOXC2 tg mice would be higher than that of the wt littermates. Thus, it was anticipated that isolated white adipocytes from FOXC2 tg mice would be more metabolically active than white adipocytes of wt mice. Finally it was hypothesized that FOXC2 tg differentiated MEFs would have higher metabolic activities than wt differentiated MEFs.

2.3. *Overall Objective*

At the level of the whole animal and in isolated adipocytes, the overall objective was to to characterize the metabolic impact of FOXC2 overexpression in adipose tissue and to determine whether the "converted" FOXC2 tg WAT is functioning as wt BAT.

2.4. *Specific Objectives*

1) To characterize O_2 consumption rates and the respiratory exchange ratios of FOXC2 tg *vs.* wt mice under various conditions. Conditions included variable environmental temperatures (24°C, 4°C, 30°C), and acute treatments with the β_3AR agonist, CL-316,243.

2) To determine the basal and FCCP-stimulated O_2 consumption of adipocytes isolated from FOXC2 tg "converted" intra-abdominal WAT in comparison to those isolated from wt BAT and WAT.

3) To compare cellular and mitochondrial ultra-structure in fat depots of FOXC2 tg and wt mice using standard light microscopy, immunohistochemistry and transmission electron microscopy (TEM).

4) To assess cellular O_2 consumption in differentiated MEFs from FOXC2 tg and wt mice using an Extracellular Flux Analyzer (XF-24; Seahorse Biosciences, North Billerica, MA).

5) To measure oxidative stress in differentiated MEFs from FOXC2 tg and wt mice by immunoblot detection of proteins modified by the lipid peroxidation product, 4-hydroxynonenal (4-HNE).

3. Methods and Design

3.1. *FOXC2 tg and wt Mice*

Male and female FOXC2 tg mice and littermate wild type (wt) C57BL/6 mice were originally provided by Dr. Sven Enerback, University of Götberg, Götberg, Sweden. They were housed at 23°C with light from 07:00 to 19:00. Initially, two groups of 20 mice were provided; half of each group were FOXC2 tg mice, and the other half were littermate wt controls. Mice from both sets were 3-4 months old upon arrival at the University of Ottawa. These mice were used for the investigations of food intake and whole body energy expenditure. A subsequent shipment of breeding pairs allowed us to establish a breeding colony of mice for all remaining experiments. Mice were fed the Teklad Global 18% Protein Rodent diet (2018S). Briefly this diet contains 18.8% crude protein, 5.7% fat, and 57.26% carbohydrate. It also contains 3.4 Kcal/g digestible energy and 3.3 Kcal/g metabolizable energy.

3.2. *Body Weight and Food Intake Measurements*

Measurements of food intake were conducted on mice between 3 and 4 months of age twice a week for three weeks at 11:00am. Body weights were recorded at the same time. Since the mice were not gaining or losing weight at the time of the study, metabolic efficiency (g gained/kCal ingested) data were not obtained. Instead, dietary energy intake (kCal/day) and body weight results were compared between FOXC2 tg and wt mice from the two sets. Dietary energy intake was calculated from the metabolizable energy content of the diet.

3.3. *Whole Body Energy Metabolism Analyses using Indirect Calorimetry*

Whole body O_2 consumption (VO_2) as well as the respiratory exchange ratio (RER) (carbohydrate vs. fatty acid oxidation) were measured over 24 hour periods using an open-circuit indirect calorimeter (customized Oxymax system; Columbus Instruments, Columbus, OH). The fuel energy oxidized is expressed in units of oxygen used and carbon dioxide released. The following equations are used to calculate VO_2, VCO_2, and RER:

a) $VO_2=ViO_2i-VoO_2o$

b) $VCO_2=VoCO_2o-ViCO_2i$

c) $RER=VCO_2/VO_2$

Vi=mass of air at chamber input per unit time

Vo=mass of air at chamber output per unit time

O_2i= O_2 fraction in Vi

CO_2i=CO_2 fraction in Vi

O_2o=O_2 fraction in Vo

CO_2o= CO_2 fraction in Vo

This instrument has automated temperature and light controls. It is a four-chamber system to allow four mice to be studied at the same time. To assess thermoregulatory characteristics of the FOXC2 tg and wt mice, measurements were conducted at three different environmental temperatures: 24°C, 4°C, and 30°C, and at 24°C after acute injections of the β_3-adrenergic agonist, CL-316,243 (1mg/g body weight; gift from Dr. J. Himms-Hagen). At thermoneutrality (30°C for mice) no energy is expended to maintain a normal body temperature, and thus determinations at this

temperature allow assessments of basal metabolic rate. In a cold environment (4°C), the main acute response is shivering thermogenesis. The β_3-adrenergic agonist, CL-316,243, allows assessments of non-shivering thermogenesis where energy is simply dissipated as heat due to uncoupling through UCP1. O_2 consumption determinations following an acute dose of the β_3-adrenergic agonist were conducted for only 3-4 hours, as the effect of the agonist diminishes greatly after 1.5 – 2 hours.

O_2 consumption and RER data were plotted and analyzed as percent relative cumulative frequency (PCRF) histograms as described in Riachi *et al* (2004) and Lui *et al* (2005). The PCRF approach was developed to analyze large sets of data gathered (*e.g.,* over a period of 24 hours) (Riachi *et al*, 2004). Using this approach, the raw data are collected and put in ascending order; subsequently the cumulative frequencies calculated. These latter are then plotted in the form of percentile curves. Group means were then determined at every tenth percentile and plotted (+/-SEM).

3.4. *Haematoxylin & Eosin (H&E) Staining of FOXC2 tg and wt Adipose Tissue Sections*

IBAT, inguinal WAT as an indicator of subcutaneous adipose tissue (SAT), and gonadal WAT as an indicator of visceral adipose tissue (VAT) from both FOXC2 tg and wt mice were fixed overnight in buffered formalin at room temperature. They were subsequently dehydrated, embedded in paraffin, and sectioned (6 microns) onto glass microscopy slides. The sections were then de-paraffined and dehydrated using xylene, then 50% xylene/ethanol, and finally 100% ethanol. The sections were then hydrated using a series of ddH_2O:ethanol mixtures with an increasing ratio of ddH_2O:ethanol until

there was an equal ratio of ddH_2O and ethanol. Sections were then stained with haematoxylin for 15 minutes at room temperature and run under tap H_20 at 35-37°C for 1 minute. Sections were then dipped in HCL ethanol in order to differentiate the stain. Sections were then stained with 54.5g/L eosin (Fisher) for 3 minutes at room temperature. Sections were then dehydrated with ethanol. Finally, they were then exposed to xylene for 5 minutes and mounted on sides using Permount (Biomedia). The magnification used to capture the images was 40x.

3.5. *Transmission Electron Microscopy (TEM) of FOXC2 tg and wt Adipose Tissue Sections*

Mice were anaesthetized using isofluorane gas. An 18-gauge needle attached to a saline-filled 30 ml syringe was then inserted into the left ventricle of the heart, and the right atrium was subsequently perforated with a scalpel; the saline was infused in order to flush out systemic blood. The mice were then perfused with a primary fixative solution: 1.6% gluteraldehyde/0.1M Na cacodylate (pH 7.2). IBAT, VAT, and SAT depots were removed, weighed, and cut into chunks with a thickness of approximately 1mm using a razorblade on dental wax. Pieces were then placed in 3ml of primary fixative solution for 24 hours at 4°C. Tissue samples were then postfixed in 1% osmium tetroxide (Marivac) in 0.1M Na cacodylate buffer and subsequently "en bloc" stained in saturated aqueous uranyl acetate (Marivac). The samples were then dehydrated in ascending grades of ethanol and embedded in Spurr epoxy resin (Marivac). Thin sections (50-90nm) were counterstained with Reynold's lead citrate (Marivac). Sections were then viewed in a Jeol 1230 TEM equipped with AMT software, allowing for analyses of tissue, cellular

and mitochondrial ultrastructures. The magnification used for the images was 1200x and 5000x.

3.6. *Immunohistochemical Analysis of UCP1 Content in Adipose Tissues*

At 4 months of age male mice were sacrificed and their adipose tissues were removed and embedded in buffered formalin (Fisher). Tissues were subsequently embedded in paraffin wax. 6μm sections of IBAT, VAT, and SAT were treated in 0.3% H_2O_2 in methanol for 5 minutes at room temperature to remove endogenous peroxidases. The tissue was then washed with phosphate buffered saline (PBS) and then exposed to normal goat serum (Vector Labs) and 4 drops per ml of Avidin D (Vector Labs) for 20 minutes at room temperature. Primary antibody (anti-mouse UCP1, Sigma) at a 1:1000 dilution in PBS was then added with 4 drops per ml of biotin solution (Vector Labs) and incubated overnight at 4°C. Tissue was then washed with PBS for 15 minutes. After this the sections were exposed to the biotinylated secondary anti-rabbit antibody (Vector Labs). Sections were then washed with PBS and exposed to an avidin-biotin complex (ABC complex; Vector Labs). Thereafter, sections were washed again with PBS and treated for 5 minutes with 3,3'-diaminobenzidine (DAB; Vector Labs) at room temperature in the dark. A haematoxylin counterstain was applied for 15-30 minutes at room temperature, followed by two dehydration steps: 80% ethanol for 1 min and 100 % ethanol for 1min. The ethanol was then cleared with xylene for 5 min at room temperature and sections were mounted on coverslips using Permount (Biomedia). The magnification used for the collection of images was 40x.

3.7. *O_2 Consumption Analysis of Primary Adipocytes from FOXC2 tg and wt Mice*

WAT (SAT and VAT) and IBAT were isolated from FOXC2 tg and wt mice and placed in Krebs-Ringer HEPES buffer (KRHB): 120mM NaCl, 10mM Na_2HPO4, 6mM KCl, 1.2mM $MgSO_4$, 10mM glucose, 5mM fructose, and 20 mM HEPES, 1% bovine serum albumin (BSA; 98%) pH 7.4, warmed to 37°C. Using a safety razor blade, the tissues were minced such that pieces were approximately 1 mm in diameter. Pieces were then transferred to a 50ml polypropylene tube (Falcon) containing 40ml of KRHB on ice. Type 2 collagenase (1mg/ml; Worthington) was then added and the capped tube was then inverted twice and placed in a gently shaking water bath (37°C) for 45 min. The adipocytes were then filtered through a 250μm nylon mesh and transferred to a new 50ml polypropylene tube and spun for 1 minute at 100 rpm to float the adipocytes. The infranatant was then removed and the cells are washed twice using KRHB 4% BSA (wash buffer). During the tissue digestion period, 96-well BD Biosensor plates (Becton and Dickinson) were prepared by adding Dulbecco's Modified Eagle Medium (DMEM; Gibco) with normal glucose (5 mM), and supplemented with 10% fetal bovine serum (Invitrogen), 100 units/ml penicillin G, and 100μg/ml streptomycin (hereafter referred to as 'Standard Medium'), inhibitors and uncouplers (as specified below). The BD plates contain the O_2 sensitive fluorophore: ruthenium (II)-tris(4,7-diphenyl-1,10-phenanthroline (Ru (DPP)3), embedded in a polydimethyl-siloxane matrix at the bottom of each well. This ruthenium-based dye is incorporated into the silicone rubber matrix and is impermeable to liquid but freely permeable to O_2. The fluorescence of this dye is quenched by the presence of O_2. 75μL of packed cells was added to each well of each BD Biosensor plate to a final volume of 150ml/well. We tested the effects of the electron

transport chain inhibitor antimycin A (50nM) and of the mitochondrial uncoupler FCCP (1μM). The plates were then sealed with ClearSeal Film (Hampton Research). Cellular O_2 consumption was detected as changes in fluorescence intensity (excitation and emission wavelengths of 485 and 580nm, respectively) in a temperature-controlled fluorimeter (FLx800, Biotek). Measurements were made over 24 hours, with readings taken every 15 minutes.

The data were collected as units of fluorescence. They were normalized to a zero value collected from wells that contained only media (*i.e.,* no cells). This was called the normalized relative fluorescence (NRF). O_2 concentration $[O_2]$ was then determined by first determining the dynamic range (DR). DR was determined using the positive control sodium sulfite, an O_2 scavenger agent. The average of the highest NRF of the positive control divided by that of the zero NRF of the positive control determines DR. k_{sv}, the Stern-Volmer constant was then calculated using the equation;

d) $k_{sv} = (DR-1)/0.209$

O_2 concentration can then be calculated using the equation;

e) $[O_2] = (DR/NRF-1)/k_{sv}$

Since the data were collected over 24 hours every 15 minutes in triplicate, the data at each time point were averaged and a curve was created. The slope of the linear part of the curve was then calculated giving the rate of O_2 consumption in nmol of O_2/hour. The average of 3 experiments was then taken for a basal as well as FCCP stimulated value for O_2 consumption of FOXC2 tg and wt IBAT, SAT and VAT.

3.8. *Culture and Adipocyte Differentiation of Mouse Embryonic Fibroblasts (MEFs)*

Mouse embryonic fibroblasts (MEFs) from wt and FOXC2 tg mice were provided by Dr. Sven Enerbäck, University of Götberg, Götberg, Sweden. MEFs were maintained in a sterile incubation chamber (37°C; 5% CO_2) in Standard Medium. Cells were maintained on gelatin-coated plates. At two days post-confluence, MEFs were differentiated into adipocytes for 5 days. The medium used to induce differentiation consisted of the Standard Medium described above, supplemented with 1μM dexamethasone, 0.5mM isobutyl-methyl-xanthine (IBMX), 10μg/ml insulin, 1μM rosiglitazone, and 20ng/ml fibroblast growth factor (FGF). After 5 days, the medium was then changed to the Standard Medium supplemented with 10μg/ml insulin, 1μM rosiglitazone, and 20ng/ml FGF. After 5 more days the media was changed back to Standard Medium. However, after 5 days of differentiation cells tended to lose adherence; therefore, O_2 consumption experiments were typically performed after 5 days of differentiation. Cells were washed with PBS and the medium was changed every 48-72 hours.

3.9. *O_2 Consumption Analysis of FOXC2 tg and wt Differentiated MEFs*

O_2 consumption of FOXC2 tg and wt differentiated MEFs was measured with an Extracellular Flux Analyzer (XF24, Seahorse Bioscience, North Billerica, MA). The novel fluorimetric technologies incorporated into this equipment allow an extremely sensitive measurement of O_2 consumption by adhered cells. The XF-24 instrument measures oxygen partial pressure and rates of O_2 consumption (OCR) are obtained by measuring the first 30 mmHg drop in O_2 per unit time. The instrument also measures the

change in extracellular proton concentration, and extracellular acidification rate (ECAR) is measured as the rate of change of pH over the duration of the measurement period (usually 2 min). For the measurements, cells were grown in the Seahorse 24-well plates. To do so, undifferentiated MEFs were washed with PBS, trypsinized with trypsin-EDTA (TE, Invitrogen), and lifted from the culture plates. MEFs were then pelleted in a 15 ml polypropylene tube (Falcon) by centrifugation at 300xg for 10 minutes. They were then resuspended in 1ml of Standard Medium. A 16µl aliquot of the cell suspension was then diluted 1:4 by Trypan blue (0.4%; Gibco), and a 10µl aliquot of this was placed in a haemocytometer (Neubauer). The viable and non-viable cells were counted in the four quadrants of the haemocytometer using a Zeiss Axioskop inverted microscope. An average of the counts in the four quadrants was determined and the following calculation applied:

[cell suspension] = Average # cells counted * $10^4(mL^{-1})$ * 1.25 (dilution factor)

The volume of the cell suspension to be added to the XF24 plates (also coated with gelatin) was then calculated for the desired concentration of 20 000 cells/well.

Volume of cell suspension (mL) = concentration of cell suspension/desired cell number

The cells were then plated in the Seahorse 24-well microplates at 20 000 cells/well. A 2-step plating procedure was used, as advised by the manufacturer. First 100 ml of the cell suspension was plated in the wells and placed at 37°C for 1 hour. Subsequently, another 150ul of media was placed in the wells. At two days post-confluence, MEFs were differentiated into adipocytes for 5 days. An hour before the plates were analyzed, the media was changed to an unbuffered DMEM (Gibco)

supplemented with 2mM Glutamax-1 (Gibco), 100μM sodium pyruvate, 30mM NaCl, and 5mM glucose. The cells were incubated at 37°C for one hour prior to analyses; during this time, the Seahorse XF24 Analyzer was calibrated; this pre-incubation period also allows cells to equilibrate in the above medium. For analyses, the cover of each culture plate was replaced by a sensor cartridge and the plate was then loaded into the Seahorse XF24 Analyzer. An analytical cycle consisted of mixing for 3 minutes, waiting for 3 minutes and then measuring cellular O_2 consumption and acidification rates for 2 min. This occurred 3 times to get basal rates of O_2 consumption and acidification before additional substrate, and either 1μM FCCP (uncoupler), or 50nm antimycin A (inhibitor) were added for the final 3 readings. Data were normalized to cellular protein concentration using the bicinchoninic acid (BCA) assay (Sigma).

3.10. *Analysis of Oxidative Stress in FOXC2 tg and wt Differentiated MEFs*

Oxidative stress was assessed in differentiated MEFs, derived from FOXC2 tg and wt mice, by immunoblot detection of proteins modified by the lipid peroxidation product 4-hydroxynonenal (4-HNE). A polyclonal rabbit primary antibody (1:1000; Calbiochem) that specifically recognizes stable fluorophores resulting from lysine-4-HNE crosslinks (Tsai *et al*, 1998) was used. Immunoblot visualization was by HRP-conjugated goat-anti-rabbit (1:1000; Santa Cruz) and ECL detection (GE HealthCare). Densitometry (Image J) was performed on the four most prominent bands, and the sum of these values was expressed as a fraction of densitometry values of nearby bands on the Coomassie-stained gel.

3.11. *Source of Chemicals*

Unless otherwise stated, all chemicals were obtained from Sigma-Aldrich.

3.12. *Statistical Analysis of Data*

Statistical differences of body weight, food intake, VO_2 and RER between FOXC2 tg and wt mice were compared using a Student T-test.

Measurements of OCR and ECAR rates were combined and an average +/-SEM was obtained under basal conditions as well as after the addition of FCCP. Analysis of the differences was done using a two-way ANOVA followed by a Bonferroni *post hoc* test.

Analysis of the differences between the rates of O_2 consumption from the isolated adipocytes involved a two-way ANOVA followed by a Bonferroni *post hoc* test.

All statistical analyses were performed using Graphpad Prism 4 software (La Jolla, CA)

4. Results

4.1. *No Difference in Body Weight Between FOXC2 tg and wt Mice*

FOXC2 tg and wt mice body weight results are presented in Figure 4. There are no differences in body weight between wt and FOXC2 tg mice. Two sets of mice were studied (set 1: received summer 2004, and set 2: received summer 2005) and the data from both sets of mice are presented to show the consistency in results (Figure 4A and B for sets 1 and 2, respectively).

Furthermore, there were no differences in liver weights between the two genotypes. Tissue weights were also obtained for IBAT, inguinal adipose tissue (as an indicator of SAT), and gonadal adipose tissue (as an indicator of VAT). Although there were no differences in IBAT weights, the SAT ($p=0.0288$) and VAT ($p<0.0001$) weights were significantly reduced in FOXC2 tg when compared with wt mice. These results are presented in Table 1.

Table 1. Comparisons of body, liver and adipose depot weights between FOXC2 transgenic and wildtype littermate control mice (non-paired t-test). Mean +/- SEM, n=27

	FOXC2 TRANSGENIC	WILDTYPE	SIGNIFICANCE
BODY WEIGHT (g)	29.7+/-0.8	29.2+/-0.9	N/S
LIVER (g)	1.16+/-0.03	1.22+/-0.04	N/S
IBAT (g)	0.234+/-0.025	0.203+/-0.022	N/S
SAT (g)	0.390+/-0.044	0.567+/-0.065	p=0.029*
VAT (g)	0.266+/-0.034	0.801+/-0.092	p<0.0001***

Figure 4. Mean body weights (+/-SEM) of two sets of FOXC2 tg and wt littermates mice. Results are presented for the two sets of mice initially received (see text for details). There were no significant differences between means in either set 1 (A) or set 2 (B) between FOXC2 tg and wt mice (non-paired t-test). Mice were approximately 3-4 months of age. Set 1: wt; n=11, FOXC2 tg; n=9, Set 2: wt; n=9, FOXC2 tg; n=9.

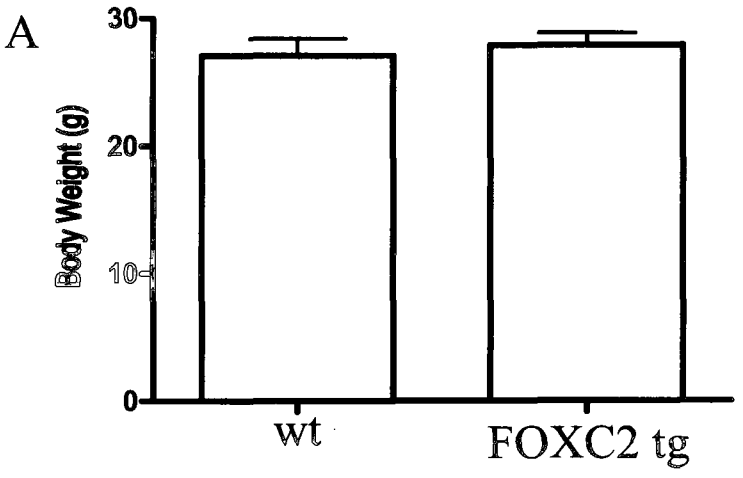
A
Body Weight (g)
30
20
10
0
wt
FOXC2 tg

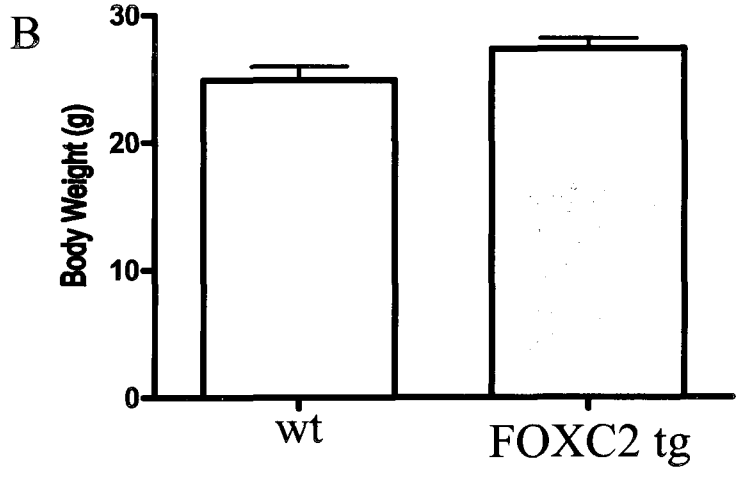
B
Body Weight (g)
30
20
10
0
wt
FOXC2 tg

4.2. *FOXC2 tg Mice are Hyperphagic Compared to wt Mice*

Daily food intake data were also collected for the 2 sets of mice. In both sets of mice, FOXC2 tg mice had a significantly greater daily food intake than wt mice. These results are presented in Figure 5A and B for sets 1 and 2, respectively. Mice were 3-4 months of age and were full grown at the time of the study making it impossible to do metabolic efficiency (g BWt gained/ Kcal ingested) calculations. Measurements were taken at the same time daily.

Figure 5. Mean food intake (+/- SEM) of two sets FOXC2 tg and wt littermate mice. Results are presented for the two sets of mice initially received. The FOXC2 tg mice had a significantly higher food intake than wt mice in both set 1 (A) and set 2 (B) (non-paired t test). Mice were approximately 3-4 months of age. * $p < 0.05$, ** $p < 0.01$. Set 1: wt; n=11, FOXC2 tg; n=9, Set 2: wt; n=9, FOXC2 tg; n=9.

A

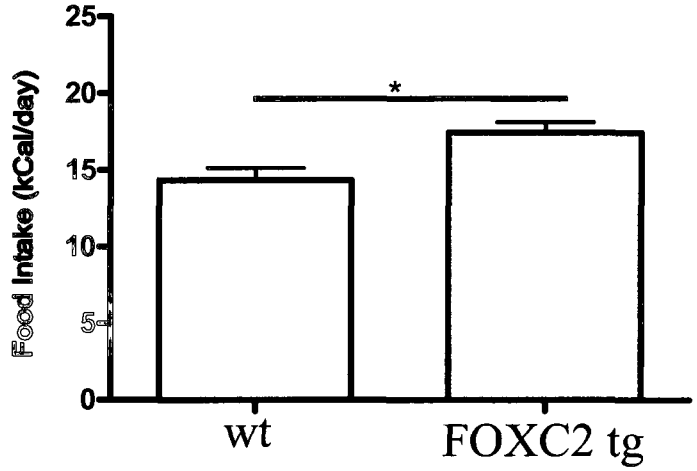
25
20
15
10
5
0
Food Intake (kCal/day)
*
wt
FOXC2 tg

B

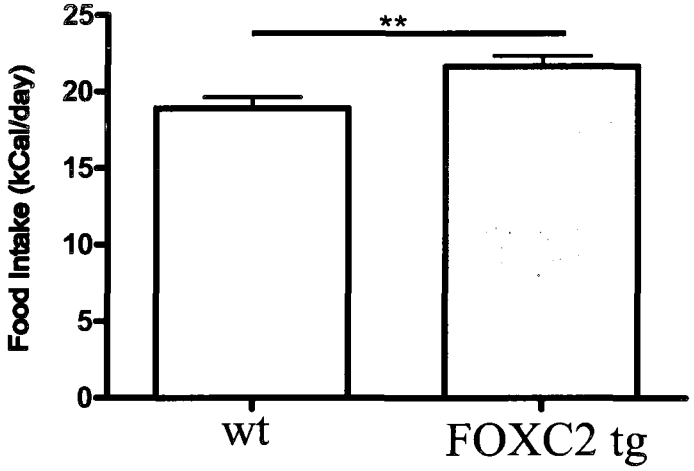
25
20
15
10
5
0
Food Intake (kCal/day)
**
wt
FOXC2 tg

4.3. *In Vivo Metabolic Studies:*

4.3.1. *FOXC2 tg Mice are Hypermetabolic but have a Blunted Response to the Selective β_3 Adrenergic Agonist, CL-316,243*

There were interesting differences in characteristics of whole body O_2 consumption between the two groups of mice. At 24°C, the FOXC2 tg mice showed an increased VO_2 (ml/min/mouse) compared to wt mice (Figure 6). At 24°C after an acute dose of the β_3-adrenergic agonist CL-316,243 (which should induce non-shivering thermogenesis and therefore increase O_2 consumption), the wt mice showed significantly greater O_2 consumption than the transgenic mice (Figure 7).

In wt mice, O_2 consumption was significantly higher after the acute dose of CL-316, 243 when compared with the mice at 24°C in the absence of agonist stimulation (Figure 8A). In contrast, significant agonist-induced increases in O_2 consumption of FOXC2 tg mice were only evident at 10%, 20%, and 30% PRCF points and the degree of stimulation was substantially smaller than in wt mice (Figure 8B). Furthermore, FOXC2 tg mice had an increased O_2 consumption at 30°C (Figure 9). No significant differences were however evident between the two groups at 4°C (Figure 10). These results indicate that while FOXC2 tg mice have a higher O_2 consumption at room temperature and thermoneutrality, they do not respond normally to an acute dose of the β_3AR agonist. This was contrary to expectations since the FOXC2 tg mice appear to have more BAT (or BAT-like cells) and therefore were originally hypothesized to have an even greater response than wt mice (see Discussion).

Figure 6. Percent relative cumulative frequency analyses of O_2 consumption of FOXC2 tg and wt mice at 24°C. Mice were housed at 24°C for 24 hours and whole body O_2 consumption data were collected using an open-circuit indirect calorimeter. Results demonstrate that the FOXC2 tg mice are hypermetabolic when compared to littermate wt mice at room temperature. Mice were approximately 4 months of age. * $p < 0.05$, ** $p < 0.01$. wt; n=11, FOXC2 tg; n=8.

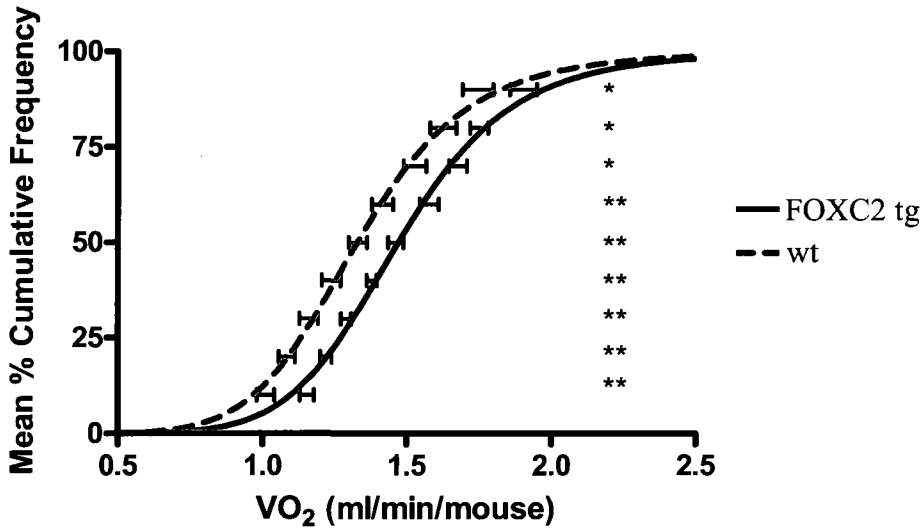
Mean % Cumulative Frequency
100
75
50
25
0
0.5
1.0
1.5
2.0
2.5
VO2 (ml/min/mouse)
*
*
*
**
**
**
**
**
**
FOXC2 tg
wt

Figure 7. Percent relative cumulative frequency analyses of O_2 consumption of FOXC2 tg and wt mice after an acute dose of CL-316,243 (24°C). Mice were housed at 24°C for ~3 hours after an injection of the β_3-adrenergic agonist CL-316,243 and whole body O_2 consumption data were collected using an open-circuit indirect calorimeter. Results indicate that whole body O_2 consumption in wt mice is dramatically greater than in FOXC2 tg mice. Note the absence of a β_3-adrenergic activation of O_2 consumption in the FOXC2 tg mice and the robust activation in the wt mice. Mice were approximately 4 months of age. ** $p < 0.01$, *** $p < 0.0001$. wt; n=11, FOXC2 tg; n=8.

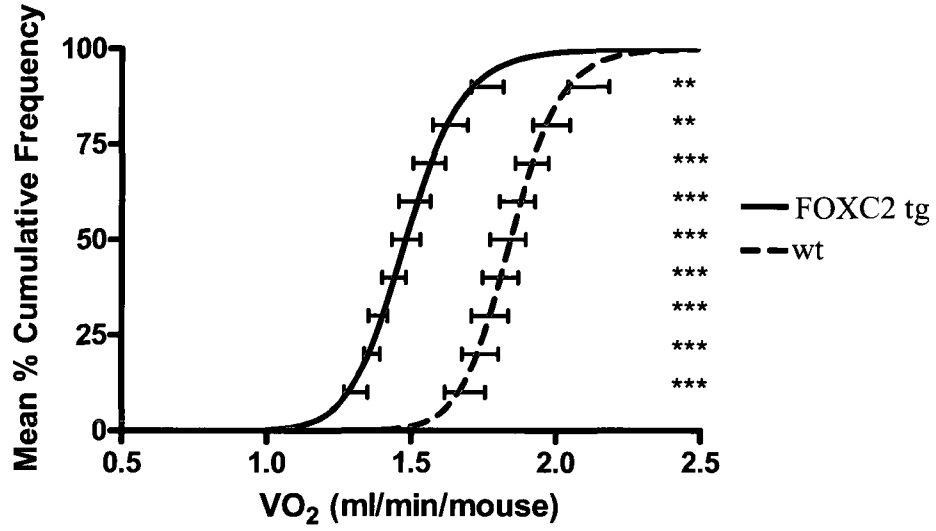
Mean % Cumulative Frequency
100
75
50
25
0
0.5
1.0
1.5
2.0
2.5
VO2 (ml/min/mouse)
**
**
***
***
***
***
***
***
***
FOXC2 tg
wt

Figure 8. Comparison of percent relative cumulative frequency analyses of the O_2 consumption of FOXC2 tg *vs.* wt mice with and without an acute dose of CL-316,243 (24°C). **A.** Percent relative cumulative frequency of O_2 consumption of wt mice housed at 24°C with and without an acute dose of CL-316,243. These results illustrate a robust increase in whole body O_2 consumption that occurs in these mice at 24°C. **B.** Percent relative cumulative frequency of O_2 consumption of FOXC2 tg mice housed at 24°C with and without an acute dose of CL-316,243. These results illustrate the remarkably blunted thermogenic response of the FOXC2 tg mice when compared to the response in wt mice. Mice were approximately 4 months of age. * $p < 0.05$, ** $p < 0.01$, *** $p < 0.0001$. wt; n=11, FOXC2 tg; n=8.

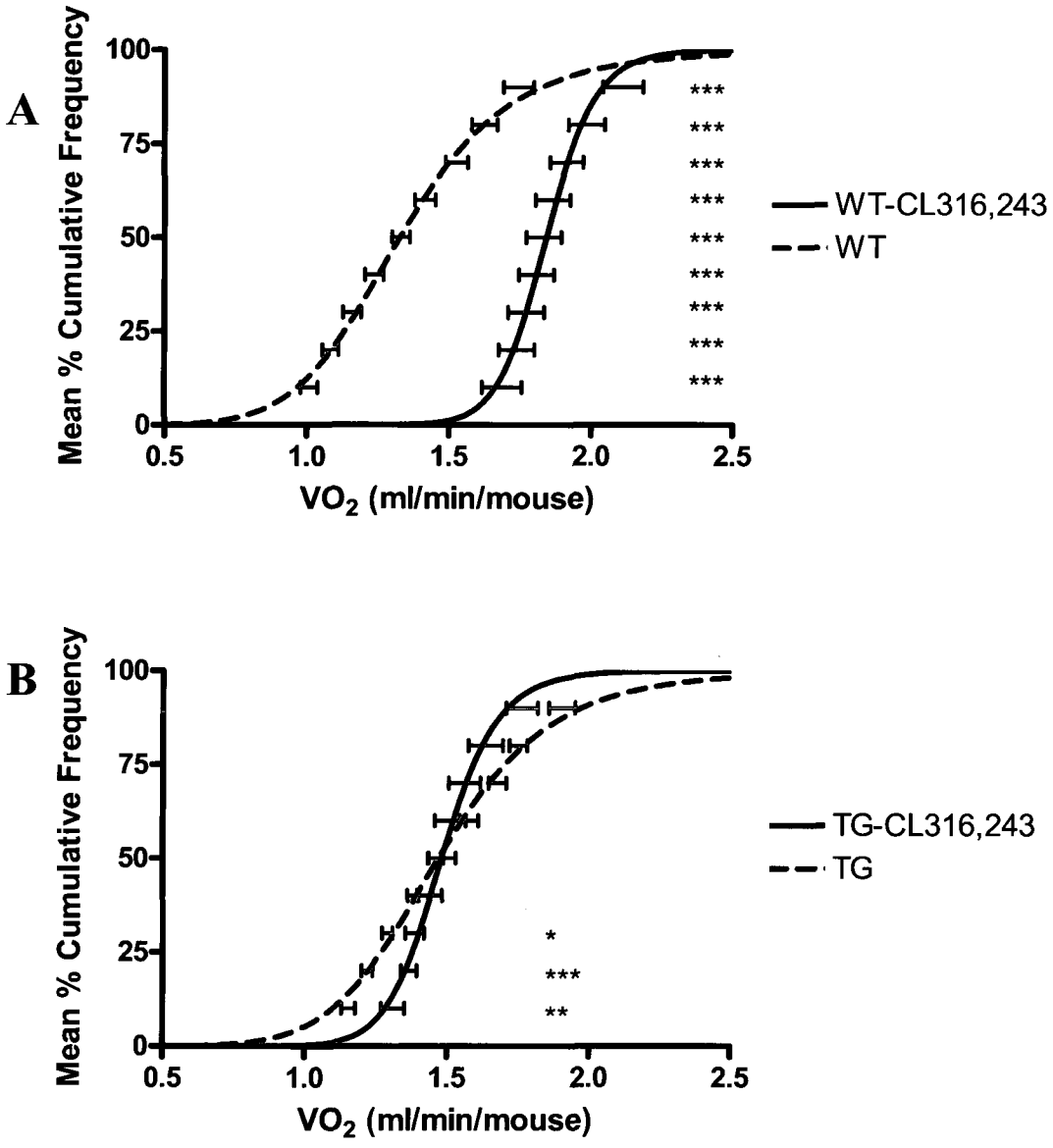
A
Mean % Cumulative Frequency
100
75
50
25
0
0.5
1.0
1.5
2.0
2.5
VO2 (ml/min/mouse)
***
***
***
***
***
***
***
***
***
WT-CL316,243
WT
B
Mean % Cumulative Frequency
100
75
50
25
0
0.5
1.0
1.5
2.0
2.5
VO2 (ml/min/mouse)
*
***
**
TG-CL316,243
TG

Figure 9. Percent relative cumulative frequency analyses of O_2 consumption of FOXC2 tg and wt mice at 30°C. Mice were housed at 30°C for 24 hours and whole body O_2 consumption data were collected using an open-circuit indirect calorimeter. FOXC2 tg mice have significant greater whole body O_2 consumption compared to wt mice. At this thermoneutral temperature, mice do not need to produce heat to maintain a normal body temperature. Mice were approximately 4 months of age. * $p < 0.05$, ** $p < 0.01$. wt; n=11, FOXC2 tg; n=8.

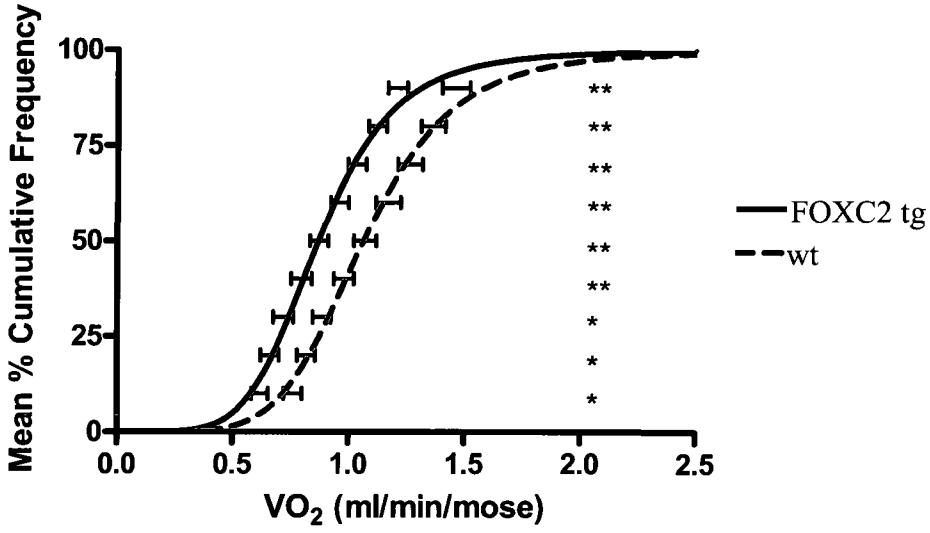
Mean % Cumulative Frequency
100
75
50
25
0
0.0
0.5
1.0
1.5
2.0
2.5
VO2 (ml/min/mose)
**
**
**
**
**
**
*
*
*
FOXC2 tg
wt

Figure 10. Percent relative cumulative frequency analyses of O_2 consumption of FOXC2 tg and wt mice studied at 4°C. Mice were housed at 4°C for 24 hours and whole body O_2 consumption data were collected using an open-circuit indirect calorimeter. Results demonstrate no significant differences between groups, indicating that the FOXC2 tg mice are no longer hypermetabolic when compared to the wt mice at 4°C. The cold environment however causes increased whole body O_2 consumption in both groups of mice (*i.e.,* compared to results at 24°C; Figure 6). Note that the results in Figure 7 describe effects of non-shivering thermogenesis, and the results here describe both shivering and non-shivering thermogenesis. Mice were approximately 4 months of age. wt; n=11, FOXC2 tg; n=8.

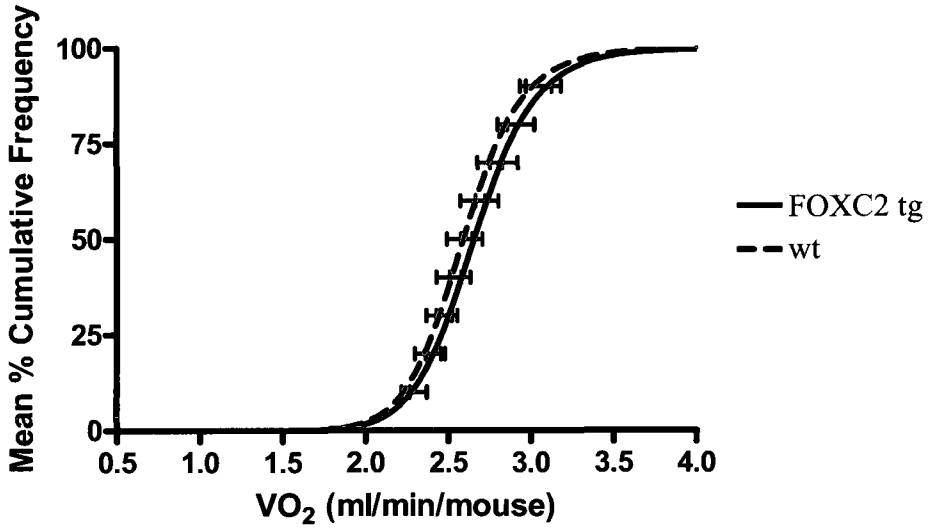
Mean % Cumulative Frequency
100
75
50
25
0
0.5
1.0
1.5
2.0
2.5
3.0
3.5
4.0
VO2 (ml/min/mouse)
FOXC2 tg
wt

4.3.2. *The Activation of Fatty Acid Oxidation by CL-316,243 is Similar in FOXC2 tg and wt Mice*

There were no differences in the RERs between wt and FOXC2 tg mice studied at 24°C (Figure 11). Moreover, there were no differences between genotypes following an acute dose of CL-316,243 (Figures 12). In both the wt and FOXC2 tg mice, RERs were lower following an acute dose of CL-316,243 (Figures 13A and B, respectively). This indicates that both the wt and FOXC2 tg mice had an increased fat oxidation (and a decreased carbohydrate oxidation) following β_3-adrenergic activation. As explained in the Discussion section, the finding that the β_3-adrenergic agonist causes a mitigated/blunted stimulation of whole body O_2 consumption, together with a normal increase in fatty acid oxidation demonstrates that the agonist changes the type of fuel oxidized without markedly inducing thermogenesis in FOXC2 tg mice. Furthermore, there were no differences in RER at 30°C (Figure 14). However, at 4°C, the FOXC2 tg mice had a significantly higher RER at all but three of the decile points, when compared to wt mice (Figure 15). These results indicate increased carbohydrate oxidation (decreased fat oxidation) in the FOXC2 tg mice, when compared to wt nice, at lower temperatures.

Figure 11. Percent relative cumulative frequency analyses of the respiratory exchange ratio (RER) of FOXC2 tg and wt mice at 24°C. Mice were housed at 24°C for 24 hours and RER data were collected using an open-circuit indirect calorimeter. Results indicate no differences in fuel utilization (carbohydrate vs. fatty acid) between the two types of mice. Mice were approximately 4 months of age. wt; n=11, FOXC2 tg; n=8.

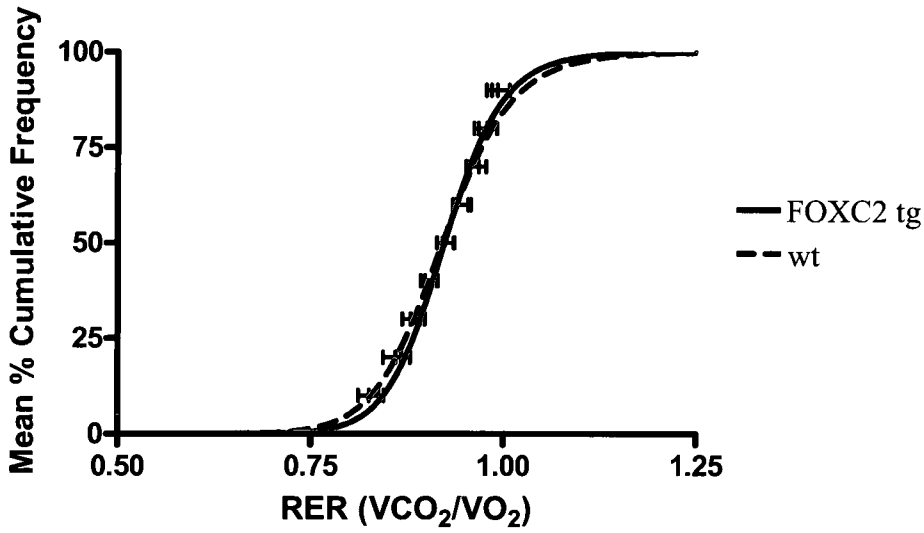
Mean % Cumulative Frequency
100
75
50
25
0
0.50
0.75
1.00
1.25
RER (VCO2/VO2)
FOXC2 tg
wt

Figure 12. Percent relative cumulative frequency analyses of the respiratory exchange ratio (RER) of FOXC2 tg and wt mice after an acute dose of CL-316,243 (24°C). Mice were housed at 24°C for ~3 hours after an injection of the β_3-adrenergic agonist CL-316,243 and RER data were collected using an open-circuit indirect calorimeter. Results indicate that there are no differences in fuel utilization (carbohydrate vs. fatty acid) between the two types of mice in response to the drug. Mice were approximately 4 months of age. wt; n=11, FOXC2 tg; n=8.

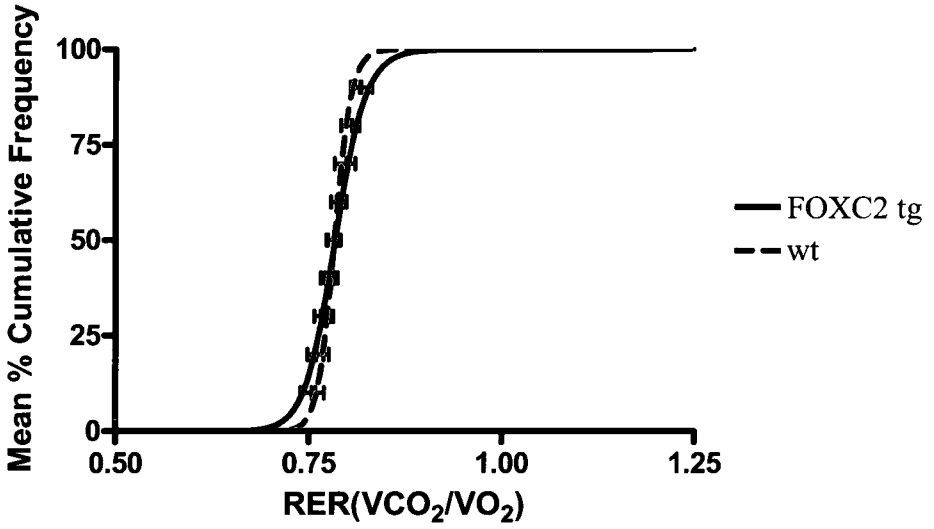
Mean % Cumulative Frequency
100
75
50
25
0
0.50
0.75
1.00
1.25
RER(VCO2/VO2)
FOXC2 tg
wt

Figure 13. Comparison of percent relative cumulative frequency analyses of the respiratory exchange ratio (RER) of FOXC2 tg *vs.* wt mice with and without an acute dose of CL-316,243 (24°C). A. Percent relative cumulative frequency of RER of wt mice housed at 24°C with and without an acute dose of CL-316,243. These results indicate that in addition to an increased O_2 consumption in the wt mice in response to the drug, the mice display a significant decrease in RER, indicative of a shift towards fat oxidation. **B.** Percent relative cumulative frequency of RER of FOXC2 tg mice at 24°C with and without an acute dose of CL-316,243. These results indicate that while there was little increase in O_2 consumption in the FOXC2 tg mice in response to the drug, the mice display the same shift towards fat oxidation as the wt mice. Mice were approximately 4 months of age. *** $p < 0.0001$. wt; n=11, FOXC2 tg; n=8.

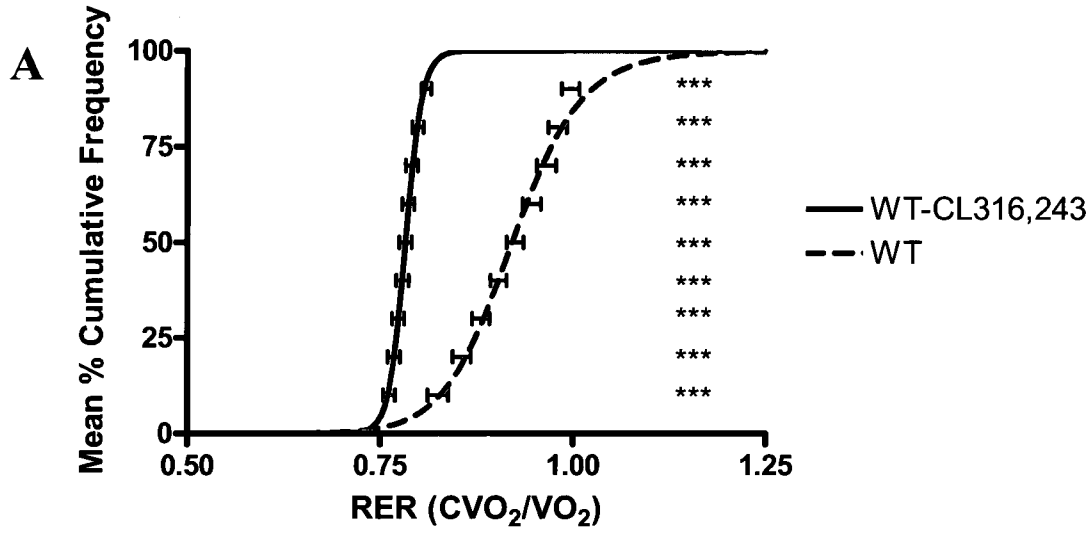
A
Mean % Cumulative Frequency
100
75
50
25
0
0.50
0.75
1.00
1.25
RER (CVO_2/VO_2)
***
WT-CL316,243
WT

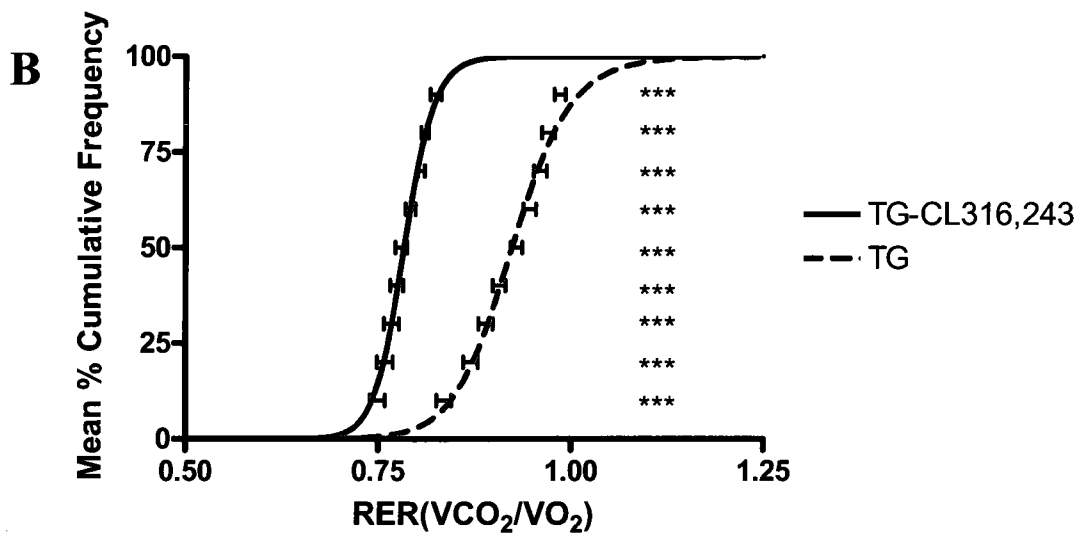
B
Mean % Cumulative Frequency
100
75
50
25
0
0.50
0.75
1.00
1.25
RER(VCO_2/VO_2)
***
TG-CL316,243
TG

Figure 14. Percent relative cumulative frequency analyses of the respiratory exchange ratio (RER) of FOXC2 tg and wt mice at 30°C. Mice were housed at 30°C for 24 hours and RER data were collected using an open-circuit indirect calorimeter. Results indicate no differences in fuel utilization (carbohydrate vs. fatty acid) between the two types of mice at thermoneutrality. Mice were approximately 4 months of age. wt; n=11, FOXC2 tg; n=8.

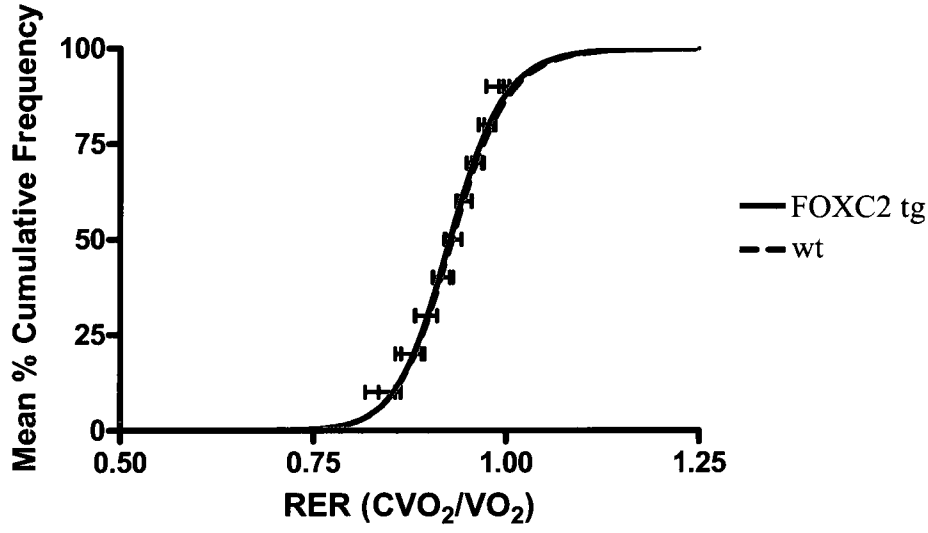
Mean % Cumulative Frequency
100
75
50
25
0
0.50
0.75
1.00
1.25
RER (CVO_2/VO_2)
FOXC2 tg
wt

Figure 15. Percent relative cumulative frequency analyses of the respiratory exchange ratio (RER) of FOXC2 tg and wt mice at 4°C. Mice were housed at 4°C for 24 hours and RER data were collected using an open-circuit indirect calorimeter. Results indicate that when the mice are housed at 4°C, wt mice have increased fatty acid oxidation (decreased carbohydrate oxidation) when compared to FOXC2 tg mice. Statistical significance is reached at 6 of the 9 points analyzed on the curves. Mice were approximately 3-4 months of age. * $p < 0.05$. wt; n=11, FOXC2 tg; n=8.

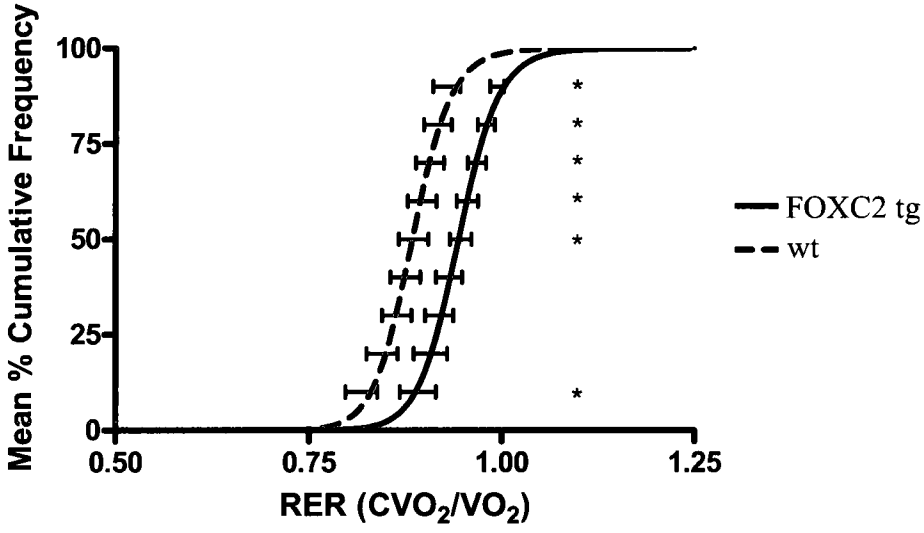
Mean % Cumulative Frequency
100
75
50
25
0
0.50
0.75
1.00
1.25
RER (CVO_2/VO_2)
FOXC2 tg
wt

4.4. *White Adipocytes from FOXC2 tg Mice have Increased Multilocularity*

Histological comparisons were performed on VAT, SAT, and IBAT sections from FOXC2 tg and wt mice. Lipid droplets in VAT from wt mice (Figure 16A) were noticeably larger than those from FOXC2 tg mice (Figure 16B). Furthermore, the size of lipid droplets from SAT of FOXC2 tg mice (Figure 16D) was reduced when compared to SAT from wt mice (Figure 16C); however the difference was not as great as that in VAT. While the lipid droplets from VAT and SAT of FOXC2 tg mice were of similar size, those from wt VAT were larger than that of wt SAT. Overall, the VAT and SAT from FOXC2 tg mice appeared to be more densely packed with an increase in lipid droplet multilocularity, when compared with wt VAT and SAT.

Brown adipocytes are normally densely packed with mitochondria and lipid droplets. Interestingly, the brown adipocytes in the IBAT sections from the FOXC2 tg mice (Figure 16F) were markedly less densely stained than those in sections from the wt mice (Figure 16E). The brown adipocytes in FOXC2 tg IBAT also had larger lipid droplets than those in wt IBAT.

Figure 16. Haematoxylin & Eosin (H&E) staining of adipose tissues from FOXC2 tg and wt mice. H&E staining was performed on sections of adipose tissue from visceral adipose tissue (VAT), subcutaneous adipose tissue (SAT), and interscapular brown adipose tissue (IBAT) of FOXC2 tg and wt mice. Figures A, C, & E depict examples of stained sections from wt VAT, SAT, and IBAT. Figures B, D, & F depicts examples of stained sections from FOXC2 tg VAT, SAT, and IBAT. The size of lipid droplets of VAT and SAT from FOXC2 tg mice appears reduced when compared with wt VAT and SAT and had a phenotype resembling that of IBAT from wt mice. Interestingly, IBAT from wt mice appeared to be more dense (less lipid) than IBAT from FOXC2 tg mice. n=3.

Magnification=40x .

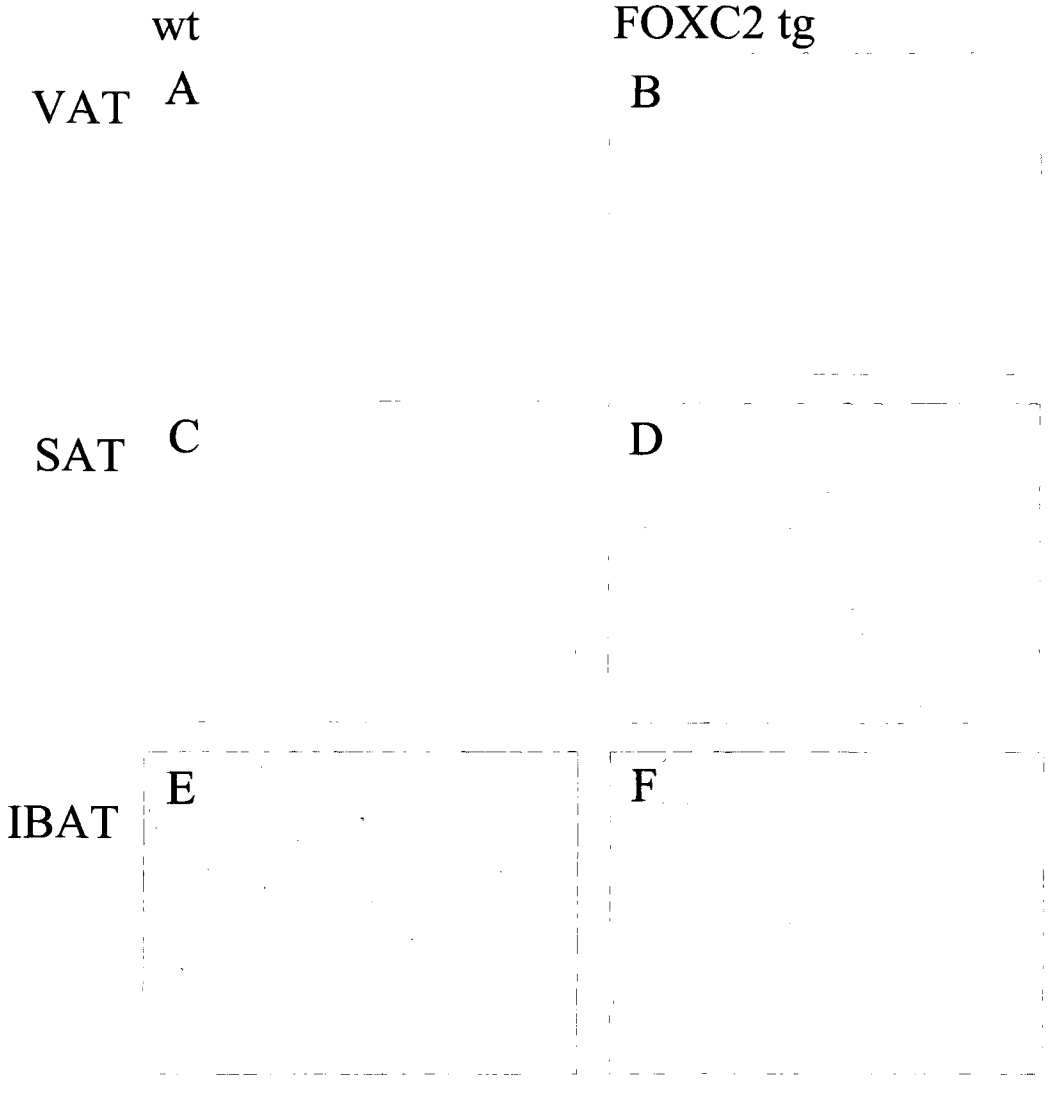
wt
FOXC2 tg
VAT
A
B
SAT
C
D
IBAT
E
F

4.5. *Ultra-Structure Evidence of Mitochondrial Fusion and Multilocularity in WAT of FOXC2 tg Mice*

The ultrastructure of adipose tissues was assessed by TEM (Figure 17). There was a large difference in the ultra-structure of wt VAT (Figure 17A) and SAT (Figure 17C) compared with FOXC2 tg VAT (Figure 17B) and SAT (Figure 17C). TEM images showed that the wt SAT and VAT adipocytes contained one large lipid droplet with all cytoplasmic contents compressed into a small space between the lipid droplet and the cell membrane. These cells had consistently fewer mitochondria containing very few cristae. In contrast, adipocytes in SAT and VAT of FOXC2 tg mice appeared to be multilocular and contained multiple clusters of mitochondria similar to the mitochondria in wt and FOXC2 tg BAT. Clusters of mitochondria in FOXC2 tg VAT were more sparse that those in FOXC2 SAT however, and the VAT adipocytes appeared to contain larger lipid droplets. Furthermore, the mitochondria appeared to be consistently misshapen in FOXC2 tg WAT. They tended to be larger and elongated. Very interestingly, the SAT and VAT from the FOXC2 mice were highly vascularized and examples of red and white blood cells were clearly evident. Examples of capillaries from VAT and SAT from FOXC2 tg mice can be seen in Figure 18 (A & B respectively).

TEM images of brown adipocytes from IBAT of both wt and FOXC2 tg mice (Figure 17E & F respectively) showed multilocularity as well as multiple clusters of mitochondria that were densely packed with cristae. The mitochondria in FOXC2 tg mice appeared to be more densely stained and in general appeared to be packed more closely together than those in wt IBAT. Mitochondria in wt BAT also appeared to be more spherical while FOXC2 tg mitochondria were clearly elongated, which may be

evidence of mitochondrial fusion (see Discussion). BAT is normally highly vascularized, and the micrographs indicated that the IBAT depots from wt and FOXC2 tg mice were well vascularized. The micrographs also clearly showed glycogen pools (G in Figure 17) although the FOXC2 tg BAT appeared to consistently contain greater amounts. Also present in IBAT from both genotypes were clusters of cholesterol crystals (images not shown).

Figure 17. Transmission Electron Microscopy (TEM) of adipose tissues from FOXC2 tg and wt mice. TEM was performed on sections of adipose tissue from VAT, SAT, and IBAT of FOXC2 tg and wt mice. Figures A, C, & E depict examples of micrographs from wt VAT, SAT, and IBAT. Figures B, D, & F depicts examples of micrographs from FOXC2 tg VAT, SAT, and IBAT. There is an apparent increase in mitochondrial content in VAT and SAT in FOXC2 tg when compared with wt VAT and SAT. Furthermore, mitochondria from all FOXC2 tg sections appear to be elongated when compared with wt sections. Note the abundance of glycogen pools (***g***). n=3. (direct mag.=5000x)

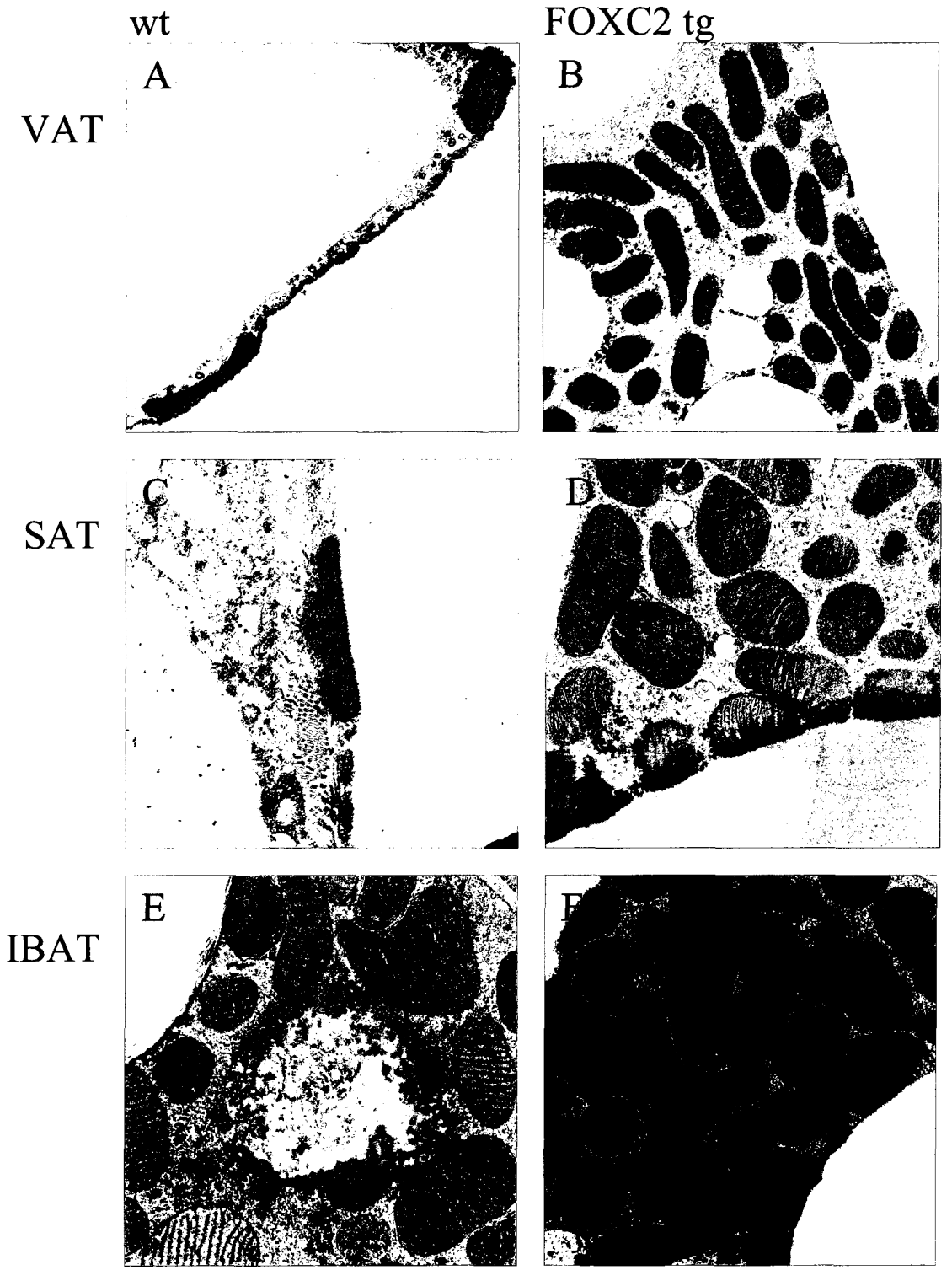
wt
FOXC2 tg
A
B
VAT
C
D
SAT
E
F
IBAT

Figure 18. TEM evidence of increased vascularity in FOXC2 tg visceral and subcutaneous adipose tissues. TEM revealed an abundance of capillaries in VAT and SAT from FOXC2 tg mice when compared with wt mice. **A.** An example of a capillary in FOXC2 tg VAT. **B.** An example of a capillary in FOXC2 tg SAT. This is indicative of an increased thermogenic capacity when compared with wt WAT, which displayed a lower extent of vascularity. Note also the circulating lymphocytes in both micrographs. Red blood cell: ***r***, white blood cell: ***w***.

(direct mag.=1200x)

FOXC2 tg VAT

FOXC2 tg SAT

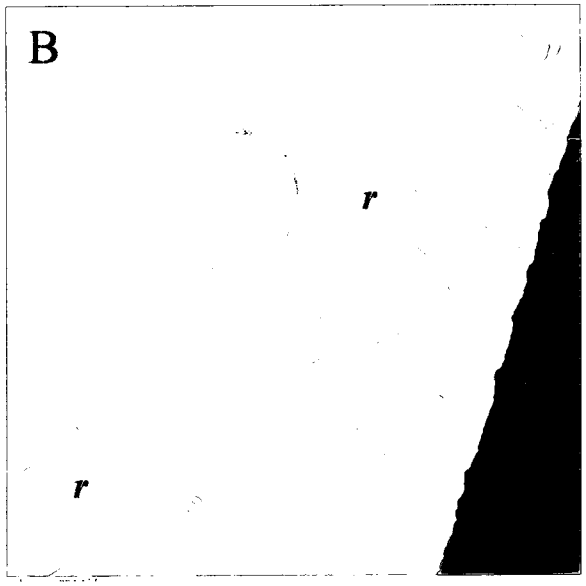

4.6. *Increased UCP-1 Protein Content in WAT of FOXC2 tg Mice*

UCP1 content was analyzed semi-quantitatively through immunohistochemical staining of VAT, SAT, and IBAT tissue sections from FOXC2 tg and wt mice. SAT from wt mice showed no UCP1 staining while SAT from FOXC2 tg mice displayed a considerable amount of UCP1 staining (Figure 19C & D respectively). UCP1 staining in FOXC2 tg VAT was harder to detect (Figure 19B), however it appeared that there was a small increase in UCP1 content in FOXC2 tg VAT when compared with wt VAT (Figure 19A), which had little-to-no staining. Both FOXC2 tg and wt IBAT stained abundantly for UCP1 (Figure 19E & F, respectively). Furthermore, the UCP1 staining in the wt IBAT tended to be clustered (see Discussion) while the staining for the FOXC2 tg IBAT was dispersed throughout the tissue sections.

Figure 19. Immunohistochemistry of UCP1 in adipose tissues from FOXC2 tg and wt mice. Sections of FOXC2 tg and wt IBAT, SAT and VAT were stained for UCP1 content using immunohistochemistry. Figures A, C, & E depict examples of UCP1 staining from wt VAT, SAT, and IBAT. Figures B, D, & F depicts examples of UCP1 staining from FOXC2 tg VAT, SAT, and IBAT. UCP1 stains a brownish colour using this method. Both FOXC2 tg and wt IBAT revealed a large amount of staining while that of wt IBAT was more clustered than that of FOXC2 tg IBAT. However, while FOXC2 tg SAT revealed a considerable amount of UCP1 staining, FOXC2 tg VAT displayed only a minimal amount of UCP1 staining. There appeared to be no UCP1 staining in wt VAT and SAT sections. n=3.

Magnification=40x

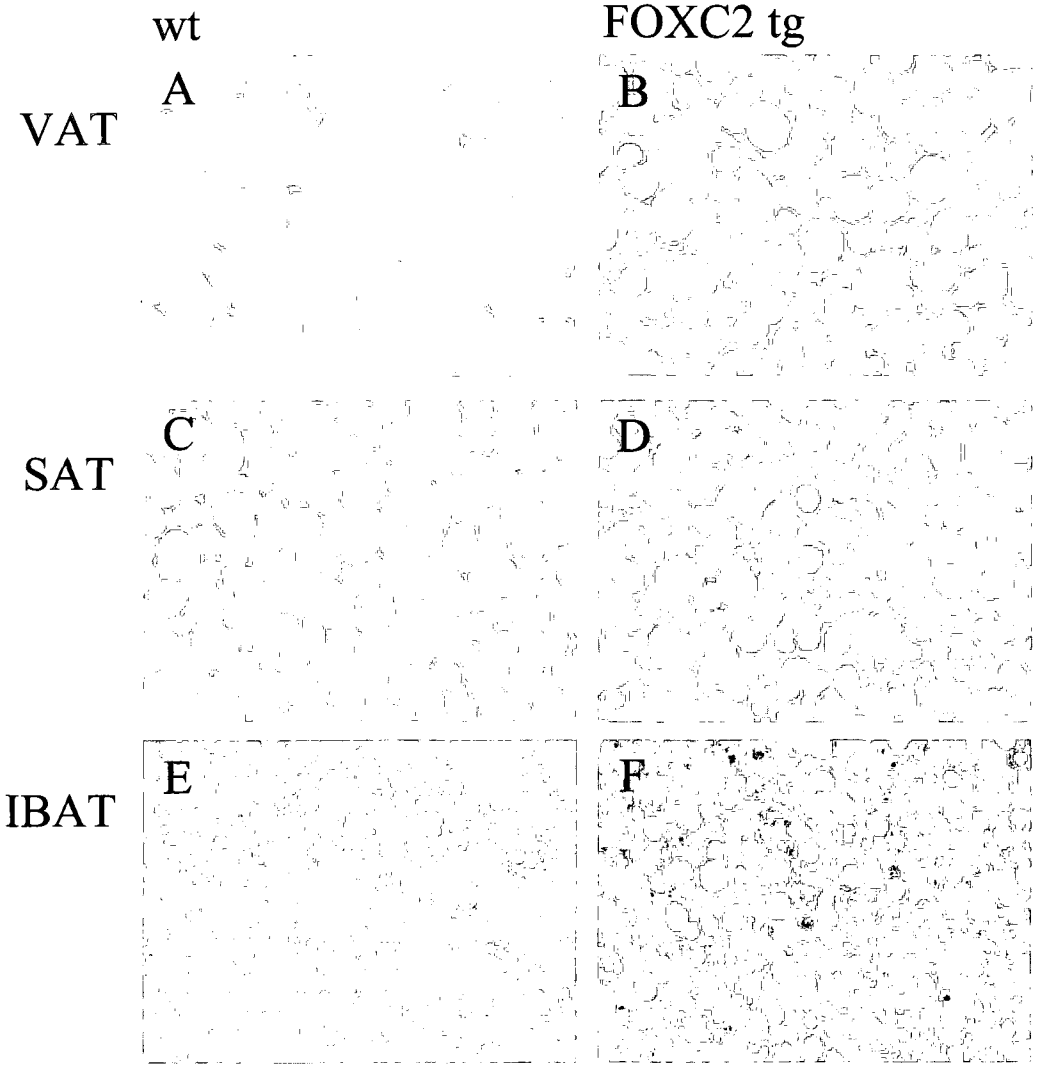
wt
FOXC2 tg
VAT
SAT
IBAT
A
B
C
D
E
F

4.7. *Increased Basal and FCCP-Stimulated O_2 Consumption in FOXC2 tg White Adipocytes*

For determinations of O_2 consumption of the isolated adipocytes, 12-15 mice were needed from each genotype. IBAT was extracted and pooled within each genotype for measurements of brown adipocytes while both inguinal (SAT) and abdominal (VAT) WAT was collected and pooled within each genotype for measurements of white adipocytes. O_2 consumption rates were then measured in aliquots of isolated adipocytes. The basal rate of O_2 consumption of FOXC2 tg white adipocytes was 7x higher ($p<0.05$) than that of white adipocytes from wt mice. Furthermore, while the basal O_2 consumption rate of wt brown adipocytes was 9x higher ($p<0.01$) than that of wt white adipocytes, there was no difference in O_2 consumption rate between wt brown adipocytes and FOXC2 tg white adipocytes (Figure 20A). Upon stimulation with the mitochondrial uncoupler FCCP, the O_2 consumption rate was again 4.5x ($p<0.05$) higher in FOXC2 tg white adipocytes when compared with wt white adipocytes. While the FCCP-stimulated O_2 consumption rate of wt brown adipocytes was 4.3x ($p<0.01$) higher than that of wt white adipocytes, there was no difference between the O_2 consumption rate of wt brown adipocytes and that of FOXC2 tg white adipocytes (Figure 20B). These results indicate that FOXC2 tg white adipocytes have bioenergetic characteristics similar to wt brown adipocytes.

Figure 20. O_2 consumption rates in isolated adipocytes from WAT and BAT of FOXC2 tg and wt mice. A. Basal O_2 consumption in isolated white and brown adipocytes from FOXC2 tg and wt mice. **B.** FCCP-stimulated O_2 consumption in isolated white and brown adipocytes from FOXC2 tg and wt mice. Results indicate that FOXC2 tg white adipocytes have a significantly higher O_2 consumption than wt white adipocytes under basal and FCCP-stimulated conditions. Furthermore, wt brown adipocytes have a significantly higher O_2 consumption than wt white adipocytes while no difference exists between wt brown adipocytes and FOXC2 tg white adipocytes under both basal and FCCP-stimulated conditions. Analysis: Two-way ANOVA, Bonferroni post hoc tests; * $p < 0.05$, ** $p < 0.01$; $n = 3$ all groups.

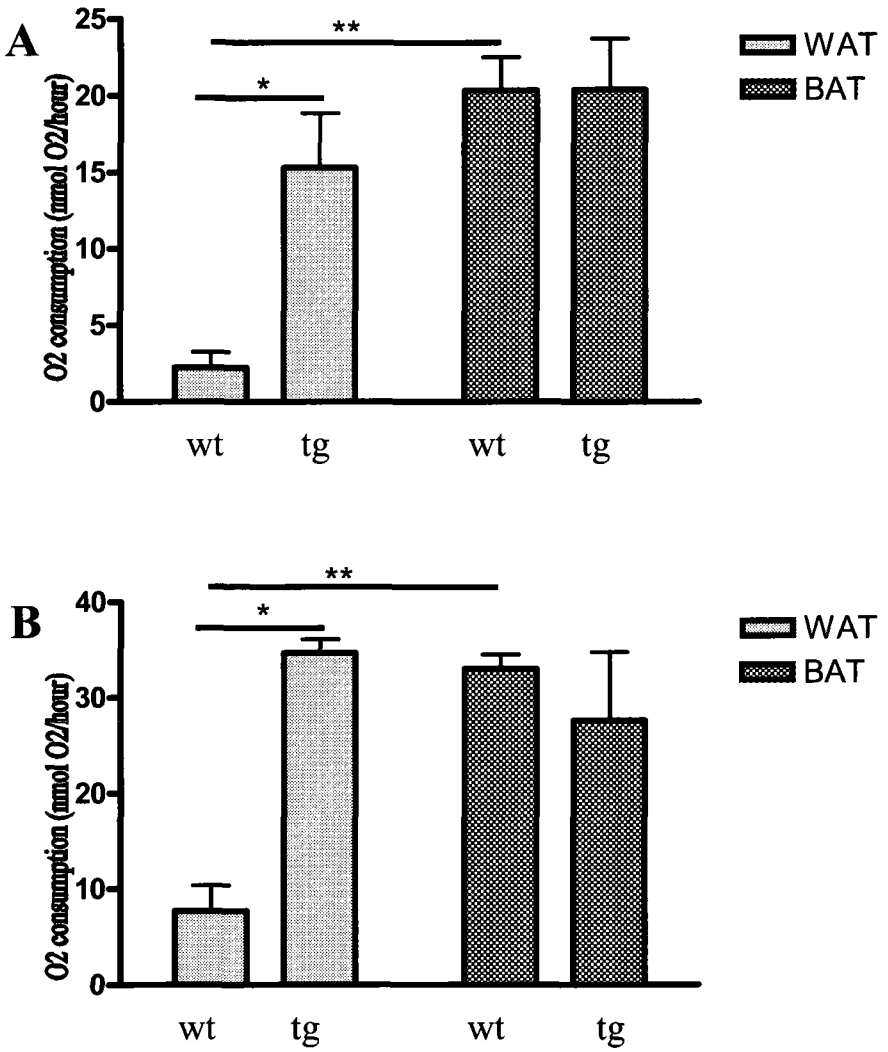
A
25
20
15
10
5
0
O2 consumption (nmol O2/hour)
**
*
WAT
BAT
wt
tg
wt
tg
B
40
30
20
10
0
O2 consumption (nmol O2/hour)
**
*
WAT
BAT
wt
tg
wt
tg

4.8. *Increased Maximal O_2 Consumption in FOXC2 tg Differentiated MEFs*

O_2 consumption rate (OCR) and extracellular acidification rate (ECAR) were measured in differentiated MEFs *in situ*, after 5 days of differentiation, using a highly sensitive Extracellular Flux Analyzer (Seahorse Bioscience XF24; North Billerica, MA), which detects changes in O_2 tension and proton concentration within the cellular microenvironment. ECAR can be taken as a surrogate measure of glycolytic activity provided that glycolysis is the main source of protons. Under basal conditions, there was no difference between the OCR of FOXC2 tg and wt differentiated MEFs. When stimulated with the uncoupler FCCP, both types of differentiated MEFs showed a remarkable increase in OCR ($p<0.0001$). However, the increase seen in the FOXC2 tg MEFs was significantly ($p=0.03$) greater than that seen in the wt MEFs. These results are presented in Figure 21A. Thus differentiated MEFs from FOXC2 tg mice have a greater aerobic capacity than the wt differentiated MEFs. There were no significant differences in ECAR values at both basal and FCCP stimulated states. Thus there were no differences in glycolytic activity at either basal or FCCP stimulated states between FOXC2 tg and wt differentiated MEFs. However, in both FOXC2 tg ($p=0.05$) and wt ($p=0.01$) differentiated MEFS, there was a significant increase in ECAR with stimulation by FCCP indicating that FCCP while causing increased O_2 consumption also causes increased glycolysis (see Discussion). The ECAR data are shown in Figure 21B.

Figure 21. O_2 consumption rates (OCR) and extracellular acidification rates (ECAR) in FOXC2 tg and wt differentiated MEFs. OCR and ECAR were measured on differentiated MEFs *in situ* using a highly sensitive extracellular flux analyzer (Seahorse Bioscience XF24; North Billerica, MA). **A.** There was no difference in OCR under basal conditions. Upon FCCP stimulation, both FOXC2 tg and wt MEFs displayed a large increase in OCR. Furthermore, the FOXC2 tg MEFs displayed an FCCP-stimulated OCR that was significantly greater than that of wt MEFs. **B.** There was no difference in ECAR values (a surrogate measurement for glycolysis) at both basal and FCCP-stimulated states however in both FOXC2 tg and wt MEFs there was a significant increase in ECAR upon stimulation with FCCP. Analysis: Two-way ANOVA, Bonferroni post hoc tests; * $p < 0.05$, ** $p < 0.01$, *** $p < 0.0001$; $n = 4$ all groups

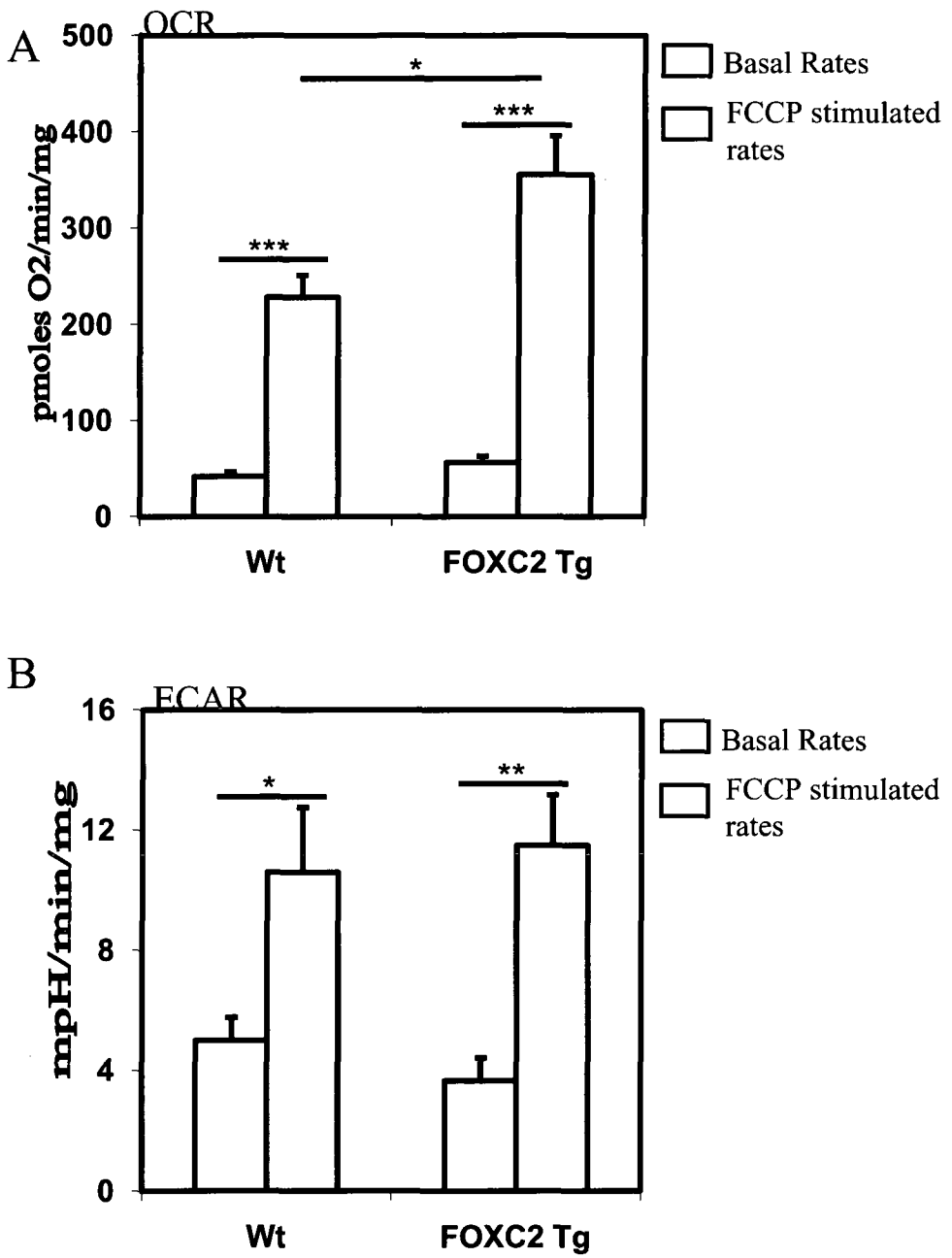
A
OCR
500
400
300
200
100
0
pmoles O2/min/mg
*
***
***
Wt
FOXC2 Tg
Basal Rates
FCCP stimulated rates
B
ECAR
16
12
8
4
0
mpH/min/mg
*
**
Wt
FOXC2 Tg
Basal Rates
FCCP stimulated rates

4.9. *Decreased Oxidative Stress in FOXC2 tg Differentiated MEFs*

Oxidative stress was assessed in differentiated MEFs from wt and FOXC2 tg mice by immunoblot detection of proteins modified by 4-HNE. 4-HNE readily reacts with histidine, cysteine and lysine residues of proteins to form stable Michael adducts (Uchida and Stadtman, 1992). For detection, an antibody that recognizes lysine-4-HNE crosslinks was used. Four prominent bands were detected in wt differentiated MEFs (Figure 22). The intensity of 2 of these bands was clearly reduced in FOXC2 tg differentiated MEFs, suggestive of decreased production of 4-HNE via free radical-initiated lipid peroxidation, or increased free radical scavenging in FOXC2 tg differentiated MEFs. Because there was no obvious reduction in protein amount on the Coomassie-stained gel, it seems unlikely that the lower detection of 4-HNE-modified proteins can be explained by reduced expression of the corresponding proteins.

Figure 22. 4-HNE-modified proteins in FOXC2 tg and wt differentiated MEFs. Shown are the immunoblot probed with an anti-4-HNE antibody (upper image) and the Coomassie-stained gel (lower image). The bar graph depicts densitometry results from the 4 most prominent bands (at and just above 55 kDa, and at 43 and 17 kDa), expressed as a fraction of values of nearby bands on the Coomassie-stained gel. * $P = 0.031$, nonpaired t-test, $n = 3$/genotype.

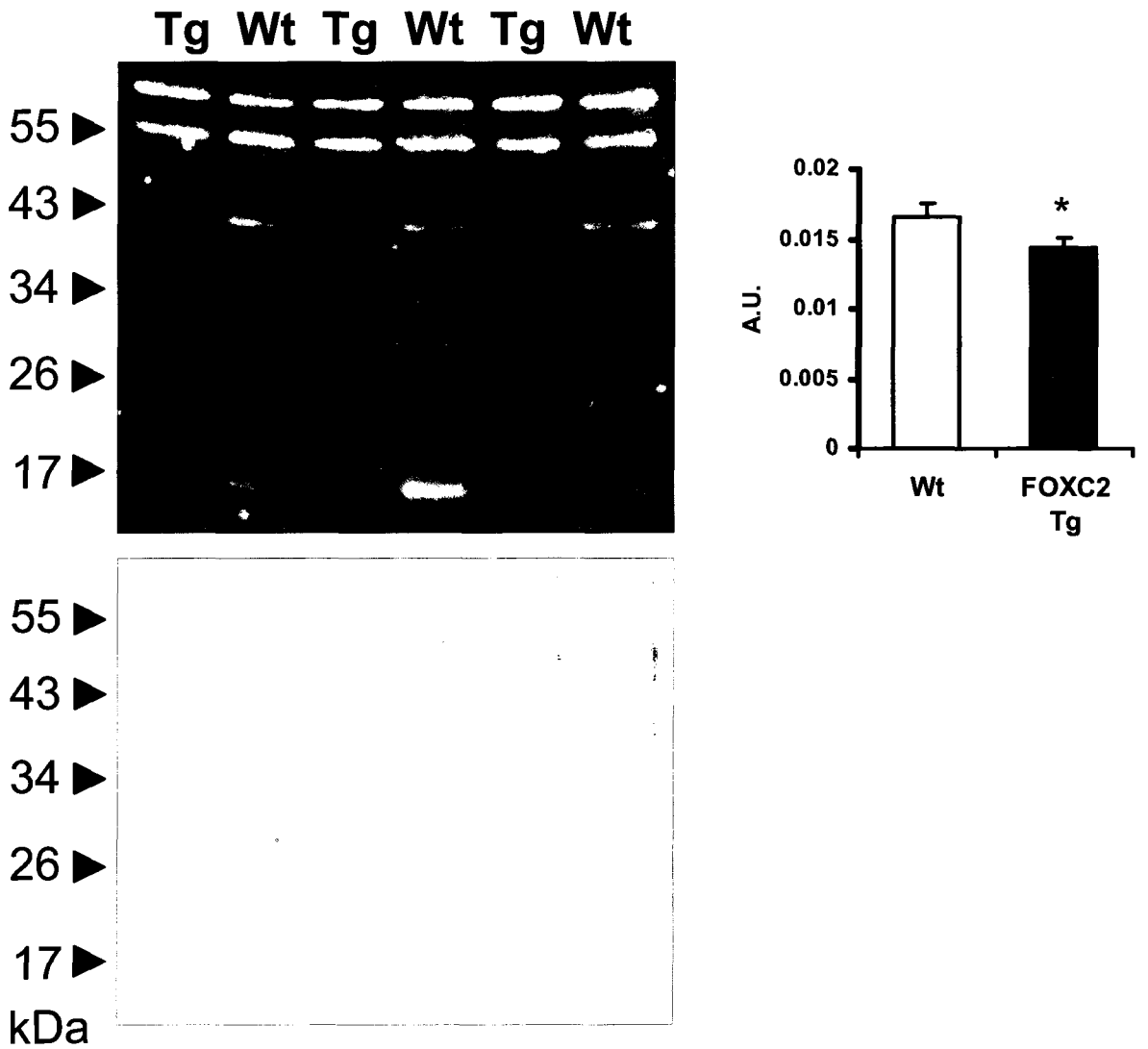
Tg Wt Tg Wt Tg Wt
55
43
34
26
17
55
43
34
26
17
kDa
0.02
0.015
0.01
0.005
0
A.U.
*
Wt
FOXC2
Tg

5. Discussion

Adaptive thermogenesis in BAT has been a major area of interest in obesity research (Nedergaard *et al*, 2007; Wijers *et al*, 2008; van Marken Lichtenbelt *et al*, 2009). Obesity increases the risk of high blood pressure, atherosclerosis, and T2DM as well as the metabolic syndrome and CVD (Gallagher *et al*, 2008). Adaptive thermogenesis is defined as the regulated production of heat in response to environmental temperature or dietary intake (Lowell and Spiegelman, 2000). Cold induced thermogenesis can be further subcategorized into shivering and non-shivering thermogenesis. Although shivering thermogenesis in skeletal muscle is thought to be the main contributor to adaptive thermogenesis in humans (Simonson *et al*, 1992), BAT is the main contributor in small mammals. BAT is highly metabolically active, and the mature brown adipocytes therein contain many mitochondria that exclusively express UCP1. Coupling of the degradation of fuel molecules and ATP synthesis is disrupted by UCP1 and the energy is released in the form of heat. This heat is then carried throughout the body due to an extensive blood supply to the BAT (Cannon and Nedergaard, 2004). Furthermore, recent evidence suggests that a metabolic pathway similar to that of muscle tissue is needed for thermogenesis in BAT (Watanabe *et al*, 2008). This indicates just how metabolically active BAT is compared to WAT. Although once thought to be negligible, there is now clear evidence of active BAT in adult humans (Nedergaard *et al*, 2007; Virtanen *et al*, 2009; Cypess *et al*, 2009; van Marken Lichtenbelt *et al*, 2009). Future research will undoubtedly aim to assess the quantitative importance of BAT in adults, and whether it can be activated for the purpose of obesity treatment in adult humans.

The FOXC2 tg mouse was chosen for these studies because previous studies have shown that the overexpression of the FOXC2 transcription factor in adipose tissue of these mice has overwhelming effects on adipocyte and muscle metabolism (Cederberg *et al*, 2001; Kim *et al*, 2005; Gronning *et al*, 2006). These mice overexpress human FOXC2 specifically in adipocytes using the adipocyte specific aP2 promotor. The WAT of these mice acquires a BAT-like appearance and presumed functionality. Mice that overexpress FOXC2 in adipose tissue are leaner than wt control mice and have increased insulin sensitivity and improved serum lipid profiles. FOXC2 tg mice are more insulin sensitive on standard and high fat diets (Cederberg *et al*, 2001). Furthermore, FOXC2 tg mice are protected from diet-induced accumulation of intramuscular fatty-acyl CoA and hepatic insulin resistance (Kim *et al*, 2005). These results indicate that increases in FOXC2 can aid in obtaining a lean, insulin sensitive phenotype that ultimately would protect against T2DM and the metabolic syndrome. Therefore, based on our interest in processes involved in the conversion of WAT to BAT and the unique characteristics of the FOXC2 tg mouse, we chose it as our model system.

The overall research goal of this M.Sc. thesis was to characterize, using a variety of *in vivo* and *in vitro* approaches, the metabolic impact of the overexpression of FOXC2 in adipose tissue.

5.1. *Effects of FOXC2 Overexpression in Adipocytes upon Characteristics of Whole Body Composition.*

We found no differences in the body weights of FOXC2 tg mice as compared to wt mice (Figure 4). This finding is consistent with that of Cederberg *et al* (2001). In fact, even though there were no differences in body weights between FOXC2 tg and wt mice, FOXC2 tg mice have been shown to consist of 20% less lipids than wt mice (Cederberg *et al*, 2001). However, inconsistent with the findings of Cederberg *et al* (2001), we found that the FOXC2 tg mice were hyperphagic when compared with wt mice (Figure 5). This inconsistency may be due to differences in the ages of the mice studied, housing, diet composition, etc. Interestingly, a decrease in leptin mRNA production by FOXC2 tg WAT when compared with wt WAT was observed by Cederberg *et al* (2001) and could help to explain the increase in food intake by FOXC2 tg mice that was observed in this study. Leptin is secreted by adipocytes and acts on the hypothalamus as a satiety signal (Farooqi and O'Rahilly, 2009). The absence of any differences in body weight despite increased food intake could be due at least partially to the increased O_2 consumption observed in FOXC2 tg mice when compared with wt mice at 24°C (Figure 6). This increase in O_2 consumption in FOXC2 tg mice would indicate that they require an increased amount of food when compared with wt mice to maintain energy balance.

WAT can be subcategorized into subcutaneous (SAT) and visceral (abdominal) adipose tissue (VAT). Increases in both are thought to contribute to the pathology of symptoms of the metabolic syndrome; however, VAT is more strongly associated with insulin resistance and other symptoms of the metabolic syndrome (Pascot *et al*, 1999;

Molenaar *et al*, 2009). Therefore, tissue weights of both depots were determined. As anticipated, the FOXC2 tg mice had significantly smaller weights of both SAT and VAT. Furthermore, the VAT depot was reduced to an even greater extent than the SAT depot (3-fold *vs.* 1.5-fold; Table 1). This indicates that increases in FOXC2 expression can have distinct effects in different WAT depots, having a specifically potent effect on VAT weight. The weights of the IBAT depots were not significantly different between the FOXC2 tg and wt mice. This is inconsistent with the finding of Cederberg *et al* (2001) that FOXC2 tg mice had enlarged IBAT depots when compared with wt mice. This difference may be due to differences in extracting the depots (*i.e.,* standard dissection practice in our lab is to remove the white fat 'cap' surrounding the IBAT). Cederberg *et al* (2001) may have incorporated surrounding 'converted' WAT into the IBAT depot while I did not. Therefore, whether or not the IBAT is enlarged or not remains unclear. Overall, my results indicate that the FOXC2 tg mice were much leaner than their wt littermates, consistent with the findings of Cederberg *et al* (2001).

5.2. *Effects of FOXC2 Overexpression in Adipocytes upon Characteristics of Whole Body O_2 Consumption.*

One of the most intriguing findings emerged from my *in vivo* studies in which we used indirect calorimetry to probe the possible functional effects at the whole body level. It was observed that while wt mice had the expected increase in O_2 consumption upon exposure to the β_3-adrenergic agonist, CL-316,243 (Figure 8A), there was little response in FOXC2 tg mice (Figure 8B). Whole body O_2 consumption of rodents (rats and mice at room temperature) normally is ~doubled by acute CL-316,243 stimulation

(Enerback *et al*, 1997). When CL-316,243 was administered chronically at 1mg/kg per day for 10-14 days, energy expenditure in rats was increased by 15% (Himms-Hagen *et al*, 1994). It was observed that β_3-adrenergic stimulation of adipose tissue prepared from FOXC2 tg WAT displayed a distinct increase in cAMP levels, while no such increase was seen in adipocytes prepared from wt WAT (Cederberg *et al,* 2001). Based on this and the previously observed increases in β_3AR mRNA expression (Cederberg *et al,* 2001), we hypothesized that FOXC2 tg mice would have a greater response to CL-316,243 than wt mice. My findings indicate that the FOXC2 tg mice are not responsive to acute β_3-adrenergic stimulation at the whole body level. However, the reasons behind this unexpected finding are unclear. Although Cederberg *et al* (2001) found an increase in the β_3AR and UCP1 mRNA, it is possible that the adipocytes from the FOXC2 mice are already oxidizing fuels at a maximal, or near-maximal rate. Therefore, it is possible that the β_3AR/cAMP/PKA pathway cannot be further amplified. It was observed by Cederberg *et al* (2001) that FOXC2 increases the sensitivity of the β_3AR/cAMP/PKA pathway by increasing the transcription and expression of the regulatory subunit RIα of PKA which binds cAMP with higher affinity than the RIIβ regulatory subunit. Furthermore, it was observed by Gronning *et al* (2006) that FOXC2 reduces the expression of phosphodiesterase-4 (PDE4) in the FOXC2 mice further amplifying the β_3AR/cAMP/PKA signal. The latter findings are indeed consistent with the possibility that fuel oxidation in FOXC2 tg adipocytes is near maximal in the absence of β_3-adrenergic agonist, and thus that there are minimal effects of CL-316,243. A similar lack of response to β_3 adrenergic stimulation was reported by Kajimura *et al*, 2009 in engineered brown fat cells created from mouse fibroblasts expressing PRDM16 and

C/EBPβ. There was no increase in respiration in response to cAMP however there was cAMP induced increases in thermogenic genes such as Ucp1 and Pgc1a .

However, as seen in Figure 8B, there was a small yet significant difference between the FOXC2 tg mice with and without the β_3-adrenergic agonist when mice were at rest (*i.e.*, at 10-30 percentile points). Low percentile values, or PCRFs (*i.e.*, <50%) represent time points at which the mice are less physically active, while high PCRFs (>50%) represent points at which the mice are more active (Riachi *et al*, 2004). This indicates that the effect of the agonist could be observed when the mice were at rest but that any effect of the agonist could be masked when the mice were physically active.

At the level of the whole body, results demonstrated several significant differences in O_2 consumption (and therefore, metabolic rate) between FOXC2 tg mice and wt control mice. Over the 24-hour period of analysis at 24°C, the FOXC2 tg mice had an increased O_2 consumption when compared with their wt littermate controls (Figure 6). This is likely due to increased activity of the β_3/cAMP/PKA pathway as described above. Presumably then, the 'converted' WAT has taken on the BAT-like function of non-shivering thermogenesis. Furthermore, results also showed that the FOXC2 tg mice, compared to wt mice have an increased whole body O_2 consumption at an environmental temperature of 30°C (Figure 9). This is consistent with the conclusion of increased basal metabolic rate in FOXC2 tg mice, since thermoregulatory energy expenditure processes do not occur at thermoneurality (30°C for mice).

Interestingly, there was no difference in O_2 consumption at 4°C between FOXC2 tg and wt mice as can be seen in Figure 10. It can be inferred from these data and those obtained at 24°C and 30°C that the wt mice would have had to increase thermogenic

mechanisms at 4°C to a greater extent than the FOXC2 tg mice. Again, this is consistent with the idea of increased basal energy expenditure in the FOXC2 tg mice. In FOXC2 tg mice, the increased heat production is presumably in the converted WAT. Wild type mice thus would have needed to activate both non-shivering and shivering thermogenesis to a greater extent to adapt to the cold. Cold-induced increases in O_2 consumption within the first 24 hours are due to shivering thermogenesis (in muscle) and acute activation of UCP1 (*i.e.*, non-shivering thermogenesis in brown adipose tissue) (Davis *et al*, 1960). After 24 hours, transcription and translation of UCP1 and other proteins involved in thermogenesis would increase (Cannon and Nedergaard, 2004).

5.3. *Effects of FOXC2 Overexpression in Adipocytes upon Characteristics of Whole Body Carbohydrate and Fatty Acid Metabolism.*

Upon stimulation with CL-316,243 there should be an increase in fatty acid oxidation and therefore a decrease in the RER of mice (Riachi *et al*, 2004). Stimulation of the β_3AR, a G-protein coupled receptor, activates adenylyl cyclase. This causes increases in cAMP which induces phosphorylation and activation of PKA. PKA is then responsible for inactivating perilipin and activating HSL. This facilitates access of HSL (as well as ATGL and MGL) to intracellular fat stores and allows for lipolysis and fatty acid release (Souza *et al*, 2007). These free fatty acids then enter the β-oxidation pathway, which in turn provides reducing equivalents for the electron transport chain. The free fatty acids also activate UCP1, freeing it from inhibition by purine nucleotides (Nichols and Rial, 1999). Interestingly, both wt and FOXC2 tg mice display this

expected shift towards fatty acid oxidation upon stimulation with CL-316,243 (Figures 13A&B, respectively), indicating that the FOXC2 tg mice are in fact responding to the β_3-adrenergic agonist with an increase in fatty acid oxidation. However, it is impossible to tell from these studies whether the activation of the β_3-adrenergic pathway is occurring in BAT, converted WAT or both. It is possible that the free fatty acids released by β_3AR activation are being utilized in areas other than adipose tissue such as muscle, and are simply being oxidized there, replacing carbohydrates as the fuel source. In other words, in FOXC2 tg mice, the only outcome is a switch in fuel source from carbohydrates to fatty acids. Thus, this paradoxical finding in FOXC2 tg mice of β_3-adrenergic activation of fatty acid oxidation in the absence of any increase in O_2 consumption needs to be investigated further.

At 4°C, although there was no difference in O_2 consumption between FOXC2 tg and wt mice, there was a difference in RER with the FOXC2 tg mice having a significantly greater RER (Figure 15). This result indicates that at this temperature, the wt mice have increased fatty acid oxidation when compared with the FOXC2 tg mice. This increased fatty acid oxidation by the wt mice in the cold may be indicative of heightened shivering thermogenesis in skeletal muscle, stemming from a greater need for cold-induced thermogenesis in wt mice compared to FOXC2 tg mice. This could be indicative of a greater basal metabolic rate of the FOXC2 tg mice when compared with the wt mice. Therefore, the FOXC2 tg mice may rely less on shivering thermogenesis in the cold because of the increased non-shivering thermogenesis presumably brought about by the overexpression of FOXC2 in adipose tissue. In future studies, body temperature of the FOXC2 tg and wt mice should be carefully monitored in a controlled

setting to test this hypothesis. These data were collected during an acute exposure to cold (*i.e.*, over the first 24-hour period) when shivering thermogenesis would be the main form of heat production, particularly in wt mice. In the future it would also be interesting to extend the time over which mice are studied at 4°C to determine if the observed differences in RER continue over an extended period of time.

5.4. *Histological Analyses of Adipose Tissues of FOXC2 tg and wt mice.*

H&E staining of adipose tissue sections and light microscopy showed that adipocytes from wt IBAT are more densely packed with smaller lipid droplets than FOXC2 tg IBAT adipocytes (Figure 16E & F, respectively). The reason for this is unclear; however, the same characteristics were noted by Cederberg *et al* (2001). Perhaps increased thermogenesis in WAT depots, most notably SAT, and an increased basal metabolic rate in FOXC2 tg mice decreases the need for BAT thermogenesis. It is also possible that the hypertrophy (*i.e.*, growth) of FOXC2 tg BAT as observed by Cederberg *et al* (2001) results in less efficient 'packing' of mitochondria and lipid droplets. To support this notion, the FOXC2 tg VAT and SAT (Figure 16B & D respectively) were more densely packed with increased multilocularity when compared with wt VAT and SAT (Figure 16A & C, respectively). Furthermore, VAT and SAT from FOXC2 tg mice have a clearly brown appearance which is presumably indicative of an increase in mitochondrial content.

Another notable difference between the genotypes was identified through immunohistochemistry of adipose tissues. The UCP1-specific staining of IBAT from wt mice appears to be localized to certain areas of cells within the sectioned tissue (Figure

19E). Such 'patchy' staining of cells has been previously observed and is known as the 'harlequin effect' in BAT (Cinti *et al*, 2002), and is believed to be due to highly variable levels of UCP1 expression in brown adipocytes due to acute adrenergic stress. However, in sections of the FOXC2 tg BAT the staining is dispersed throughout the sections much more evenly (Figure 19F), indicating that the harlequin effect is not as prominent in BAT of FOXC2 tg mice. The previous work of Cederberg *et al* (2001) demonstrated upregulated UCP1 mRNA expression in IBAT from FOXC2 tg mice when compared with wt mice. These authors also observed UCP1 mRNA expression in WAT from FOXC2 tg mice but not in that of wt mice (Cederberg *et al*, 2001). Therefore, the distribution of UCP1 in FOXC2 tg IBAT may be more evenly distributed because of its increased expression while the distribution of UCP1 in wt IBAT is based on adrenergic stress (*i.e.*, cold-induced).

Interestingly, my findings show that while there was a considerable amount of UCP1 staining in SAT from FOXC2 tg mice (Figure 19D), there was little in VAT from FOXC2 tg mice (Figure 19B). This, along with the large decrease in weight of VAT from FOXC2 tg mice, suggest that FOXC2 expression may have different effects on SAT and VAT. These findings support the idea that SAT appears to be converted into BAT, while VAT is not as fully converted. Tissue weight results however show that the VAT depot is significantly decreased (Table 1) as a result of increased FOXC2 expression. Therefore, the main effect on VAT appears to be a reduction in the actual amount of tissue. This may be due to the increased resting metabolic rate. It is well known that metabolic characteristics vary between different depots of WAT. For example, a metabolic distinction between VAT and SAT was observed by Walker *et al*

(2008) who found that in humans SAT was much more responsive to the TZD rosiglitazone than VAT. Furthermore, in the Framingham heart study, results (in humans) indicated that VAT was more strongly associated with adverse metabolic risk than was SAT (Fox *et al*, 2007). While it appears that VAT is less responsive to both the overexpression of FOXC2 and TZDs, results indicate that FOXC2 effectively reduces the size of VAT. Decreasing the size of VAT may be of key importance in reversing obesity-related pathophysiologies since obese patients with the metabolic syndrome generally have a large VAT distribution (Lebovitz, 2003).

Even with these differences in UCP1 staining between IBAT of FOXC2 tg and wt mice, there was no difference in basal O_2 consumption (Figure 20A) or FCCP-stimulated maximal O_2 consumption (Figure 20A) between isolated brown adipocytes from the IBAT of FOXC2 tg and wt mice. This finding is consistent with the conclusions 1) that UCP1 content does not affect the thermogenic capacity of the tissue, or 2) that there may be differences in the amount or activity of other factors such as regulatory/signaling factors in IBAT from FOXC2 tg and wt mice and that these differences may supersede the importance of total UCP1 content (*i.e.,* in terms of overall thermogenic activity of the tissue). It was discovered by Ukropec *et al* (2006), that Ucp1 -/- mice could still acquire cold-induced brown adipocyte phenotypes, such as increased fat oxidation, in white adipose depots (inguinal), even though they do not express UCP1. This suggests that thermogenesis can occur without UCP1 or that more likely, cold can induce the expression of genes involved in thermogenesis without the expression of UCP1. However, UCP1 is believed to be necessary for optimal thermogenesis and unique in its function to mediate adaptive thermogenesis in BAT

(Golozoubova *et al*, 2006). The importance of UCP1 in non-shivering thermogenesis was also made evident in a study by Enerback *et al* (1997) where UCP1 ablated mice were shown to be cold intolerant and have low responses to acute treatment with the β_3-adrenergic agonist CL-316,243. Furthermore, UCP1 deficient mice kept at neutrality and therefore not exposed to thermal stress are prone to obesity on a normal diet and obesity is augmented on a high-fat diet (Feldmann *et al*, 2009).

5.5. *Effects of FOXC2 Overexpression in Adipocytes upon Ultrastructural Characteristics of Adipocytes.*

Using TEM, it was observed that IBAT from wt and FOXC2 tg mice (Figure 17E & F, respectively) had a similar ultrastructure characterized by many condensed mitochondria surrounding multilocular lipid droplets. These results were anticipated and are similar to those observed by Cinti *et al* (2002) who used TEM to study the ultrastructure of BAT in cold- (4°C) and warm-acclimated rats. The IBAT of FOXC2 tg and wt animals resembled that of the cold-acclimated rats.

It was observed that the VAT and SAT from wt mice (Figure 17A & C, respectively) had very little mitochondrial content, vascularity, and UCP1 staining. This is what was anticipated, based on the well-known structural and functional characteristics of WAT (Frühbeck, 2008). FOXC2 SAT displayed much higher amounts of mitochondrial, vascularity, and UCP1 staining. Based on results from H&E staining of tissue sections for light microscopy, it was clear that SAT from FOXC2 tg mice (Figure 16D) had increased multilocularity when compared with wt SAT (Figure 16C). This was confirmed by TEM images which showed clusters of mitochondria

around multilocular lipid droplets in FOXC2 tg SAT (Figure 17D). These structural findings are consistent with the conclusion that the FOXC2 SAT acquires structural characteristics of BAT. Using TEM, the cells from wt VAT and SAT appeared to contain one large lipid droplet with a few mitochondria between it and the cell wall. Furthermore, the wt VAT and SAT mitochondria had very little cristae indicating that they are not very metabolically active. The cristae in mitochondria of the FOXC2 tg SAT were more numerous and the mitochondria appeared to congregate around small lipid droplets. Overall these differences are consistent with the idea that FOXC2 tg SAT is more thermogenic than wt VAT and SAT.

Compared with the FOXC2 tg SAT, the VAT from the FOXC2 tg mice was much harder to characterize using TEM (Figure 17A). Lipid droplet multilocularity in FOXC2 tg VAT was sparse compared with that of FOXC2 tg SAT. The mitochondrial clusters were also fewer and farther between, indicating a less complete 'conversion' of FOXC2 tg VAT from WAT to BAT. The observed histological differences between FOXC2 tg VAT and SAT may be due to underlying differences in metabolic pathways between VAT and SAT. Evidence suggests that FOXC2 is able to convert SAT more completely into active brown-like tissue than it is able to convert VAT. However, both FOXC2tg VAT (Figure 18A) and SAT (Figure 18B) displayed an increase in vascularity when compared to wt VAT and SAT; increased vascularity is important for the provision of nutrients and, in the case of BAT, for the export of heat. It must be noted that these conclusions are based on qualitative observations and differences between SAT and VAT should be further investigated quantitatively. To support this observation, it was observed quantitatively by Xue *et al* (2008) that the FOXC2 tg WAT

and BAT contained a higher density of vascular plexuses when compared with wt WAT and BAT. It has been observed previously by Kim *et al* (2005) that FOXC2 tg mice had a greater lean muscle mass than wt mice. This increase in muscle mass would lead to an increase in energy expenditure and perhaps is the cause of the large decrease in VAT observed in FOXC2 tg mice.

Another interesting finding from the TEM analyses was that mitochondria from IBAT, SAT, and VAT of FOXC2 tg mice appeared to be elongated when compared with mitochondria from the corresponding wt adipose depots (Figure 17). These elongated mitochondria were also seen by Westergren *et al* (2009; submitted) in differentiated MEFs from FOXC2 tg mice when compared with wt differentiated MEFs. These observations are consistent with the possibility that increased FOXC2 expression causes mitochondrial fusion. Moreover, it was observed by Westergren *et al* (2009; submitted) that adipocytes with enhanced FOXC2 expression had increased mRNA expression of mitofusin (Mfn) 1 and 2 which are known to facilitate mitochondrial fusion (Griffin *et al*, 2006). In muscle cells, mitochondrial fusion allows mitochondria to form elongated filaments and suppression of this fusion disrupts mitochondrial function and increases obesity and obesity-related characteristics (Bach *et al*, 2003). Furthermore, reduced mitochondrial fusion has been reported to be linked with increased insulin resistance (Civitarese and Ravussin, 2008). Therefore, this presumed enhanced mitochondrial fusion might be important in enhancing the function of the mitochondria in these adipocytes.

5.6. *Effects of FOXC2 Overexpression in Adipocytes upon Oxidative Characteristics of Isolated Cells.*

To determine the role of FOXC2 on the metabolic activity of adipose tissue, cells from WAT and BAT were isolated from FOXC2 tg and wt mice. For these determinations of cellular O_2 consumption, 12-15 mice at 3-4 months of age were needed from each genotype for each experiment. This hindered the pace in performing multiple experiments. VAT and SAT depots were pooled since a relatively large amount of adipose tissue was required for each experiment. As anticipated, basal O_2 consumption of adipocytes from FOXC2 tg and wt BAT was 9-fold higher than that of wt WAT (Figure 20A). Of great interest was the 7-fold increase in O_2 consumption in the adipocytes from WAT of FOXC2 tg mice when compared with adipocytes from WAT of wt mice. This large increase in O_2 consumption indicates unequivocally the functional thermogenic effects of FOXC2 in WAT. These are the first results to clearly demonstrate that the isolated white adipocytes from FOXC2 tg WAT have increased O_2 consumption. This difference is in accordance with, and even greater than that found by Cederberg *et al* (2001) who observed a 4-fold increase in O_2 consumption in isolated pieces of FOXC2 tg WAT when compared with wt WAT. Furthermore, FOXC2 tg WAT displayed a 4.5-fold greater maximal O_2 consumption when compared with wt WAT (Figure 20B) further indicating an increased thermogenic capacity. The implications of this are important because they indicate that the WAT from FOXC2 tg mice is indeed highly metabolically active. Because of the differences observed in the ultrastructure of FOXC2 tg VAT and SAT, further experiments should examine O_2 consumption of SAT and VAT separately in order to determine whether FOXC2 has

distinct effects in these two tissues. Perhaps the O_2 consumption of SAT would be even greater when studied in the absence of VAT, and it is likely that the VAT would have O_2 consumption characteristics similar to wt WAT.

5.7. *Metabolic Effects of FOXC2 Overexpression in Differentiated MEFs.*

The results herein indicated that the FOXC2 tg differentiated MEFs had an oxidative capacity that exceeded that of wt differentiated MEFs (Figure 21A). Thus FOXC2 tg MEFs differentiate into adipocytes that contain more functional mitochondria when compared with wt MEFs, further supporting a function for FOXC2 in facilitating thermogenesis. FOXC2 tg MEFs displayed an increase in mitochondrial DNA, and TEM of these cells showed increased mitochondrial volume/content and a fused phenotype (Westergren *et al,* 2009; submitted). These results indicate that FOXC2 is involved in mitochondrial biogenesis. A limitation of our study was that for metabolic assessments in the Extracellular Flux Analyzer, the differentiation period was only 5-6 days. Confluent, adhered cells are imperative for these measurements and after 6-8 days of differentiation, the adipocytes tended to lift off of the cell culture plates. However, the visual characteristics of the cells after 5-6 days were consistent with that of differentiated adipocytes and we are confident that our findings are meaningful.

5.8. *Reduced Oxidative Stress in FOXC2 tg Differentiated MEFs*

Oxidative stress is caused by an imbalance in the production of reactive oxygen species (ROS) and the cell's ability to detoxify these species (*e.g.,* de Farrenti and Mozzaffarian, 2008). Oxidative damage is known to play a large role in the foundation

and progression of insulin resistance and T2DM (Houstis *et al*, 2006; Rosen *et al*, 2001; Green *et al*, 2004). It is also well known that there is increased oxidative stress in the accumulated fat of obese individuals and that this stimulates the progression of the metabolic syndrome (Furukawa *et al*, 2004). ROS are generated along the electron transport chain and the greatest rates of ROS production occur when the electron transport chain is fully reduced (Korshunov *et al*, 1997). UCP1 decreases mitochondrial membrane potential and stimulates electron transport chain activity and therefore, can effectively reduce ROS production (Green *et al*, 2004). It was therefore important to analyze what effect the overexpression of FOXC2 would have on oxidative stress in adipocytes with the hypothesis that oxidative stress would be decreased in the adipocytes overexpressing FOXC2. Results indeed indicated that FOXC2 overexpression in differentiated MEFs can lead to decreased oxidative stress (Figure 22). This identifies a potential role for FOXC2 in the prevention of T2DM and the metabolic syndrome by decreasing ROS production and/or by increasing ROS detoxification.

5.9. *Summary of the Role of FOXC2 in Energy Metabolism and Future Directions*

It was observed by our collaborators that mice that overexpress human FOXC2 in adipose tissue have an apparent conversion of WAT to BAT. These FOXC2 tg mice are leaner, have increased insulin sensitivity, and improved serum lipid profiles when compared with littermate wt controls. Furthermore, the WAT of FOXC2 tg mice acquires a brown appearance. It was shown by Cederberg *et al* (2001) that this conversion was brought about by an amplification of the β_3AR/cAMP/PKA pathway.

FOXC2 increases the expression of the RIα regulatory subunit of PKA which binds cAMP with higher affinity than the RIIβ subunit also found in adipocytes. This is depicted in Figure 23. Moreover, this amplification of the β_3-adrenergic pathway presumably caused the increased O_2 consumption in isolated pieces of white adipose tissue of FOXC2 tg mice as reported by Cederberg *et al* (2001).

Some observations of previous and ongoing studies were verified in this thesis while others were elaborated on with novel approaches and findings. My thesis showed the novel findings of increased O_2 consumption in FOXC2 tg mice and in isolated white adipocytes (as opposed to pieces of adipose tissue) from FOXC2 tg mice. Moreover, this thesis revealed differences in whole body O_2 consumption and the RERs of mice at various temperatures and in response to the selective β_3 agonist CL-316,243. Furthermore, an increased capacity for O_2 consumption was detected in differentiated MEFs from FOXC2 tg mice.

Histological analysis of adipocyte sections confirmed the increased multilocularity and mitochondrial content in FOXC2 tg WAT when compared with wt WAT and similar to that of wt BAT as was observed by Cederberg *et al* (2001). The increased UCP1 mRNA expression observed in FOXC2 tg WAT by Cederberg *et al* (2001) was confirmed in this thesis at a semi-quantitative level using immunohistochemistry of UCP1 in histological samples of adipocytes. Furthermore, WAT and BAT from FOXC2 tg mice displayed evidence of mitochondrial fusion. The increased mitochondrial fusion observed using TEM on adipocytes from FOXC2 tg and wt mice was confirmed by Westergren *et al* (2009) in FOXC2 tg MEFs.

Figure 23. The mechanism by which FOXC2 increases the sensitivity of the β_3/cAMP/PKA pathway. PKA is composed of regulatory (R) and catalytic (c) subunits. cAMP binds the regulatory subunits releasing the catalytic subunits. The kinase activity of the catalytic subunits causes expression of genes involved in the thermogenic response. The PKA regulatory subunits RIα and RIIβ are expressed in BAT and WAT. FOXC2 increases expression of the RIα subunit which is more readily bound by cAMP. Increases in the amount of the RIα subunit increases the sensitivity of the β_3/cAMP/PKA pathway. FOXC2 also increases expression of itself further attenuating this amplification.

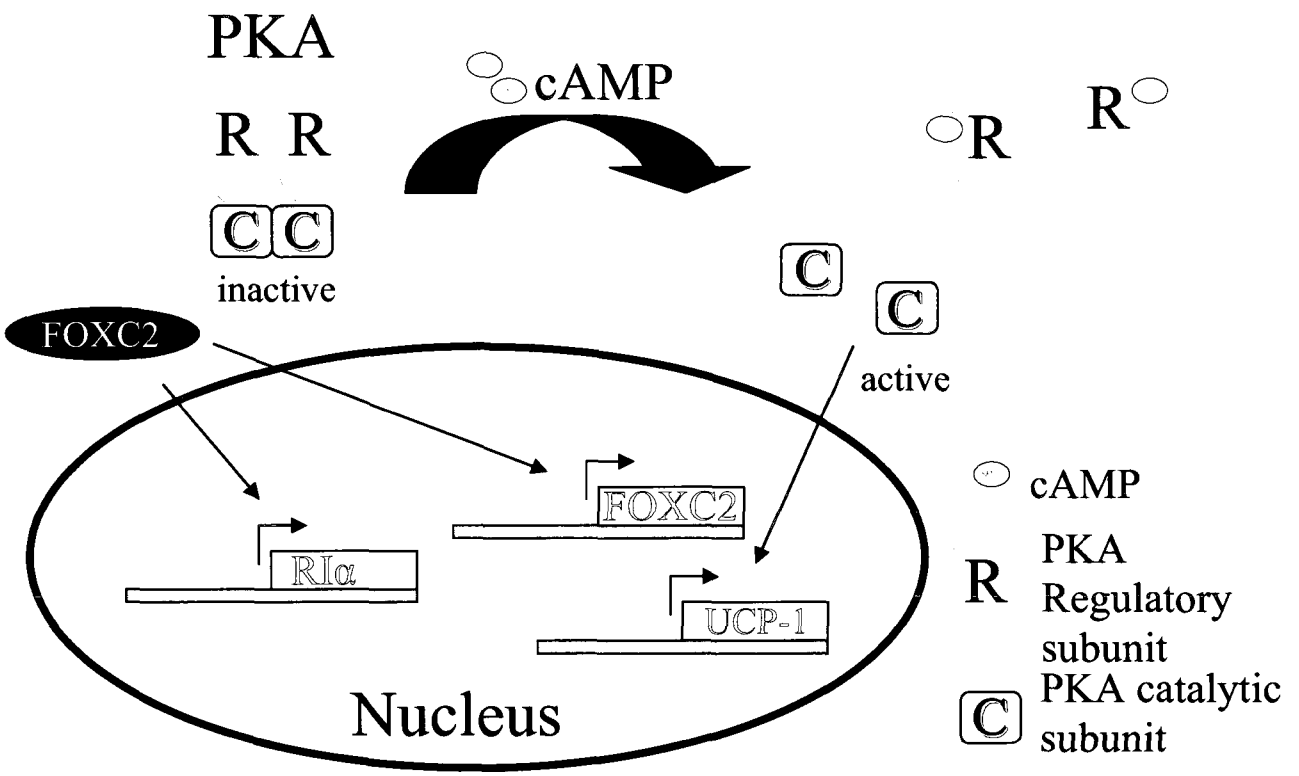
PKA
R R
C C
inactive
cAMP
R
R
C
C
active
FOXC2
FOXC2
RIα
UCP-1
Nucleus
cAMP
R
PKA
Regulatory
subunit
C
PKA catalytic
subunit

Furthermore, in this thesis the novel finding that FOXC2 tg MEFs displayed reduced oxidative stress possibly because of increased UCP1-mediated mitochondrial uncoupling was reported.

Current research shows that FOXC2 directly activates certain genes involved in diverse areas of metabolism such as IRS1, UCP1, GLUT4, HSL, and FOXC2 itself (Westergren et al, 2009; submitted). However, other adipogenic proteins such as adiponectin, adipsin and LPL, all known to be upregulated in WAT of FOXC2 tg mice are not directly activated by FOXC2 (Westergren *et al*, 2009; submitted). Moreover, while FOXC2 expression induces increased expression of PGC1α mRNA, the expression of PGC1α is not dependant on FOXC2. Perhaps the amplification of the β_3-adrenergic pathway by FOXC2 causes an increase in PGC1α. Furthermore, FOXC2 was shown to upregulate Tfam expression and Tfam is upregulated in FOXC2 tg mice. It is well known that Tfam is involved in mtDNA transcription and replication and the effects of FOXC2 on mitochondrial fusion may occur through this transcription factor as well as through Mfn 1 and 2. Phosphodiesterases (PDEs) cleave cAMP and therefore decrease the activity of PKA. It was found that PDE4 and PDE4A5 activity and expression levels were decreased in FOXC2 tg WAT when compared with wt WAT (Gronning *et al*, 2006). Thus the decreased expression of these PDEs most likely contributes to the phenotype of the FOXC2 tg mice.

The use of human FOXC2 in the rodent models, such as the FOXC2 tg mouse, implicates FOXC2 not only in rodent energy metabolism, but also in humans. Indeed, studies in human populations in which mutant forms of FOXC2 have been identified have implicated this transcription factor in energy metabolism in humans. As most

studies however have been conducted in rodents, future studies should be directed at deducing the mechanisms further in rodents and eventually in humans. Figure 24 summarizes the known roles of FOXC2 in adipocyte energy metabolism.

Figure 24. A summary of the known roles of FOXC2 in adipocyte energy metabolism. In humans, mutations in the FOXC2 gene have been identified that are associated with obesity and insulin resistance (IR). In rodents, FOXC2 has been shown to amplify the β_3AR/camp/PKA pathway by increasing transcription of the RIα subunit of PKA. Furthermore PDE4 levels are decreased in FOXC2 tg mice amplifying this pathway further. This leads to increased UCP1 and PGC1α expression, BAT differentiation, and thermogenesis. FOXC2 also increases the expression of Tfam and Mfn causing increased mitochondrial biogenesis and fusion. Moreover, FOXC2 increases the expression of GLUT4, IRS1, and HSL which are involved in a range of functions in adipocyte metabolism. The net result of increased FOXC2 expression is an increase in energy expenditure in the adipocyte by favouring a brown adipocyte phenotype. This leads to a phenotype that is lean and insulin sensitive.

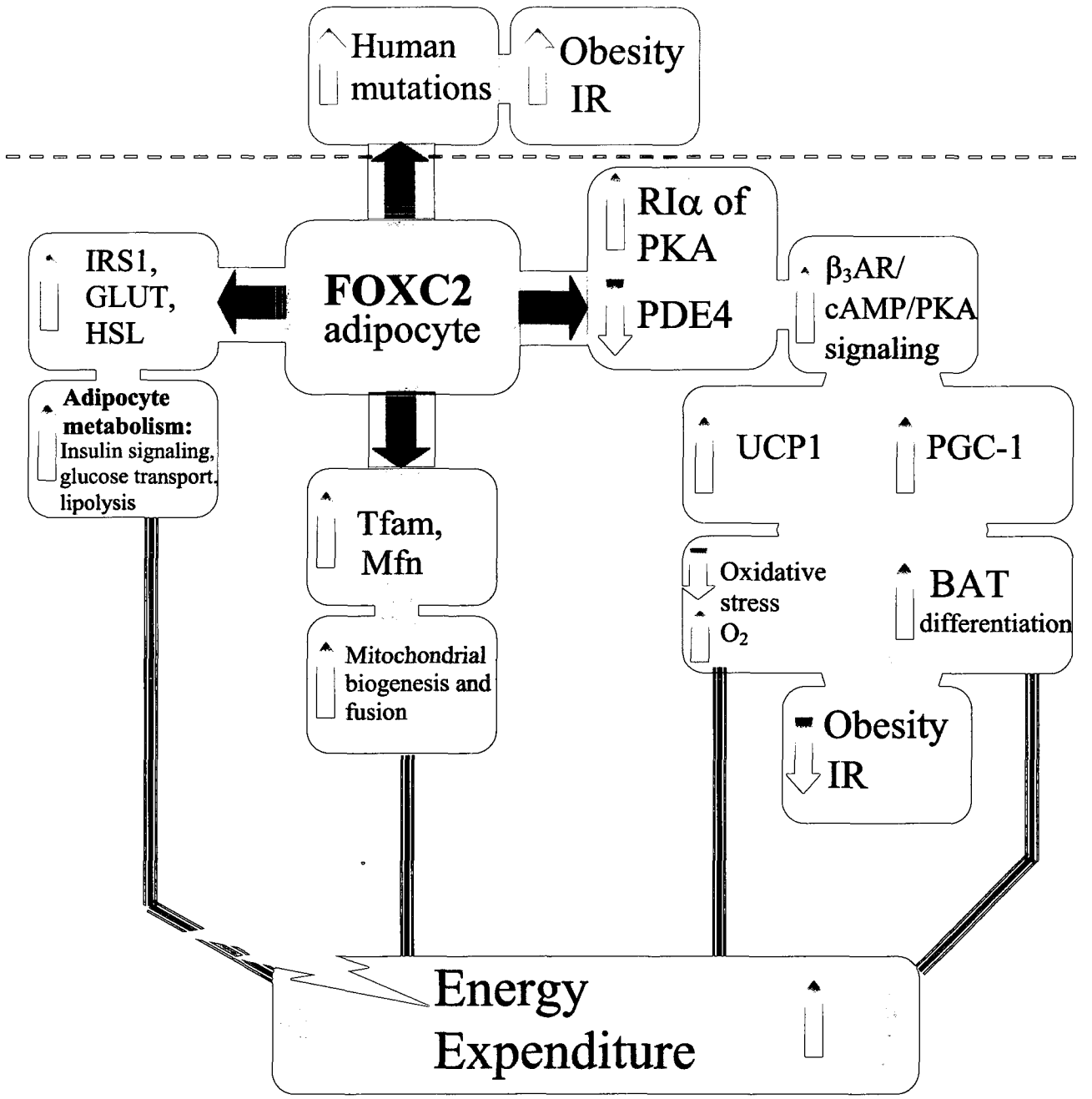
Human mutations
Obesity IR
RIα of PKA
PDE4
IRS1, GLUT, HSL
FOXC2 adipocyte
β3AR/ cAMP/PKA signaling
Adipocyte metabolism: Insulin signaling, glucose transport, lipolysis
UCP1
PGC-1
Tfam, Mfn
Oxidative stress
O2
BAT differentiation
Mitochondrial biogenesis and fusion
Obesity IR
Energy Expenditure

Conclusion

Conversion of white adipose tissue to brown adipose tissue in humans has been an exciting area of obesity research for almost twenty years. Many studies have focused on the identification of a selective β_3AR agonist that would be effective in humans much like the effectiveness of CL-316,243 in rodents. However, human β_3-adrenergic agonists have not as yet proven to be effective. Early β_3-adrenergic receptor agonists were developed using the rodent β_3AR (Arch, 2002). Unfortunately the human β_3AR, cloned in 1989, is sufficiently different from the rodent receptor, and the correspondingly developed agonists were relatively ineffective (they also crossreacted with the human β_1 and β_2 adrenoreceptors) (Hoffstedt *et al* 1996). Thus there is an ongoing challenge to develop an agonist that will selectively stimulate the low number of β_3ARs in human white adipocytes and the β_3ARs in human BAT (Arch, 2002, Chamberlain *et al*, 1999). Altogether, our results indicate that FOXC2 may be an important target for increasing energy expenditure in humans by increasing the thermogenic capacity of white adipose tissue. FOXC2 has been shown to increase the expression of the β_3AR which would be imperative for stimulation of human white adipocytes by β_3-adrenergic agonists (Cederberg *et al*, 2001). FOXC2 has also been shown to increase the sensitivity of the β_3/cAMP/PKA pathway which would be additionally beneficial. Furthermore, as revealed by my research and that of others, increased FOXC2 expression in adipose stimulates a BAT-like phenotype in WAT, and this increases insulin sensitivity and energy expenditure. One of the drawbacks of the use of TZDs in the treatment of T2DM is weight gain. It is proposed that a therapy involving FOXC2 would have similar clinical benefits as TZDs but would not cause

weight gain. All of the research findings to-date arising from studies of increased FOXC2 expression in adipocytes are consistent with the idea that increased expression in adipose tissue could provide an ideal therapy for obesity and obesity related pathologies. Future research will need to more completely characterize the pathways through which FOXC2 expression can be safely stimulated. Further research in cellular systems and animal models is needed.

6. Literature Cited

Abdul-Ghani, MA, and DeFronzo, RA. (2009). Pathophysiology of prediabetes. *Curr Diab Rep.* 9(3): 193-199.

Almind, K, Manieri, M, Sivitz, WI, Cinti, S, and Kahn, CR. (2007). Ectopic brown adipose tissue in muscle provides a mechanism for differences in risk of metabolic syndrome in mice. *Proc Natl Acad Sci U S A.* 104(7): 2366-2371.

Arch, JRS. (2002). β_3-Adrenoreeptor agonists: potential, pitfalls and progress. *Eur J Pharmacol.* 440(2-3): 99-107.

Bach, D, Pich, S, Soriano, FX, Vega, N, Baumgartner, B, Oriola, J, Daugaard, JR, Lloberas, J, Camps, M, Zierth, JR, Rabasa-Lhoret, R, Wallberg-Henriksson, H, Laville, M, Palacín, M, Vidal, H, Rivera, F, Brand, M, and Zorzano, A. (2003). Mitofusion-2 determines mitochondrial network architecture and mitochondrial metabolsm. A novel regulatory mechanism altered in obesity. *J Biol Chem.* 278: 17190-17197.

Bouillaud, F, Raimbault, S, and Ricquier, D. (1988). The gene for rat uncoupling protein: complete sequence, structure of primary transcript and evolutionary relationship between exons. *Biochem Biophys Res Commun.* 157(2): 783-792.

Bouillaud, F, Ricquier. D, Thibault, J, and Weissenbach, J. (1985). Molecular approach to thermogenesis in brown adipose tissue: cDNA cloning of the mitochondrial uncoupling protein. *Proc Natl Acad Sci U S A.* 82(2): 445-448.

Bronnikov, G, Houstek, J, and Nedergaard, J. (1992). B-Adrenergic, cAMP-mediated stimulation of proliferation of brown fat cells in primary culture. Mediation via β_1 but not via β_3 receptors. *J Biol Chem.* 267: 2006-2013.

Bukowiecki, L, Collet, AJ, Follea, N, Guay, G, and Jahjah, L. (1982). Brown adipose tissue hyperplasia: a fundamental mechanism of adaptation to cold and hyperphagia. *Am. J. Physiol.* 242(6): E353-E359.

Cannon, B, and Nedergaard, J. (1996). Adrenergic regulation of brown adipocyte differentiation. Biochem Soc Trans. 24(2): 407-412.

Cannon, B, and Nedergaard, J. (2004). Brown Adipose Tissue: Function and Physiological Significance. *Physiol Rev.* 84: 277-359.

Cannon, B, and Nedergaard, J. (2001). Respiratory and thermogenic capacity of cells and mitochondria from brown and white adipose tissue. *Methods Mol Biol.* 155: 295-303.

Carlsson, E, Almgren, P, Hoffstedt, J, Groop, L, and Ridderstråle, M. (2004). The FOXC2 C-512T polymorphism is associated with obesity and dyslipidemia. *Obes Res.* 12(11): 1738-1743.

Carlsson, E, Groop, L, and Ridderstrale, M (2005). Role of the FOXC2 512 C>T polymorhism in type 2 diabetes: a possible association with the dismetabolic syndrome. *Int J Obes.* 29(3): 268-274.

Cassard, AM, Bouillaud, F, Mattei, MG, Hentz, E, Raimbault, S, Thomas, M, and Ricquier, D. (1990). Human uncoupling protein gene: structure, comparison with rat gene, and assignment to the long arm of chromosome 4. *J Cell Biochem.* 43(3): 255-264.

Cederberg, A, Gronning, LM, Ahren, B, Tasken, K, Carlsson, P, and S, Enerback. (2001). FOXC2 is a winged helix gene that counteracts obesity, hyperglyceridemia, and diet induced insulin resistance. *Cell.* 106: 563-573.

Celi, FS. (2009). Brown adipose tissue--when it pays to be inefficient. *N Engl J Med.* 360(15): 1553-1556.

Chamberlain, PD, Jennings, KH, Paul, F, Cordell, J, Berry, A, Holmes, SD, Park, J, Chambers, J, Sennitt, MV, Stock, MJ, Cawthorne, MA, Young, PW, and Murphy, GJ. (1999). The tissue distribution of the human beta3-adrenoceptor studied using a monoclonal antibody: direct evidence of the beta3-adrenoceptor in human adipose tissue, atrium and skeletal muscle. *Int J Obes Relat Metab Disord.* 23(10): 1057-1065.

Cinti, S. (2006). The role of brown adipose tissue in human obesity. *Nutr Metab Cardiovasc Dis.* 16(8): 569-574.

Cinti, S, Cancello, R, Zingaretti, MC, Ceresi, E, De Matteis, R, Giordano, A, Himms-Hagen, J, and Ricquier, D. (2002). CL316,243 and cold stress induce heterogeneous expression of UCP1 mRNA and protein in rodent brown adipocytes. *J Histochem Cytochem.* 50(1): 21-31.

Civartese, A-E, and Ravussin, E. (2008). Mitochondrial energetics and insulin resistance. *Endocrinology.* 149: 950-954.

Clark, KL, Halay, ED, Lai, E, and Burley, SK. (1993). Co-crystal structure of the HNF-3/fork head DNA-recognition motif resembles histone H5. *Nature.* 364: 412-420.

Collins, S, and Surwit, RS. (2001). The β-Adrenergic Receptors and the Control of Adipose Tissue Metabolism and Thermogenesis. *Endocrine Society.* 309-328.

Cousin, B, Bascands-Viguerie, N, Kassis, N, Nibbelink, M, Ambid, L, Casteilla, L, and Pénicaud, L. (1996). Cellular changes during cold acclimatation in adipose tissues. *J Cell Physiol.* 167(2): 285-289.

Cummings, DE, Brandon, EP, Planas, JV, Motamed, K, Idzerda, RL, and McKnight, GS. (1996). Genetically lean mice result from targeted disruption of the RIIβ sbunit of protein kinase A. *Nature.* 383(6592): 622-626.

Cypess, AM, Lehman, S, Williams, G, Tal, I, Rodman, D, Goldfine, AB, Kuo, FC, Palmer, EL, Tseng, YH, Doria, A, Kolodny, GM, and Kahn, CR. (2009). Identification and importance of brown adipose tissue in adult humans. *N Engl J Med.* 360 (15): 1509-1517.

Davis, TR, Johnston, DR, Bell, FC, and Cremer, BJ. (1960). Regulation of shivering and non-shivering heat production during acclimation of rats. *Am J Physiol.* 198: 471-475.

Davis, KE, Moldes, M, and Farmer, SR. (2004). The forkhead transcription factor FoxC2 inhibits white adipocyte differentiation. *J Biol Chem.* 279(41): 42453-42461

de Ferranti, S, and Mozaffarian, D. (2008). The perfect storm: obesity, adipocyte dysfunction, and metabolic consequences. *Clin Chem.* 54(6): 945-955.

Dicker, A, Cannon, B, and Nedergaard, J. (1995). Cold acclimation-recruited nonshivering thermogenesis: the Syrian hamster is not an exception. *Am J Physiol.* 269(4 Pt 2): R767-R774.

Dostmann, WR, Taylor, SS, Genieser, HG, Jastorff, B, Doskeland, SO, and Ogreid, D. (1990). Probing the cyclic nucleotide binding sites of cAMP-dependent protein kinases I and II with analogues of adenosine 3',5'-cyclic phosphorothioates. *J Biol Chem.* 265(18): 10484-10491.

Emorine, LJ, Fève, B, Pairault, J, Briend-Sutren, MM, Nahmias, C, Marullo, S, Delavier-Klutchko, C, and Strosberg, DA. (1992). The human beta 3-adrenergic receptor: relationship with atypical receptors. *Am J Clin Nutr.* 55(1 Suppl): 215S-218S.

Enerbäck, S., Jacobsson, A, Simpson, EM, Guerra, C, Yamashita, H, Harper, M-E, and Kozak, LP. (1997). Mice lacking mitochondrial uncoupling protein are cold sensitive but not obese. *Nature.* 387: 90-94.

Fain, JN, Madan, AK, Hiler, ML, Cheema, P, and Bahouth, SW. (2004). Comparison of the release of adipokines by adipose tissue, adipose tissue matrix, and adipocytes from visceral and subcutaneous abdominal adipose tissues of obese humans. *Endocrinology.* 145(5): 2273-2282.

Farooqi, IS, and O'Rahilly, S. (2009). Leptin: a pivotal regulator of human energy homeostasis. *Am J Clin Nutr.* 89(3): 980S-984S.

Feldmann, HM, Golozoubova, V, Cannon, B, and Nedergaard, J. (2009). UCP1 ablation induces obesity and abolishes diet-induced thermogenesis in mice exempt from thermal stress by living at thermoneutrality. *Cell Metab.* 9(2): 203-209.

Fox, CS, Massaro, JM, Hoffmann, U, Pou, KM, Maurovich-Horvat, P, Liu, CY, Vasan, RS, Murabito, JM, Meigs, JB, Cupples, LA, D'Agostino, RB Sr, and O'Donnell, CJ. (2007). Abdominal visceral and subcutaneous adipose tissue compartments: association with metabolic risk factors in the Framingham Heart Study. *Circulation.* 116(1): 39-48.

Frühbeck G. (2008). Overview of adipose tissue and its role in obesity and metabolic disorders. *Methods Mol Biol.* 456: 1-22.

Furukawa, S, Fujita, T, Shimabukuro, M, Iwaki, M, Yamada, Y, Nakajima, Y, Nakayama, O, Makishima, M, Matsuda, M, and Shimomura, I. (1993). Increased oxidative stress in obesity and its impact on metabolic syndrome. *J Clin Invest.* 114(12): 1752-1761.

Gallagher, EJ, LeRoith, D, and Karnieli, E. (2008). The metabolic syndrome--from insulin resistance to obesity and diabetes. *Endocrinol Metab Clin North Am.* 37(3): 559-579.

Ghorbani, M, and Himms-Hagen, J. (1998). Appearance of brown adipocytes in white adipose tissue during CL 316,243-induced reversal of obesity and diabetes in Zucker fa/fa rats. *Int J Obes Relat Metab Disord.* 21(6): 465-475.

Golozoubova, V, Cannon, B, and Nedergaard, J. (2006). UCP1 is essential for adaptive adrenergic nonshivering thermogenesis. *Am J Physiol Endocrinol Metab.* 291(2): E350-E357.

Gomez-Ambrosi, J, Fruhbeck, G, and Martinez, JA. (2001). Rapid in vivo PGC-1 mRNA upregulation in brown adipose tissue of Wistar rats by a beta(3)-adrenergic agonist and lack of effect of leptin. *Mol Cell Endocrinol.* 176: 85–90.

Green, K, Brand, MD, and Murphy, MP. (2004). Prevention of mitochondrial oxidative damage as a therapeutic strategy in diabetes. *Diabetes.* 53:(Suppl. 1): S110–S118.

Gregoire, FM. (2001). Adipocyte differentiation: from fibroblast to endocrine cell. *Exp Biol and Med.* 226(11): 997-1002.

Griffin, EE, Detmer, SA, and Chan, DC. (2006) Molecular mechanism of mitochondrial membrane fusion. *Biochim Biophys Acta.* 1763(5-6): 482-489.

Grønning, LM, Baillie, GS, Cederberg, A, Lynch, MJ, Houslay, MD, Enerbäck S, and Taskén, K. (2006). Reduced PDE4 expression and activity contributes to enhanced catecholamine-induced cAMP accumulation in adipocytes from FOXC2 transgenic mice. *FEBS letters.* (17): 4126-4130.

Hajer, GR, van Haeften, TW, and Visseren, FL. (2008). Adipose tissue dysfunction in obesity, diabetes, and vascular diseases. *Eur Heart J.* 29(24): 2959-2971.

Hamann, A, Flier, JS, and Lowell, BB. (1996). Decreased brown fat markedly enhances susceptibility to diet-induced obesity, diabetes, and hyperlipidemia. *Endocrinology.* 137(1): 21-29.

Hauner, H. (2005). Secretory factors from human adipose tissue and their functional role. *Proc Nutr Soc.* 64(2): 163-169.

Heaton, GM, Wagenvoord, RJ, Kemp, AJ, and Nicholls, DG. (1978). Brown-adipose-tissue mitochondria: photoaffinity labelling of the regulatory site of energy dissipation. *Eur J Biochem.* 82(2): 515-21.

Himms-Hagen, J, Cui, J, Danforth, E Jr, Taatjes, DJ, Lang, SS, Waters, BL, and Claus, TH. (1994). Effect of CL-316,243, a thermogenic beta3-agonist, on energy balance and brown and white adipose tissues in rats. *Am J Physiol.* 266(4 Pt 2): R1371-1382.

Himms-Hagen, J, Melnyk, A, Zingaretti, MC, Ceresi, E, Barbatelli, G, and Cinti, S. (2000). Multilocular fat cells in WAT of CL-316243-treated rats derive directly from white adipocytes. *Am J Physiol Cell Physiol.* 279(3): C670-C681.

Himms-Hagen, J. (2001). Does brown adipose tissue (BAT) have a role in the physiology or treatment of human obesity? *Rev Endocr Metab Disord.* 2001 2(4): 395-401.

Hoffstedt, J, Lönnqvist, F, Shimizu, M, Blaak, E, and Arner, P. (1996). Effects of several putative beta 3-adrenoceptor agonists on lipolysis in human omental adipocytes. *Int J Obes Relat Metab Disord.* 20(5): 428-434.

Houstis, N, Rosen, ED, and Lander, ES. (2006). Reactive oxygen species have a causal role in multiple forms of insulin resistance. *Nature.* 440(7086): 944-948.

Huang, PL. (2009). A comprehensive definition for metabolic syndrome. *Dis Model Mech.* 2(5-6): 231–237.

Ito, M, Grujic, D, Abel, ED, Vidal-Puig, A, Susulic, VS, Lawitts, J, Harper, ME, Himms-Hagen, J, Strosberg, AD, and Lowell, BB. (1998). Mice expressing human but not murine beta3-adrenergic receptors under the control of human gene regulatory elements. *Diabetes.* 47(9): 1464-1471.

Imaizumi-Scherrer, T, Faust, DM, Benichou, JC, Hellio, R, and Weiss, MC. (1996). Accumulation in fetal muscle and localization to the neuromuscular junction of cAMP-dependent protein kinase A regulatory and catalytic subunits RIα and Cα. *J Cell Biol.* 134(5): 1241-1254.

Kaestner, KH, Knochel, W, and Martinez, DE. (2000). Unified nomenclature for the winged helix/forkhead transcription factors. *Genes Dev.* 14: 142-146.

Kahn, BB, and Flier, JS. (2000). Obesity and insulin resistance. *J Clin Invest.* 106(4): 473-481.

Kajimura, S, Seale, P, Kubota, K, Lunsford, E, Frangioni, JV, Gygi, SP, and Spiegelman, BM, (2009). Initiation of myoblast to brown fat switch by a PRDM16-C/EBP-beta transcriptional complex. *Nature*. 460(7259): 1154-8.

Karamanlidis, G, Karamitri, A, Docherty, K, Hazlerigg, DG, and Lomax, MA. (2007). C/EBPbeta reprograms white 3T3-L1 preadipocytes to a Brown adipocyte pattern of gene expression. *J Biol Chem*. 282(34): 24660-24669.

Kim, JK, Kim, HJ, Park, SY, Cederberg, A, Westergren, R, Nilsson, D, Higashimori, T, Cho, YR, Liu, ZX, Dong, J, Cline, GW, Enerback, S, and Shulman, GI. (2005). Adipocyte-specific overexpression of FOXC2 prevents diet-induced increases in intramuscular fatty acyl CoA and insulin resistance. *Diabetes*. 54(6): 1657-1663.

Kleiwer, SA, Umesono, K, Noonon, D, Heyman, R, and Evans, RM. (1992). Convergence of 9-cis retinoic acid and peroxisome proliferators sigmalling pathways through heterodimer formation of there receptors. *Nature*. 358: 771-774.

Klingenspor, M. (2003). Cold-induced recruitment of brown adipose tissue thermogenesis. *Exp Physiol*. 88(1): 141-148.

Korshunov, SS, Skulachev, VP, and Starkov, AA. (1997). High protonic potential actuates a mechanism of production of reactive oxygen species in mitochondria. *FEBS Lett*. 416: 15–18.

Kozak, LP, and Harper, ME. (2000). Mitochondrial uncoupling proteins in energy expenditure. *Annu Rev Nutr*. 20: 339-363.

Kume, T, Jiang, H, Topczewska, JM, and Hogan, BL. (2001). The murine winged helix transcription factors, Foxc1 and Foxc2, are both required for cardiovascular development and somitogenesis. *Genes Dev*. 15: 2470-2482.

Lafontan, M, Sengenes, C, Galitzky, J, Berlan, M, De Glisezinski, I, Crampes, F, Stich, V, Langin, D, Barbe, P, and Riviere, D. (2000). Recent developments on lipolysis regulation in humans and discovery of a new lipolytic pathway. *Int J Obes Relat Metab Disord*. 24 (Suppl 4): S47-S52.

Lai, CS, Fisher, SE, Hurst, JA, Vargha-Khadem, F, and Monaco, AP. (2001). A forkhead-domain gene is mutated in a severe language and speech disorder. *Nature*. 413: 519-523.

Lai, E, Prezioso, VR, Smith, E, Litvin, O, Costa, RH, and Darnell, JEJ. (1990). HNF-3A, a hepatocyte-enriched transcription factor of novel structure is regulated transcriptionally. *Genes Dev*. 4: 1427–1436.

Lai, E, Prezioso, VR, Tao, WF, Chen, WS, and Darnell, JEJ. (1991). Hepatocyte nuclear factor 3 alpha belongs to a gene family in mammals that is homologous to the *Drosophila* homeotic gene fork head. *Genes Dev*. 5: 416–427.

Larsson, NG, Wang, J, Wilhelmsson, H, Oldfors, A, Rustin, P, Lewandoski, M, Barsh, GS, and Clayton, DA. (1998). Mitochondrial transcription factor A is necessary for mtDNA maintenance and embryogenesis in mice. *Nat Genet.* 18(3): 199-200.

Lebovitz, HE. (2003). The relationship of obesity to the metabolic syndrome. *Int J Clin Pract Suppl.* (134): 18-27.

Lehmann, OJ, Ebenezer, ND, Jordan, T, Fox, M, Ocaka, L, Payne, A, Leroy, BP, Clark, BJ, Hitchings, RA, Povey, S, Khaw, PT, and Bhattacharya, SS. (2000). Chromosomal duplicationinvolving the forkhead transcription factor gene FOXC1 causes iris hypoplasia and glaucoma. *Am. J. Hum. Genet.* 67: 1129-1135.

Lehmann, JM, Moore, LB, Smith-Oliver, TA, Wilkison, WO, Willson, TM, and Kliewer, SA. (1995). An antidiabetic thiazolidinedione is a high affinity ligand for peroxisome proliferator-activated receptor gamma (PPAR gamma). *J Biol Chem.* (22): 12953-12956.

Lehmann, OJ, Sowden, JC, Carlsson, P, Jordan, T, and Bhattacharya, SS. (2003). Fox's in development and disease. *TRENDS* 19(6): 339-344.

Liu, X, Rossmeisl, M, McClaine, J, Riachi, M, Harper, ME, and Kozak, LP. (2003). Paradoxical resistance to diet-induced obesity in UCP1-deficient mice. *J Clin Invest.* 111: 399–407.

Lowell, BB, and Spiegelman, BM. (2000). Towards a molecular understanding of adaptive thermogenesis. *Nature.* 404: 652-660.

Lupien, JR, Glick, Z, Saito, M, and Bray, GA. (1985). Guanosine diphosphate binding to brown adipose tissue mitochondria is increased after single meal. *Am J Physiol.* 249(6 Pt 2): R694-R698.

Ma, SW, and Foster, DO. (1989). Brown adipose tissue, liver, and diet-induced thermogenesis in cafeteria diet-fed rats. *Can J Physiol Pharmacol.* 67(4): 376-381.

Medina-Gomez, G, Gray, S, and Vidal-Puig, A. (2007). Adipogenesis and lipotoxicity: role of peroxisome proliferator-activated receptor gamma (PPARgamma) and PPARgammacoactivator-1 (PGC1). *Public Health Nutri.* 10(10A): 1132-1137.

Molenaar, EA, Massaro, JM, Jacques, PF, Pou, KM, Ellison, RC, Hoffmann, U, Pencina, K, Shadwick, SD, Vasan, RS, O'Donnell, CJ, and Fox, CS. (2009). Association of lifestyle factors with abdominal subcutaneous and visceral adiposity: the Framingham Heart Study. *Diabetes Care.* 32(3): 505-510.

Muoio, DM, and Newgard, CB. (2008). Mechanisms of disease: molecular and metabolic mechanisms of insulin resistance and beta-cell failure in type 2 diabetes. *Nat Rev Mol Cell Biol.* 9(3): 193-205.

Must, A, Spadano, J, Coakley, EH, Field, AE, Colditz, G, and Dietz, WH. (1999). The disease burden associated with overweight and obesity. *JAMA.* 16(282): 1523-1529.

Nedergaard, J, Bengtsson, T, and Cannon, B. (2007). Unexpected evidence for active brown adipose tissue in adult humans. *AM J Physiol Endocrinol Metab.* 293(2): E444-E452.

Nedergaard, J, Golozoubova, V, Matthias, A, Asadi, A, Jacobsson, A, and Cannon, B. (2001). UCP1: the only protein able to mediate adaptive non-shivering thermogenesis and metabolic inefficiency. *Biochim Biophys Acta.* 1504(1): 82-106.

Nedergaard, J, Petrovic, N, Lindgren, EM, Jacobsson, A, and Cannon, B. (2005). PPARgamma in the control of brown adipocyte differentiation. *Biochim Biophys Acta.* 1740(2): 293-304.

Nicholls, DG, and Rial, E. (1999). A history of the first uncoupling protein, UCP1. *J Bioenerg Biomembr.* 5: 399-406.

Ocloo, A, Shabalina, IG, Nedergaard, J, and Brand, MD. (2007). Cold-induced alterations of phospholipid fatty acyl composition in brown adipose tissue mitochondria are independent of uncoupling protein-1. *Am J Physiol Regul Integr Comp Physiol.* 293(3):R1086-R1093.

O'Rahilly, S. (1997). Science, medicine, and the future non-insulin dependent diabetes mellitus: the gathering storm. *BMJ.* 314: 955-959.

Pascot, A, Lemieux, S, Lemieux, I, Prud'homme, D, Tremblay, A, Bouchard, C, Nadeau, A, Couillard, C, Tchernof, A, Bergeron, J, and Despres, JP. (1999). Age-related increase in visceral adipose tissue and body fat and the metabolic risk profile of premenopausal women. *Diabetes Care.* 22:1471–1478.

Pelleymounter, MA, Cullen, MJ, Baker, MB, Hecht, R, Winters, D, Boone, T, and Collins, F. (1995). Effects of the obese gene product on body weight regulation in ob/ob mice. *Science.* 269(5223): 540-543.

Porter, RK. (2008). Uncoupling protein 1: a short-circuit in the chemiosmotic process. *J Bioenerg Biomembr.* 40: 45-461.

Puigserver, P, Wu, Z, Park, CW, Graves R, Wright, M, and Spiegelman, BM. (1998). A cold-inducible coactivator of nuclear receptors linked to adaptive thermogenesis. *Cell.* 92(6): 829-39.

Rau, H, Reaves, BJ, O'Rahilly, S, and Whitehead, JP. (1999). Truncated human leptin (delta133) associated with extreme obesity undergoes proteasomal degradation after defective intracellular transport. *Endocrinology.* 140(4): 1718-1723.

Ravussin, E, and Kozak, LP. (2009). Have we entered the brown adipose tissue renaissance? *Obes Rev.* 10(3): 265-268.

Riachi, M, Himms-Hagen, J, and Harper, ME. (2004). Percent relative cumulative frequency analysis in indirect calorimetry: application to studies of transgenic mice. *Can J Physiol Pharmacol.* 82(12): 1075-1083.

Ridderstråle, M, Carlsson, E, Klannemark, M, Cederberg, A, Kösters, C, Tornqvist, H, Storgaard, H, Vaag, A, Enerbäck, S, and Groop, L. (2002). FOXC2 mRNA Expression and a 5' untranslated region polymorphism of the gene are associated with insulin resistance. *Diabetes.* 51(12): 3554-3560.

Rösen, P, Nawroth, PP, King, G, Möller, W, Tritschler, HJ, and Packer, L. (2001). The role of oxidative stress in the onset and progression of diabetes and its complications: a summary of a Congress Series sponsored by UNESCO-MCBN, the American Diabetes Association and the German Diabetes Society. *Diabetes Metab Res Rev.* 17(3): 189-212.

Rosen, ED, and Spiegelman, BM. (2000). Molecular Regulation of Adipogenesis. *Annu. Rev. Cell Dev.* 16: 145-171.

Rothwell, NJ, and Stock, MJ. (1979). A role for brown adipose tissue in diet induced thermogenesis. *Nature.* 281: 31-35.

Seale, P, Bjork, B, Yang, W, Kajimura, S, Chin, S, Kuang, S, Scimè, A, Devarakonda, S, Conroe, HM, Erdjument-Bromage, H, Tempst, P, Rudnicki, MA, Beier, DR, and Spiegelman, BM, (2008). PRDM16 controls a brown fat/skeletal muscle switch. *Nature.* 454(7207): 961-7.

Seale, P, Kajimura, S, and Speigelman, BM. (2009). Transcriptional control of brown adipocyte development and physiological function-of mice and men. *Genes Dev.* 23: 788-797.

Seale, P, Kajimura, S, Yang, W, Chin, S, Rohas, LM, Uldry, M, Tavernier, G, Langin, D, and Spiegelman, BM. (2007). Transcriptional control of brown fat determination by PRDM16. *Cell Metab.* 6(1): 38-54.

Sell, H Deshaies, Y, and Richard, D. (2004). The brown adipocyte: update on its metabolic role. *Int J Biochem Cell Biol.* 36(11): 2098-2104.

Silva, J, Kohler, M, Graff C, Oldfors, A, Magnuson, MA, Berggren, PO, and Larsson, NG. (2000). Impaired insulin secretion and beta-cell loss in tissue-specific knockout mice with mitochondrial diabetes. *Nat Genet.* 26(3): 336-340.

Simonsen, L, Bulow, J, Madsen, J, and Christensen, NJ. (1992). Thermogenic response to epinephrine in the forearm and abdominal subcutaneous adipose tissue. *AM J Physiol.* 263: E850-E855.

Skeberdis, VA. (2004). Structure and function of β3-adrenergic receptors. *Medicina (Kaunas.* 40(5): 407-413.

Smith, RE. (1961). Thermogenic activity of the hibernating gland in cold-acclimated rats. *Physiologist.* 4: 113.

Smith, RE. (1962). Thermoregulation by brown adipose tissue in cold. *Federation Proc.* 21: 221.

Smith, RE, and Horwitz, BA. (1969). Brown fat and thermogenesis. *Physiological Reviews.* 49(2): 330-425.

Souza, SC, Christoffolete, MA, Ribeiro, MO, Miyoshi, H, Strissel, KJ, Stancheva, ZS, Rogers, NH, D'Eon, TM, Perfield, JW 2nd, Imachi, H, Obin, MS, Bianco, AC, and Greenberg, AS. (2007). Perilipin regulates the thermogenic actions of norepinephrine in brown adipose tissue. *J Lipid Res.* 48(6): 1273-1279

Statistics Canada. *Canadian Community Health Survey: Nutrition*, 2004. (http://www.statcan.gc.ca/cgi-bin/imdb/p2SV.pl?Function=getSurvey&SDDS=5049&lang=en&db=imdb&adm=8&dis=2)

Tiraby, C., and Langin, D. (2003). Conversion of white to brown adipocytes: a strategy for the control of fat mass. *Trends Endocrinol Metab.* 14(10); 439-441.

Tontonoz, P, and Spiegelman, BM. (2008). Fat and beyond: the diverse biology of PPARgamma. *Annu Rev Biochem.* 77: 289-312.

Tsai, L, Szweda, PA, Vinogradova, O, and Szweda, LI. (1998). Structural characterization and immunochemical detection of a fluorophore derived from 4-hydroxy-2-nonenal and lysine. *Proc Natl Acad Sci U S A.* 95(14): 7975-7980.

Uchida, K, and Stadtman, ER. (1992). Modification of histidine residues in proteins by reaction with 4-hydroxynonenal. *Proc Natl Acad Sci U S A.* 89(10): 4544-4548

Ukropec, J, Anunciado, RP, Ravussin, Y, Hulver, MW, and Kozak, LP. (2006). UCP1-independent thermogenesis in white adipose tissue of cold-acclimated Ucp1-/- mice. *J Biol Chem.* 281(42): 31894-31908.

van Marken Lichtenbelt, WD, Vanhommerig, JW, Smulders, NM, Drossaerts, JM, Kemerink, GJ, Bouvy, ND, Schrauwen, P, and Teule, GJ. (2009). Cold-activated brown adipose tissue in healthy men. *N Engl J Med.* 360(18): 1500-1509.

Virtanen, KA, Lidell, ME, Orava, J, Heglind, M, Westergren, R, Niemi, T, Taittonen, M, Laine, J, Savisto, NJ, Enerbäck, S, and Nuutila P. (2009). Functional brown adipose tissue in healthy adults. *N Engl J Med.* 360 (15): 1518-1525.

Walker, GE, Marzullo, P, Verti, B, Guzzaloni, G, Maestrini, S, Zurleni, F, Liuzzi, A, and Di Blasio, AM. (2008). Subcutaneous abdominal adipose tissue subcompartments: potential role in rosiglitazone effects. *Obesity.* 16(9): 1983-1991.

Wang, P, Mariman, E, Renes, J, and Keijer, J. (2008). The secretory function of adipocytes in the physiology of white adipose tissue. *J Cell Physiol.* 216(1): 3-13.

Watanabe, M, Yamomoto, T, Mori, C, Okada, N, Yamazaki, N, Kajimoto, K, Kataoka, M, and Shinohara, Y. (2008). Cold-Induced Changes in Gene Expression n Brown Adipose Tissue: Implications for the Activation of Thermogenesis. *Biol Pharm Bull.* 31(5): 775-784.

Weigel, D, and Jackle, H. (1990). The fork head domain: a novel DNA binding motif of eukaryotic transcription factors. *Cell.* 63: 455-456.

Weigel, D, Jurgens, G, Kuttner, F, Seifert, E, and Jackle, H. (1989). The homeotic gene fork head encodes a nuclear protein and is expressed in the terminal regions of Drosophila embryo. *Cell.* 57: 645-658.

Westergren, R, Seifert, E, Heglind, M, Gowing, A, Arani, Z, Bell, M, Rodrigo-Blomqvist, S, Fernandez-Rodriguez, J, Nilsson, T, Harper, M-E, and Enerback, S. (2009). The adipocyte expressed fork head transcrption factor Foxc2 links metabolism to mitochondrial fusion and biogenesis. Submitted.

Wijers, SL, Saris, WH, and van Marken Lichtenbelt, WD. (2009). Recent advances in adaptive thermogenesis: potential implications for the treatment of obesity. *Obes Rev.* 10(2): 218-226.

Wozniak, SE, Gee, LL, Wachtel, MS, and Frezza, EE. (2008). Adipose tissue: the new endocrine organ? A review article. *Dig Dis Sci.* 54(9): 1847-1856.

Xue, Y, Cao, R, Nilsson, D, Chen, S, Westergren, R, Hedlund, EM, Martijn, C, Rondahl, L, Krauli, P, Walum, E, Enerbäck, S, and Cao, Y. (2008). FOXC2 controls Ang-2 expression and modulates angiogenesis, vascular patterning, remodeling, and functions in adipose tissue. *Proc Natl Acad Sci U S A.* 105(29): 10167-10172.

Yang, X, Enerback, S, and Smith, U. (2003). Reduced Expression of FOXC2 and Brown Adipogenic Genes in Human Subjects with Insulin Resistance. *Obes Res.* 11(10): 1182-1191.

Yildirim-Toruner, C, Subramanian, K, El Manjra, L, Chen, E, Goldstein, S, Vitale, E. (2004). A novel frameshift mutation of FOXC2 gene in a family with hereditary lymphedema-distichiasis syndrome associated with renal disease and diabetes mellitus. *Am J Med Genet A.* 131(3): 281-286.

Young, P, Arch, JR, and Ashwell, M. (1984). Brown adipose tissue in the parametrial fat pad of the mouse. *FEBS Lett.* 167(1): 10-14.

Zechner, R, Strauss, JG, Haemmerle, G, Lass, A, and Zimmermann, R. (2005). Lipolysis: pathway under construction. *Curr Opin Lipidol.* 16(3): 333-340.

Zhang, Y, Proenca, R, Maffei, M, Barone, M, Leopold, L, Friedman, JM. (1994). Positional cloning of the mouse obese gene and its human homologue. *Nature.* 372(6505): 425-32.

Zimmermann, R, Strauss, JG, Haemmerle, G, Schoiswohl, G, Birner-Gruenberger, R, Riederer M, Lass, A, Neuberger, G, Eisenhaber, F, Hermetter, A, and Zechner, R. (2004). Fat mobilization in adipose tissue is promoted by adipose triglyceride lipase. *Science.* 306 (5700): 1383-1386.

Curriculum Vitae

Adrienne Gowing B.Sc., M.Sc. Candidate

Formal Education

M.Sc. Candidate in Biochemistry
University of Ottawa, Ottawa ON, 2004-2009

B.Sc. in Biochemistry S.S.P. (Hon)
Queen's University, Kingston ON, 2004

O.A.C.D. (Ontario Scholar)
St. Francis Xavier Catholic High School, Hammond ON, 2000

O.S.S.D.
St. Francis Xavier Catholic High School, Hammond ON, 1999

Experience

2004-2009
M.Sc. Candidate in Biochemistry
Faculty of Medicine, University of Ottawa
Supervisor: Dr. Mary-Ellen Harper
Dissertation: Metabolic Characterization of Human FOXC2 in Adipose Tissue

September 2005-April 2006
Teaching Assistant/Laboratory Demonstrator
Faculty of Science, University of Ottawa

January 2004-April 2004
Research Student
Department of Biochemistry, Queen's University
Supervisor: Dr. Christopher Mueller

September 2003-December 2003
Research Student
Department of Biochemistry, Queen's University
Supervisor: Dr. Michael Nesheim

May 2003-August 2003
Research Student/NSERC
Department of Biochemistry, Queen's University
Supervisor: Dr. Zongchao Jia C.R.C.

Awards

September 2005-August 2006
NSERC PGS-M ($17,300)
University of Ottawa

September 2005-August 2006
Ontario Graduate Scholarship ($15,000)
University of Ottawa *(Declined)*

September 2005-August 2006
Excellence Scholarship ($5,000)
University of Ottawa

September 2004-August 2005
Ontario Graduate Scholarship ($15,000)
University of Ottawa

September 2004-August 2005
Excellence Scholarship ($5,000)
University of Ottawa

May 2003-August 2003
USRA-NSERC ($4,000)
Queen's University

September 2000-April 2001
Entrance Bursary ($3,000)
Queen's University

2000-2004
Dean's List
Queen's University

Published Papers and Abstracts

Refereed Papers

Westergren, R, Seifert, E, Heglind, M, **Gowing, A**, Arani, Z, Bell, M, Rodrigo-Blomqvist, S, Fernandez-Rodriguez, J, Nilsson, T, Harper, M-E, and Enerback, S. (2009). The adipocyte expressed fork head transcrption factor Foxc2 links metabolism to mitochondrial fusion and biogenesis. Submitted.

Costford, S, **Gowing, A,** and Harper, M-E. (2007). Mitochondrial uncoupling as a target in the treatment of obesity. *Curr Opin Clin Nutr Metab Care*. 10(6): 671-678.

Costford, SR, Seifert, EL, Bézaire, V, Gerrits, MF, Bevilacqua, L, **Gowing, A**, and Harper, M-E. (2007). The energetic implications of uncoupling protein-3 in skeletal muscle. *Appl Physiol Nutr Metab*. 32(5): 884-894.

MacLellan, JD, Gerrits, MF, **Gowing, A,** Smith, PJS, Sivitz, W, Wheeler, MB, and Harper, M-E. (2005). Uncoupling protein 3 increases fatty acid but not glucose oxidation in L6 myotubes. *Diabetes*. 54(8): 2343-2350.

Refereed Published Abstracts
Gowing, A, Enerback, S, and Harper, M-E. Metabolic characterization of the overexpression of FOXC2, a winged helix transcription factor in adipocytes. *Second International Meeting on Physiology and Pharmacology of Temperature Regulation.* Phoenix AZ. March 3-6, 2006.

Gowing, A, Enerback, S, and Harper, M-E. Metabolic characterization of mice overexpressing foxc2 in adipose tissue. *Canadian Federation of Biological Societies' Northern Lights meeting.* Guelph, June 2005.

Non-Refereed
Oral Presentation (2006), Department of Biochemistry, Microbiology, and Immunology, University of Ottawa (Graduate Seminar Day).

Poster Presentation (2005, 2007), Department of Biochemistry, Microbiology, and Immunology, University of Ottawa (Graduate Poster Day).

Oral Presentation (2004), Department of Biochemistry, Queen's University (Undergraduate Honours Thesis; Oral Presentation).

References
Upon Request